PERFORMANCE CHARACTERISTICS OF SELF-COMPACTING CONCRETE CONTAINING IRON SLAG

A Thesis
Submitted in fulfillment of the requirement
for the award of the degree of

DOCTOR OF PHILOSOPHY
IN
CIVIL ENGINEERING

GURPREET SINGH
Registration No. 951202001

DEPARTMENT OF CIVIL ENGINEERING
THAPAR UNIVERSITY, PATIALA – 147004
PUNJAB (INDIA)
2017

CERTIFICATE

This is to certified that thesis entitled, **"Performance Characteristics of Self-Compacting Concrete Containing Iron Slag"**, submitted by Mr. Gurpreet Singh in partial fulfillment of requirements, for the award of degree of Doctor of Philosophy in Civil Engineering submitted in the Department of Civil Engineering, Thapar University.
Patiala is a record of the candidate original research work carried out by him under the guidance and supervision.

The matter embodied in this thesis has not been submitted into any other university or institute for the award of any degree.

Siddique 15/3/17

Rafat Siddique, Ph.D.
Senior Professor, Civil Engineering Department
Thapar University
Patiala – 147004, India

DECLARATION

I hereby certify that the work which is being presented in the thesis entitled, **"Performance Characteristics of Self-Compacting Concrete Containing Iron Slag"** being in partial fulfillment of the requirements for the award of the degree of Doctor of Philosophy in Civil Engineering submitted in Civil Engineering Department of Thapar University Patiala is an authentic record of my own work carried out by me under the supervision of Dr. Rafat Siddique and refers other research's work duly listed in the reference section.

The matter presented in this thesis has not been submitted in part or full to any other university or institution for the award of any degree in India or abroad.

(Gurpreet Singh)

ACKNOWLEDGEMENT

- Foremost, I thank the almighty whose blessing have enabled me to accomplish this research work.
- I would like to express my sincere gratitude to my advisor Dr. Rafat Siddique, Sr. Professor, Department of Civil Engineering, Thapar University, Patiala for the continuous support of my Ph.D study and research, for his patience, motivation, enthusiasm, and immense knowledge. His guidance helped me in all the time of research and writing of this thesis. I could not have imagined having a better advisor and mentor for my Ph.D study.
- Besides my advisor, I would like to thank the rest of my thesis committee: Dr. Maneek Kumar, Dr. Shweta Goyal and Dr. Kulbir Singh for their valuable suggestions and feedbacks. The inputs provided by Dr. Naveen Kawatra, Head Department of Civil Engineering, his interest and critical appraisal during the early stage of this research are invaluable.
- The help and support provided by technical staff Er. Varinder Sharma and Shri Ram Sumiran during the entire research period are greatly appreciated
- I would also like to show our gratitude to Dr. Malkit Singh for sharing their pearls of wisdom with me during the course of this research.
- I also acknowledge the support of SAI labs, Thapar University for SEM and XRD analysis.
- Special thanks to my parents, my wife and son Avraj singh for their patience, understanding and constant support during the whole research program.

(Gurpreet Singh)

PUBLICATIONS

Journal Publications

1. Singh, G and Siddique, R. Strength properties and micro-structural analysis of self-compacting concrete made with iron slag as partial replacement of fine aggregates. ***Construction and Building Materials (ELSEVIER), Vol.127, November 2016, Pages 144-152.***
2. Singh, G and Siddique, R. Effect of iron slag as partial replacement of fine aggregates on the durability characteristics of self-compacting concrete. ***Construction and Building Materials (ELSEVIER), Vol.128, December 2016, Pages 88-95.***
3. Singh, G and Siddique, R. Abrasion resistance and strength properties of self-compacting concrete containing iron slag. **(Under Submission)**

Conference

1. Singh, G., and Siddique, R. Properties of Self-Compacting Concrete Incorporating Iron Slag as Replacement of Fine Aggregate, 10th ACI/RILEM International Conference on Cementitious Materials and Alternative Binders for Sustainable Concrete. Montreal, Canada. October 2-4, 2017 **(Paper Accepted)**

ABSTRACT

In India, an approximate production of iron and steel slag is 10 million tons annually. Large quantity of slag is used in cement industry but except that it is dumped on land adjoining sites of iron and steel mills, and becoming environmental hazard to the community. The constructive use of iron slag is the better way to mitigate the issue associated with disposal. The utilization of such material in self compacting concrete helps in reducing the disposal problem. Hence in this study, perceptions for using iron slag as replacement of fine aggregates are explored.

The current study has been carried out to evaluate the feasibility of the use iron slag as fine aggregates in self-compacting concrete (SCC). Control SCC was made with fly ash (10% addition as supplementary cementing material) designed to achieve 28-day compressive strength of 30 – 40MPa. In control SCC, fine aggregates were replaced with iron slag at 10, 25 and 40% contents. A total four SCC mixtures SCC-CM, SCC-IS10, SCC-IS25 and SCC-IS40 were developed; SCC-CM (control mix) was developed without replacement of iron slag with fine aggregates, SCC-IS10 with 10% replacement of iron slag, SCC-IS25 with 25% replacement of iron slag and SCC-IS40 with 40% replacement of iron slag. Slump flow, L-box, U-box and V-funnel tests were performed to evaluate passing and filling abilities of SCC in fresh state. Tests for compressive strength, splitting tensile strength, flexural strength, modulus of elasticity, water absorption, sorptivity, sulphate resistance, rapid chloride permeability, abrasion resistance and ultra-sonic pulse velocity were conducted up to the age of 365 days.

Test results indicate that fresh properties such as slump flow, L-box, U-box and V-funnel of SCC mixes with or without replacement of iron slag were within the specified range as specified by EFNARC. Compressive strength of SCC mixtures increased with the inclusion of iron slag as well as with age. At the age of 7 days, SCC mixes with iron slag achieved higher compressive strength. 28-day compressive strength of SCC with iron slag varied between 37.1 N/mm^2 to 45.1 N/mm^2 at 10 to 40% replacement of iron slag as compared to 35.7 N/mm^2 of control SCC. Splitting tensile strength increased with the increase in iron slag and with age as well. 28-day splitting tensile strength of SCC with iron slag was varied between 2.8 N/mm^2 to 3.4 N/mm^2 at from 10 to 40% replacement of

iron slag. However, 28-days splitting tensile strength of control SCC were 2.7 N/mm^2. Flexural strength of SCC increases with the inclusion of iron slag as compared with control SCC. Modulus of elasticity of SCC mix with iron slag mixes was in the range of 28.19 – 28.87 GPa at 28-days age against 27.9 GPa of control SCC.

Water absorption and sorptivity decreased with the increase in iron slag content. However, in case of compressive strength loss in sulphate resistance, control SCC performed slightly better than SCC with iron slag content. Chloride permeability of SCC mixes reduced with iron slag. Further, chloride permeability decreased with age, and decreased at faster rate than that of control SCC mixture. Abrasion resistance of SCC with iron slag content was higher than control SCC. The effect of iron slag on pulse velocity value of SCC was significant. All value of pulse velocity was graded as excellent concrete quality.

Micro-structural analysis reveals that SCC matrix gets denser and pore structure improves with the inclusion of iron slag content. X-ray diffraction spectrum reveals that the phase composition of powder SCC paste was not changing qualitatively, the change of phases was observed on the use of iron slag dose in SCC. In the statically analysis the correlation of strength properties, strength and durability properties shows that there is good relation between regression curve and data points and good coefficient of determination.

Strength and durability results indicate that iron slag could be suitably used in making SCC.

CONTENTS

LIST OF TABLES

LIST OF FIGURES

LIST OF UNITS

Units		Word(s)
Kg	-	Kilogram
g	-	Gram
mg	-	Milligram
°C	-	Degree Celsius
%	-	Percent
m	-	Meter
cm	-	Centimeter
mm	-	Millimeter
µm	-	Micrometer
N	-	Newton
MPa	-	Mega Pascal
GPa	-	Giga Pascal
Kg/m^3	-	Kilogram per cubic meter
N/mm^2	-	Newton per square millimeter
KN	-	Kilo Newton
hr	-	Hour
min	-	Minute
Sec	-	Second
C	-	Coulombs
m/s	-	Meter per second
km/s	-	Kilometer per second
θ	-	Theta

ABBREVIATIONS

Abbreviations		Word(s)
ACI	-	American Concrete Institute
ASTM	-	American Society for Testing Materials
BIS	-	Bureau of Indian Standards
C	-	Calcite
CA	-	Coarse Aggregates
CM	-	Control Mix
CH	-	Calcium Hydroxide
CS	-	Calcium Silicate
CSH	-	Calcium Silicate Hydrates
CTM	-	Compression Testing Machine
E	-	Ettringite
EDS	-	Energy Dispersive X-ray spectroscopy
FA	-	Fly Ash
IS	-	Iron Slag
ITZ	-	Inter Transition Zone
OPC	-	Ordinary Portland Cement
Q	-	Quartz
RCPT	-	Rapid Chloride Permeability Test
SCC	-	Self-compacting Concrete
SEM	-	Scanning Electron Microscopy
UPV	-	Ultra-sonic Pulse Velocity
XRD	-	X-ray Diffraction

CHAPTER-1

INTRODUCTION

This unit deals with general introduction about (i) self-compacting concrete (SCC), definition of self-compacting concrete by various authors, advantages and limitations of SCC, how self-compacting concrete differs from vibrated concrete, global growth of self-compacting concrete, applications of self-compacting concrete, (ii) Industrial by-products such as waste foundry sand, coal bottom ash, steel slag, copper slag, marble sludge powder, quarry dust, boiler slag, manufactured sand, iron slag, production, consumption, price, types of iron-blast furnace slag, physical properties of iron slag, chemical composition of iron slag, environment impact of iron slag, applications of iron slag; (iii) fly ash, classifications of fly ash, properties of fly ash, applications of fly ash, objectives and scope of the work, and organization of thesis.

1.1 SELF-COMPACTING CONCRETE

The development of self-compacting concrete is considered as a milestone achievement in concrete technology due to several advantages. In order to be self-compactable the fresh concrete must show high fluidity besides good cohesiveness (*Corinaldesi and Moriconi, 2011).* In general practices, concrete is compacted by internal vibration to expel the entrapped air, thus making it dense and homogeneous; Compaction is the key to producing good concrete with optimum strength and durability (*The Concrete Society and BRE, 2005*). However, in Japan in the early 1980's, because of the increasing reinforcement volumes with smaller steel bars and a shortage in skilled construction workers, proper compaction was difficult task, leading to poor compaction and quality of concrete (*Okamura and Ouchi, 1999*).

Professor Okamura therefore proposed a concept for a design of concrete without the need for compaction. Ozawa and Maekawa produced the first prototype of SCC at the University of Tokyo in 1988 (*Ozawa et al., 1989; RILEM TC 174 SCC, 2000*).

Since that time SCC has gone from a laboratory to practical applications. Research published every year that deal with all aspects of SCC, e.g. mix design, rheological and physical properties and applications in practice indicate research on this technology is

Thriving. Recommendations on the design and applications of SCC in construction have now been developed by many professional societies, including the American Concrete Institute (ACI), the American Society for Testing and Materials (ASTM), Centre for Advanced Cement-Based Materials (ACBM), Precast Consulting Services (PCI) and (RILEM) etc. Symposiums and workshops on this topic have been organized by these societies and several test methods have been or are in the process of standardization.

SCC with its outstanding properties, impressive deformability, gives designers and architects more freedom of creativity that was not possible previously. Lighter and slender members can be made from SCC, larger span bridges can be developed, and underwater structures can be built, making SCC a highly promising material for the future of the in-situ and pre-cast construction industries. Since its early use in Japan, SCC has now started to be an alternative to vibrated concrete across the world in such areas where normal vibrated concrete is difficult or impossible to pour and vibrate. However those applications are still few and vibrated concrete is still considered as the standard concrete. As more and more investigations are done into SCC, it is likely to move from being a fringe technology to becoming a concrete of choice for construction because of reduced health concerns, i.e. no vibration-induced noise. Improvements to concrete will have a large impact in the construction and building sector. As the attention is drawn towards energy-efficient and zero emission buildings of concrete will be important *(Serina et al.(2015)).*

Depending on its composition, SCC can have a wide range of different properties; from a normal to an ultra-high compressive strength, from a poor to an extremely high durability. The mix of SCC is strongly dependent on the composition and characteristics of its constituents in its fresh state. The properties of SCC in its fresh state have a great influence on its properties in the hardened state. Therefore it is critical to understand its flow behavior in the fresh state. Since the SCC mix is essentially defined in terms of its flow-ability, the characterization and control of its rheology is crucial for its successful production.

When there is no need for compacting, the quality assurance of the vibrating as an uncertain factor, regarding the final result of the concrete, is ruled out. The most used

argument for not using SCC is that it is more expensive than regular vibrated concrete. Despite the high expenses of SCC compared to regular concrete, it is probably more profitable in use by reducing the expenses of vibrating, and by quicker casting. In addition there are several other benefits with using SCC; With no need for vibrating, the working environment is better, the surfaces are improved, there is less need for rework, the execution is more rational, and we get more homogeneous concrete which gives better durability.

1.1.1 Self-Compacting Concrete Definition

The British Standard *(BS EN 206-9, 2010)* defines "SCC is the concrete that is able to flow and compact under its own weight; fill the formwork with its reinforcement, ducts, box outs etc, whilst maintaining homogeneity".

(EFNARC, 2005) defines 'Self-compacting concrete (SCC) is an innovative concrete that does not require vibration for placing and compaction. It is able to flow under its own weight, completely filling formwork and achieving full compaction, even in the presence of congested reinforcement'.

Other researchers *(Ozawa et al., 1989; Bartos and Marrs, 1999; Khayat, 1999)* have defined SCC in almost the same terms as a highly flow-able concrete that should meet the following requirements:

- Flow-ability: SCC should flow under its own weight and fill all parts of formwork without any external aid or vibration.
- Passing ability: SCC should pass through heavy reinforcing steel bars.
- Segregation resistance: SCC should maintain its homogeneity without any migration or separation of its large components (aggregates or/and fibers).

1.1.2 Advantages of Using Self-Compacting Concrete

- Eliminating need of vibration
- Reducing the noise pollution
- Easy placement and filling

- Better surface finish
- Reduce manpower and construction time
- Decrease permeability and improve the quality
- Improve durability
- Higher Strength
- The ability to cast narrow and confined zones where it could be difficult or impossible to cast and compact conventional type concretes.
- Economic advantages with SCC are essentially linked to changes to construction processes; the ability to reduce the number and skill level of operatives achieved through the removal of the compaction process *(Damtoft et al, 2008; Goodier, 2003; Bernabeu, 2000).*

However, also mention the possible disadvantages of using SCC compared with conventional concrete can include the high cost of materials which can subsequently be overcome by the low cost of labor. Another disadvantage can be related to the nature of SCC, because of its high fluidity, handling and transporting SCC becomes a bit delicate, although the outstanding results would definitely overcome these disadvantages.

1.1.3 How Self-Compacting Concrete Differs From Vibrated Concrete

SCC consists of cement, aggregates, water and admixtures which are quite similar to the composition of conventional vibrated concrete, however, the reduction of coarse aggregates, the large amount of fines, the incorporation of super-plasticizer, the low water to cement ratio, is what led to self-compact ability. The specific mix design of SCC, which guarantees its self-compacting ability in fresh state, inevitably influences the performance of hardened concrete. For instant, the higher control of fine aggregates (by adding fillers) affects the whole micro-structure, making the interfacial transition zone of SCC stronger and consequently increasing the compressive and tensile strength, compared to vibrated concrete with the same w/c ratio.

1.1.4 Global Growth of Self-Compacting Concrete

Europe and Sweden, was the first region outside Japan to begin development of SCC *(Holton, 2004)*. Consequently development spread throughout the rest of Europe, initially

with other Scandinavian countries, France and the UK all becoming key developers, with a number of other major European countries undertaking some level of research *(Holton, 2004)*. It is difficult to determine who the world leader in the development is currently and use of SCC *(Damtoft et al., 2008)*.

Historically, the development of SCC began within academia in Japan with the first reference to a modern SCC in 1992 *(Ozawa, 1992)*. Development transfer from academia to the research departments of large construction companies followed *(Goodier, 2003*). Industrial development of SCC led to the commencement of major construction projects utilizing and employing SCC, moving the material from design to reality *(Goodier, 2003)*. Early projects which adopted SCC included the construction of the Akashi Kaiko Bridge anchor blocks (The Concrete Society and BRE, 2005) and part of a large LNG (Liquid Natural Gas) tank owned by the Osaka Gas Company *(Kitamura, 1999).* Initial research and development in Europe was driven by the creation of several task groups, such as the RILEM Technical Committee, who were set up to review current SCC technology. Swedish trials led to the creation of the Brite-EuRam project group, tasked with establishing a vibration-free production system in order to reduce the cost of insitu concrete construction *(Goodier, 2003*). European development continued with research being led by the University of Paisley, including several European trade Introduction 11 groups‡ 1.3.4 SCC IN THE UK, to address the lack of test methods and standards *(Holton, 2004; Goodier, 2003).* The result was the specification and guideline document, "The Guidelines for Self-Compacting Concrete" (2005). The guidelines covered details from engineering properties and constituent materials to the specification and placement of SCC. Following this work began on developing a supplement for European Standard EN 206 (2000) to address the additional concerns regarding the conformance of SCC with existing standards. The standard was subsequently published in 2010 as "EN 206 Part 9: Additional Rules for self-compacting concrete" (2010).

1.1.5 Applications of Self-Compacting Concrete

The past decade has witnessed a rapid development of self-compacting concrete (SCC) and its frequent use in many construction applications. Nowadays, SCC forms vital parts of infrastructure and substructures in the world that can be exposed to external

environmental attack. In particular, medium strength SCC has been used widely for various precast concrete elements and it is planned for many other applications *(Viacava et al., 2012).* This widespread use of medium strength SCC could increase the probability of its exposure to severe natural environments. With the extensive use of this type of concrete, it is becoming increasingly difficult to ignore the influence of its microstructure and hydration on the durability. SCC is applicable for the production of architectural and textures surfaces.SCC is applicable in case of containment vessels, chimneys, nuclear reactors, storage structure like water tank, crude oil storage tanks etc. it is applicable in highways, tunnel linings, under water concreting, high rise buildings, bridges and repair of concrete building.SCC is applicable where poring of concrete only of single point is possible.

Dragon Bridge (2012), Alcalá De Guadaira, Seville, Spain. This spectacular 124 m long bridge, distributed in four spans, stands out due to its unique shape. The concrete structure represents a dragon that seems to emerge from the Guadaira river in the province of Seville.

Burj Khalifa (2010) at over 828 meters (2,716.5 ft) and 166 stories, in Dubai holds the record of the tallest building and free standing structure in the world with the largest number of stories. Self-compacting concrete is playing a greater role in high-rise construction to overcome the problem of congested reinforcement and ease of placement.

The Sodra Lanken (1997) 800 million dollar Project in Sweden notably was one of the largest infrastructure projects that used SCC. The six kilometres long four-lane highway in Stockholm involved seven major junctions, and rock tunnels totalling over 16 km partly lined with concrete and over 225,000 cubic meters of concrete. Incorporating SCC was ideal to cope with the density of reinforcement required and the highly uneven rock surfaces.

The Ritto Bridge on the New Meishin Expressway in Japan. The highest pier is 65-meter high. High strength concrete and reinforcements, of which specified compressive strength and yield strength are 50 MPa and 685 MPa respectively, were applied to the construction of the pier to meet the earthquake resistance. Arrangement of reinforcement

was very dense; therefore SCC was chosen to obtain good workability for the pier construction.

Kaiga Project, (India) to reduce the cycle time and to enhance quality, the innovative concept of self compacting concrete (SCC) is being considered in large scale for the construction work of Kaiga- 3&4.

1.2 INDUSTRIAL BY-PRODUCTS

It is obvious that the level of annual aggregate production has a significant impact on the environment. It is our responsibility to reduce consumption of natural mineral resources and to increase the use of secondary materials *(Milicevic et al., 2016).* Since the industrial revolution, industrial operations have been accompanied by a problem: industrial waste which may be toxic, ignitable, and corrosive. Waste management is very difficult problem and in the near future an important task will be to increase recycling and economic utilization while lowering storage *(Smarzewski and Hunek, 2016).* If not properly managed, this waste can pose dangerous health and environmental consequences. Environmental pollution is a global problem. Unsustainable production of goods, improper treatment of the waste, emissions to air and water, and inadequate legislation causes growing problems to human beings and nature. The urgent need for reducing environmental load coming from industry, and communities demands for novel ways of thinking. The productive use of industrial solid waste is the best way to alleviate the problems associated with their disposal. The use of industrial by products is an important factor in the economics of many industries. Concrete could be a viable solution to environmental problems since it is also possible to re-use solid by-products from other industries for concrete production (Tittareli and Moriconi, 2010). The industrial by-products can be utilized depending upon their physical and chemical properties. Industrial by-products can use in construction industry as full or partial replacement with fine and coarse aggregates based upon their properties. The use of waste materials in concrete, compressive strength increase and chloride permeability decreases *(Mishra et al., 1994).* Instead of wasting construction material (recycled aggregates), good concrete can be produced with the use of recycled coarse aggregates *(Rakshvir and Barai, 2006).* Compressive strength, splitting tensile strength and modulus of elasticity increase on the

incorporation of stone dust as fine aggregates *(Sahu et al., 2003). Cachim et al. (2014)* observed that because of increasing environmental concerns and sustainable issues, the utilization of solid waste materials is the need of the hour. The shortage of natural aggregates in some parts of the world and current environmental policies have made the reuse and recycling of C&DW a very attractive solution *(Gayarre et al., 2017).*

Earth's natural resources are finite and face increasing human pressure. Over the last few decades, concern has been growing about resource efficiency and the environmental impact of material consumption. The construction industry is responsible for the consumption of a relevant part of all produced materials, however, only recently has this industry started to worry about its environmental impacts *(Torgal, 2014).*

With the increased industrialization, generation of industrial by-products has increased significantly. There are many types of industrial by-products depending upon the industry given in Table 1.1. Utilization of such types of by-products has become an enormous challenge *(Siddique and Bannacer, 2012),* such solid industrial by-products such as coal bottom ash, marble dust, foundry sand, slag, waste plastic, glass waste, ceramic waste, crusher stone dust, recycled aggregates etc. have been tried as replacement of aggregates in the production of concrete. These are very beneficial for concrete industry and environment. Government should provide incentives for using and managing industrial solid waste materials in more eco-friendly manners *(Regev et al.,2014).*

Table 1.1: Different industrial by-products used in self-compacting concrete

Ingredients of Concrete	Industrial By-Products (Replacement)
Cement (Binder)	Fly Ash Silica Fume Metakaolin Granulated Blast Furnace Slag Municipal Solid Waste Incinerator Ash Rice Husk Ash Wood Ash Cement Kiln Dust Marble Dust
Fine Aggregates (Sand)	Waste Foundry Sand Coal Bottom Ash Steel Slag Marble powder Copper Slag Boiler Slag Quarry Dust Manufactured Sand Iron Slag
Coarse Aggregates	Crushed Glass Rubber Aggregates Marble Waste

1.2.1 Waste Foundry Sand

Foundry industry produces a large amount of by-product material during casting process. The ferrous metal casts in foundry are cast iron and steel, non ferrous metal are aluminum, copper, brass and bronze. Over 70% of the total by-product material consists of sand because moulds usually consist of molding sand, which is easily available, inexpensive, resistance to heat damage, easily bonded with binder, and other organic material in mould. Foundry industry use high quality specific size silica sand for their molding and casting process. This is high quality sand than the typical bank run or natural sand. Foundries successfully recycle and reuse the sand many times in foundry.

When it can no longer be reused in the foundry, it is removed from the foundry, and is termed as "foundry sand" (*Khatib and Ellis, 2001)*. It is also known as spent foundry sand (SFS) and used-foundry sand (UFS).

Waste foundry sand are by-products which appears to possess the potential to partially replace regular sand as a fine aggregate in concretes, providing a recycling opportunity for them. If such types of materials can be substituted partly/fully for natural sand (fine aggregates) in concrete mixes without sacrificing or even improving strength and durability, there are clear economic and environmental gains. Currently, very limited literature is available on the use of these by-products in concrete. Waste foundry sand (WFS) is one of the major issues in the management of foundry waste. WFS are black in color and contain large amount of fines. The typical physical and chemical property of WFS is dependent upon the type of metal being poured, casting process, technology employed, type of furnaces (induction, electric arc and cupola) and type of finishing process (grinding, blast cleaning and coating). Physical properties and chemical composition of foundry sand is given in Table 1.2 and 1.3 respectively.

Table 1.2: Physical properties of waste foundry sand

Property	Naik et al. (2001)	Guney et al. (2010)	Siddique et al. (2011)
Specific gravity	2.79	2.45	2.61
Fineness modulus	2.32	-	1.78
Unit Weight (kg/m^3)	1784	-	1638
Absorption (%)	5.0	-	1.3
Moisture content (%)	-	3.25	-
Clay lumps and friable particles	0.4	-	0.9

Table 1.3: Chemical composition of foundry sand

Constituent	Value (%)		
	Guney et al. (2010)	Etxeberria et al. (2010)	Siddique et al. (2011)
SiO_2	98	95.10	78.81
Al_2O_3	0.8	1.47	6.32
Fe_2O_3	0.25	0.49	4.83
CaO	0.035	0.19	1.88
MgO	0.023	0.19	1.95
SO_3	0.01	0.03	0.05
Na_2O	0.04	0.26	0.10
LOI	-	1.32	2.15

1.2.2 Coal Bottom Ash

Coal bottom ash and boiler slag are the coarse, granular, incombustible by-products that are collected from the bottom of furnaces that burn coal for the generation of steam, the production of electric power, or both. The majority of these coal by-products are produced at coal-fired electric utility generating stations, although considerable bottom ash are also produced from many smaller industrial or institutional coal-fired boilers and from coal-burning independent power production facilities. The type of by-product (i.e., bottom ash or boiler slag) produced depends on the type of furnace used to burn the coal.

At present, India is the 3rd largest consumer of coal. Approximate 410 million tons of coal is burnt in thermal power plants annually. They are the main source of production of coal ash. Indian coals have higher ash content up to 40% based upon the source of coal and results in large volume of coal ash. Physical properties and chemical composition of coal bottom is given in Table 1.4 and 1.5 respectively.

Table 1.4: Physical properties of coal bottom ash

Physical Property	Value		
	Kim et al. (2005)	Singh and Siddique, (2014)	Yuksel and Genc (2007)
Specific gravity	2.32	1.39	1.39
Water absorption (%)	-	31.58	6.10
Fineness modulus	-	1.37	-

Table 1.5: Chemical composition of coal bottom ash

Chemical composition	Value (%)		
	Yuksel and Genc (2007)	Baite et al. (2016)	Singh and Siddique (2014)
Silicon dioxide (SiO_2)	57.90	62.32	56.44
Aluminum oxide (Al_2O_2)	22.60	27.21	29.24
Iron oxide (Fe_2O_3)	6.50	3.57	8.44
Calcium oxide (CaO)	2.00	0.5	0.75
Magnesium oxide (MgO)	3.20	0.95	0.40
Sodium oxide (Na_2O)	0.086	0.7	0.09
Loss of ignition (LOI)	2.40	-	0.89

1.2.3 Steel Slag

Steel slag, a by-product of steel making, is produced during the separation of the molten steel from impurities in steel-making furnaces. The slag occurs as a molten liquid melt and is a complex solution of silicates and oxides that solidifies upon cooling. Virtually all steel is now made in integrated steel plants using a version of the basic oxygen process or in specialty steel plants (mini-mills) using an electric arc furnace process. The open hearth furnace process is no longer used. In the basic oxygen process, hot liquid blast furnace metal, scrap, and fluxes, which consist of lime (CaO) and dolomitic lime (CaO, MgO or "dolime"), are charged to a converter (furnace). A lance is lowered into the converter and high-pressure oxygen is injected. The oxygen combines with and removes the impurities in the charge. These impurities consist of carbon as gaseous carbon monoxide, and silicon, manganese, phosphorus and some iron as liquid oxides, which

combine with lime and dolime to form the steel slag. At the end of the refining operation, the liquid steel is tapped (poured) into a ladle while the steel slag is retained in the vessel and subsequently tapped into a separate slag pot. There are many grades of steel that can be produced, and the properties of the steel slag can change significantly with each grade. Grades of steel can be classified as high, medium, and low, depending on the carbon content of the steel. High-grade steels have high carbon content. To reduce the amount of carbon in the steel, greater oxygen levels are required in the steel-making process. This also requires the addition of increased levels of lime and dolime (flux) for the removal of impurities from the steel and increased slag formation. Physical properties and chemical composition of steel slag is given in Table 1.6 and 1.7 respectively.

Table 1.6: Physical properties of steel slag

Properties	Value		
	(www.fhwa.dot.gov)	Maruthachalam and Palaniamy (2014)	Shalabi et al. (2016)
Specific gravity	3.2- 3.6	2.89	3.2
Unit weight (kg/m^3)	1600 - 1920	1611	-
Absorption (%)	Up to 3%	1.90	4.5

Table 1.7: Chemical composition of steel slag

Chemical composition	Value (%)		
	Netinger et al. (2013)	Sabapathy et al. (2106)	Ahmer et al. (2016)
Silicon dioxide (SiO_2)	17.08	13.81	7.40
Aluminum oxide (Al_2O_2)	5.40	2.53	30.55
Iron oxide (Fe_2O_3)	25.45	28.93	19.14
Calcium oxide (CaO)	24.98	36.96	21.82
Magnesium oxide (MgO)	10.58	7.46	11.67
Sodium oxide (Na_2O)	0.12	0.057	-

1.2.4 Copper Slag

Copper slag is a by-product of copper extraction by smelting. During smelting, impurities become slag which floats on the molten metal. Slag that is quenched in water produces angular granules which are disposed of as waste or utilized. Copper slag, which is produced during pyrometallurgical production of copper from copper ores, contains

materials like iron, alumina, calcium oxide, silica etc. For every tone of metal production about 2.2 ton of slag is generated. Dumping or disposal of such huge quantities of slag cause environmental and space problems. During the past two decades attempts have been made by several investigators and copper producing units all over the world to explore the possible utilization of copper slag. Physical properties and chemical composition of copper slag is given in Table 1.8 and 1.9 respectively.

Table 1.8: Physical properties of copper slag

Properties	Value		
	Brindha et al. (2010)	Madheswaran et al. (2014)	Srinivas and Muranal (2015)
Color	Black and glassy	Black and glassy	Black and glassy
Specific gravity	3.91	4.12	3.44
Hardness	6 to 7 Moh's scale	-	-
Absorption (%)	0.3 to 0.4%	-	0.19%

Table 1.9: Chemical composition of copper slag

Chemical composition	Value (%)		
	Brindha et al. (2010)	Madheswaran et al. (2014)	Srinivas and Muranal (2015)
Silicon dioxide (SiO_2)	25.84	27-33	37.26
Aluminum oxide (Al_2O_2)	0.22	<3	3.95
Iron oxide (Fe_2O_3)	68.29	<10	47.45
Calcium oxide (CaO)	0.15	1-3.5	2.38
Magnesium oxide (MgO)	0.22	-	-
Sodium oxide (Na_2O)	0.58	-	0.65

1.2.5 Marble Powder

Marble cutting industry produces large amounts of solid wastes on large areas, which are expected to increase as construction is continuously increased, owing to the fact that the world production of marble industry has been increasing annually in the recent years. All natural stones including marble, granite and slate, which can be cut to sizes, polished and used for construction purposes, are referred to as dimensional. Dimensional stones are

characterized by aesthetics/acoustics and practicality in use. Marble is a crystalline, compact variety of metamorphosed limestone, consisting primarily of calcite (CaCO3), dolomite (CaMg (CO3)2) or a combination of both minerals.

In India, marble processing industry generates around 7 million tons of wastes mainly in the form of powder during sawing and polishing processes. These are dumped in the open which pollute and damage the environment. The pollution issue is a serious cause of concern in the state of Rajasthan since there are around 4000 marble mines and about 1100 marble cutters in medium sector spread over 16 districts of Rajasthan. Out of the total waste generated in India, contribution from Rajasthan state itself is 95% of the total accounting to 6 million tons annually. Chemical composition of marble sludge powder is given in Table 1.10.

Table 1.10: Chemical composition of marble powder

Chemical composition	Value (%)		
	Hameed and Sekar (2009)	Omar et al. (2012)	Aliabdo et al. (2014)
Silicon dioxide (SiO_2)	64.86	14.08	1.12
Aluminum oxide (Al_2O_2)	4.45	2.69	0.73
Iron oxide (Fe_2O_3)	11.99	1.94	0.05
Calcium oxide (CaO)	1.58	42.14	83.22
Magnesium oxide (MgO)	6.13	2.77	0.52
Sodium oxide (Na_2O)	2.08	0.91	1.12

1.2.6 Quarry Dust

Quarry dust is a byproduct of the crushing process which is a concentrated material to use as aggregates for concreting purpose, especially as fine aggregates. In quarrying activities, the rock has been crushed into various sizes; during the process the dust generated is called quarry dust and it is formed as waste. So it becomes as a useless material and also results in air pollution. Therefore, quarry dust should be used in construction works, which will reduce the cost of construction and the construction material would be saved and the natural resources can be used properly. Most of the

developing countries are under pressure to replace fine aggregate in concrete by an alternate material also to some extent or totally without compromising the quality of concrete. Quarry dust has been used for different activities in the construction industry, such as building materials, road development materials, aggregates, bricks, and tiles. Physical properties and chemical composition of quarry dust is given in Table 1.11 and 1.12 respectively.

Table 1.11: Physical properties of quarry dust

Properties	Value	
	Balamurgan and Perumal	Rai et al. (2014)
Color	Black	
Specific gravity	2.57	2.54
Bulk density	1850	1800
Absorption (%)	-	1.2
Fineness modulus	2.41	-

Table 1.12: Chemical composition of quarry dust

Chemical composition	Value (%)	
	Hameed and Sekar (2009)	Ilangovana et al. (2008)
Silicon dioxide (SiO_2)	62.48	62.41
Aluminum oxide (Al_2O_2)	14.45	18.72
Iron oxide (Fe_2O_3)	6.99	6.54
Calcium oxide (CaO)	4.58	4.83
Magnesium oxide (MgO)	3.14	2.56
Sodium oxide (Na_2O)	Nil	-

1.2.7 Boiler Slag

Boiler slag is a by-product produced from a wet-bottom boiler, a special type of boiler designed to keep bottom ash in a molten state before it is removed. These types of boilers (slag-tap and cyclone boilers) are much more compact than pulverized coal boilers used by most large utility generating stations. They can burn a wide range of fuels and generate a higher proportion of bottom ash than fly ash (50 to 80% bottom ash vs. 15 to 20% bottom ash for pulverized coal boilers). These are some of the reasons they are

typically used by industrial manufacturing plants and smaller utilities. With wet-bottom boilers, the molten ash is withdrawn from the boiler and allowed to flow into quenching water. The rapid cooling of the slag causes it to immediately crystallize into a black, dense, fine-grained glassy mass that fractures into angular particles, which can be crushed and screened to the appropriate sizes for several uses such as in concrete manufacturing. Since boiler slag is angular, dense and hard, it is often used as a wear-resistant component in surface coatings of asphalt in road paving. Finer-sized boiler slag can be used as blasting grit and is commonly used for coating roofing shingles. Other uses include raw material for the manufacture of cement and in colder climates, it is spread onto icy roads for traction control.

1.2.8 Manufactured Sand

Manufactured sand is a substitute of river for construction purposes sand produced from hard granite stone by crushing. The crushed sand is of cubical shape with grounded edges, washed and graded to as a construction material. The size of manufactured sand (M-Sand) is less than 4.75mm. Manufactured sand is an alternative for river sand. Due to fast growing construction industry, the demand for sand has increased tremendously, causing deficiency of suitable river sand in most part of the word. Due to the depletion of good quality river sand for the use of construction, the use of manufactured sand has been increased. Another reason for use of M-Sand is its availability and transportation cost. Since this sand can be crushed from hard granite rocks, it can be readily available at the nearby place, reducing the cost of transportation from far-off river sand bed. Thus, the cost of construction can be controlled by the use of manufactured sand as an alternative material for construction. The other advantage of using M-Sand is, it can be dust free, the sizes of m-sand can be controlled easily so that it meets the required grading for the given construction.

1.2.9 Iron Slag

Iron slag is non-metallic product consisting essentially of silicates and alumino-silicates of calcium and other bases that is "developed in a molten condition simultaneously with iron in a blast furnace." In addition the blast furnace is the primary means for reducing iron oxides to molten, metallic iron. It is continuously charged with iron oxide sources

(ores, pellets, sinter), flux stone (limestone and dolomite), and fuel (coke). Molten iron collects in the bottom of the furnace and the liquid slag floats on it, and both are periodically tapped from the furnace. The other important point slag consists primarily of the impurities from the iron ore (silica and alumina), combined with calcium and magnesium oxides from the flux stone. Sulfur and ash that may come from the coke will also be contained in the slag, which comes from the furnace as a liquid at temperatures about 1500°C. It is a man-made molten rock, similar in many respects to volcanic lavas. There are many different types of iron slag, some were produced by smelting, others by smithing; some are large, some so tiny they are invisible to the naked eye when in the soil, some are magnetic, others not. Generally the blast-furnace slag in cement began to develop, fears arose that the sulfur in slag could oxidize and cause expansion of the concrete, that it could generate acid and corrode the reinforcing steel. These fears were transferred to aggregate usage with the idea that adjacent metals or concrete could be attacked, more ghosts were raised - the voids in slag could cause failures in freezing and thawing, the presence of magnesia might result in the formation of expansive periclase and disrupt structures; "falling" slag might fall or disintegrate after incorporation in structure rather than at the time of cooling, none of these horrible things have happened in a century of use of more than one and one-half billion tons of blast-furnace slag in the U.S. It is doubtful that any such disasters took place anywhere, the specifications for slag’s in many countries impose unnecessary and unreasonable restrictions designed to prevent something that has never occurred in practice. Such restrictions have a habit of spreading, and finding application in one area solely because it is customary that such a limit should be imposed and it really doesn't do any harm – all of the available slag pass the test, in the case of aggregates area unnecessary requirements can, and do in some countries, prevent the use of perfectly usable materials sometimes because of efforts to make slag fit the requirements believed reasonable for natural aggregates. The Blast-furnace slag is a different material, different in particle shape, mineralogy, porosity characteristics, and density.

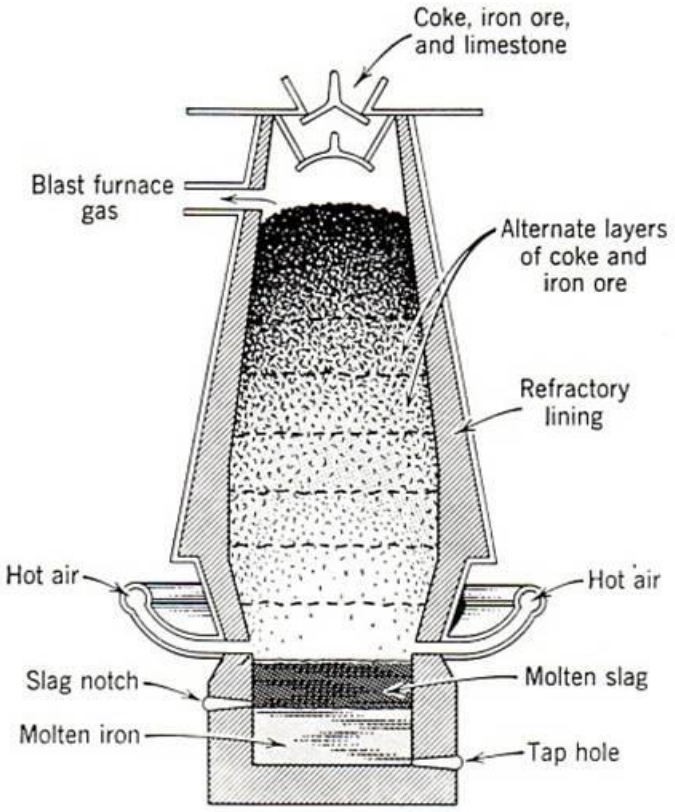

Fig 1.1: Production of iron slag in blast furnace

1.2.9.1. Production

The amount of slag tapped from the furnaces is not routinely measured and not all of the slag formed is tapped during a heat; accordingly, data on annual production of slag are generally unavailable. Output levels can, however, be estimated broadly based on typical slag to metal production ratios, which in turn are related to the chemistry of the ferrous feeds to the furnaces, but it is estimated that annual world iron slag output in 2014 was on the order of 310 to 370 million tons, and steel slag about 170 to 250 million tons, based on typical ratios of slag to crude iron and steel output *(Hendrik, 2014).*

As per the report of the working group on cement industry for the 12th Plan about 10 million tons of iron slag produced annually in India. The main source of production is metallurgical industry.

1.2.9.2. Consumption and Price

Hiltunen (1998) reports that iron slag is almost 100% reused in most countries and steel slag 75-80% reused. The principal uses for the latter are in civil engineering, road construction and the cement industry. As per Indian bureau of mines, India, report (2013-2014), blast furnace slag in India is used mainly in the cement manufacture, depending upon the quality; the slag is used in the range of 70% in the manufacture of Portland slag cement (PSC) and in other unorganized work, such as, landfills and railway ballast. A small quantity is also used by the glass industry for making slag wool fibers.

The prices of iron slag vary from plant to plant. As per the information available with Indian bureau of mines (IBM), the price of blast furnace slag, during 2012-13, varied from Rs.350 to Rs.974 per ton. Depending upon the distance between cement plants and the steel plants, much variation is observed in prices of furnace slag.

1.2.9.3. Physical Properties

Iron slag has angular, irregular, porous and rough textured particles. The particles of iron slag range from fine sand to fine gravels. Iron slag has particles appearance and particle size distribution similar to river sand. Particles of iron slag have interlocking characteristics. Iron slag is light and more brittle than river sand. Physical properties of iron slag are given in Table 1.13.

Table 1.13: Physical properties of iron slag

Property	Value	
	Ouda and Gawwad (2015)	Raharjo et al., (2013)
Appearance	Black, glassy	-
Unit weight (kg/m^3)	1870	1809
Specific gravity	2.71	-
Clay and fine materials (%)	19.60	-

1.2.9.4 Chemical Composition

Chemical composition of waste iron slag depends on the type of metal molded, type of binder and combustible used. 20 % of the total mass in iron production is formed into

slag. Different slags are a result of different cooling methods applied. Chemical composition of iron slag is given in Table 1.14.

Table 1.14: Chemical composition of iron slag

Constituents	Value (%)		
	Monshi and Asgarani (1999)	Raharjo et al., (2013	Ouda and Gawwad (2015)
Silicon dioxide (SiO_2)	36.80	35.67	8.20
Aluminium oxide (Al_2O_3)	9.84	3.62	2.12
Iron oxide (Fe_2O_3)	1.50	41.39	38.89
Calcium oxide (CaO)	35.80	6.12	39.52
Magnesium oxide (MgO)	1.88	4.27	0.88
Sodium dioxide (Na_2O)	0.15	0.81	-
Sulfur trioxide (SO_3)	1.08	1.83	0.24
TiO_2	4.85	-	0.22
LOI	4.45	-	3.45

1.2.9.5. Environment Impact

The current method of disposal of iron slag dumping in open area poses dangerous to human health and to environment. The industrial wastes, in general, are disposed off in wet form into open area, which not only occupy vast tracts of valuable cultivable land but also create environmental pollution and ecological problems.

The utilization of the industrial solid wastes in concrete production will not only help in solving the environmental pollution problems associated with the disposal of these wastes but also help in conservation of natural resources (such as limestone, sand etc.) which are fast depleting. The other benefits to cement industry include lower cost of cement production and lower green house gas emission per ton of cement production. This may also enable cement industries to take benefits of carbon trading.

1.2.9.6. Applications

Iron slag can be beneficially utilized in a variety of manufacturing construction applications, such as:

- As a blending material for the manufacture of slag cement, super sulphated cements, pozzolana metallurgical cement.
- Non-Portland cement.
- Manufacture of expansive cement, oil well,
- Colored cement and high early-strength cement In refractory and in ceramic as sital.
- As a structural fill (air-cooled slag).
- As aggregate in concrete.
- Land filling
- Road making.
- Railway ballast.
- Paving bases Patching pot holes.
- High stress applications i.e. storage yard, heavy vehicles parking loads. Where native ground is incapable of withstanding heavier loads.
- Ready mix concrete.
- Concrete blocks.
- Pipe bedding.
- Concrete admixtures

1.3 FLY ASH

During the combustion of pulverized coal in suspension-fired furnaces of modern thermal power plants, the volatile matter is vaporized and the majority of the carbon is burned off. The mineral matter associated with the coal, such as clay, quartz and feldspar disintegrate or slag to varying degree. The slaged particles and unburned carbon are collected as ash. The coarser particles fall in the bottom of the furnace and are collected as bottom ash or boiler slag. The finer particles that escape with flue gases are collected as fly ash using cyclone separators, electrostatic precipitators or bag houses. Depending upon the collection system varying from mechanical to electrical precipitators or bag houses and

fabric filters, about 85 to 99.9% of the ash from the flue gases is retrieved in the form of fly ash. Fly ash, accounts for 75 to 85% of the total coal ash, and the remainder is collected as bottom ash or boiler slag. Fly ash because of its mineralogical composition, fine particle size and amorphous character is generally pozzolanic and in some cases also self cementitious. The bottom ash and boiler slag are much coarser and are not pozzolanic in nature. It is thus important to recognize that all the ash is not fly ash and the fly ashes produced by different power plants are not equally pozzolanic and, therefore, are not always suitable for use as mineral admixture in concrete.

The amount of fly ash released annually by thermal plants all over the world around 780 million tons. The amount of fly ash released annually by thermal plants in India is above 100 million tons and the percentages use in concrete is 25% (approx.) of the total cementitious material.

1.3.1 Classification

ASTM – C 618-93 categorizes natural pozzolans and fly ashes into the following three categories: -

1. Class N Fly ash: Raw or calcined natural pozzolans such as some diatomaceous earths, opaline chert and shale, stuffs, volcanic ashes and pumice come in this category. Calcined kaolin clay and laterite shale also fall in this category of pozzolans.

2. Class F Fly ash: Fly ash normally produced from burning anthracite or bituminous coal falls in this category. This class of fly ash exhibits pozzolanic property, but rarely if any, self-hardening property.

3. Class C Fly ash: Fly ash normally produced from lignite or sub- bituminous coal is the only material included in this category. This class of fly ash has both pozzolanic and varying degree of self cementitious properties. (Most class C fly ashes contain more than 15 % CaO. But some class C fly ashes may contain as little as 10 % CaO.

1.3.2 Physical Properties

Physical properties of fly ash are given below:

Partial morphology: fly ash particles usually consist of spongy aggregate and clear glassy spheres ranging in diameter from 1 to 150 micron, the majority being less than 44 micron as seen under dispersive x-ray analysis.

Fineness: Fineness is one of the primary physical characteristics of fly ash that relates to its pozzolanic activity. A large fraction of ash particles is smaller than 3μm in size. In bituminous ashes, the particle sizes range from less than 1 to over 100μm.

Specific gravity: Specific gravity of fly ash is related to shape as well as chemical composition of particles. Specific gravity of fly ash usually varies from 1.35 to 4.7. Coal particles with some minerallic impurities have specific gravity in between 1.3 to 1.6.

1.3.3 Chemical Properties

Chemical properties of fly ash are given in Table 1.15.

Table 1.15: Chemical properties of fly ash

Constituents	Value (%)		
	Brouwers & Eijk (2003)	Ismail et al. (2007)	Omran et al. (2017)
Silica (SiO_2)	51.96	59.00	52.4
Iron oxide (Fe_2O_3)	4.65	3.70	8.3
Alumina (Al_2O_3)	25.89	21.00	27.2
Calcium oxide (CaO)	2.83	6.90	4.5
Magnesium oxide (MgO)	1.82	1.40	0.96
Total sulphur (SO_3)	0.08	0.07	-

1.3.4 Morphology

The study carries out by Tanikella and Olek, (2010) indicates that relatively smaller number of un-burnt carbon particles, which is consistent with higher LOI values in class F ashes, many hollow particles present, particles with rugged surface is generally magnetic, wide range of spherical particles.

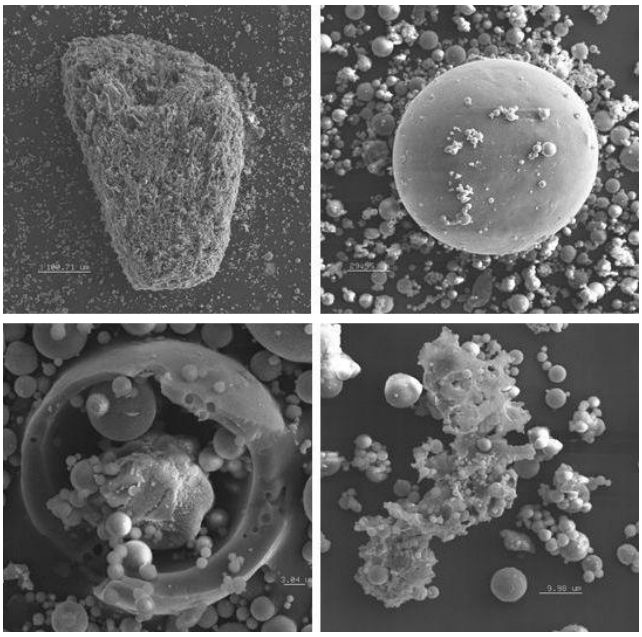

Fig 1.2: SEM images of fly ash (Tanikella and Olek, 2010)

1.3.5 Applications

Fly ashes are widely used in project backfilling, road engineering, concrete or mortar projects, bricks and insulating materials. The grinded ash and compound ash have become the essential components of the pump concrete because of its excellent flow ability and low hydration heat.

1.4 SIGNIFICANCE IN RESEARCH AREA

With ever increasing quantities of industrial by products and waste material, solid waste management has become the principal environment concern globally. The utilization of such material in concrete not only makes it economical, but also do help in reducing disposal problems. One of such by product is iron slag (IS). Slag is a partially vitreous by-product of the process of smelting ore, which separates the desired metal fraction from the unwanted fraction. Slag is usually a mixture of metal oxides and silicon dioxide. However, slag can contain metal sulfides and metal atoms in the elemental form. The slag is molten by-products of high temperature processes that are primarily used to separate the metal and non-metal constituents contained in the bulk ore. When cooled, the molten slag converts to granular material. In India, million tons of IS generated. Not much work

has been reported on strength, and especially durability aspects of self-compacting concrete made with iron slag.

1.5 GAP IN THE RESEARCH AREA

The advancement in recycling and using industrial processes for utilizing waste will lead to better use of world resources. In the exiting research in the area of iron slag as fine aggregates in concrete, the strength parameters has been considered as the prime objective but has not been reported extensively ever from strength point of view, not to mention of durability aspects. In the proposed research proposal, SCC using iron slag as fine aggregates would be studied for the strength and durability parameters so that its suitability for use in SCC could be established.

1.6 RESEARCH OBJECTIVES

- Development and characterization of SCC containing iron slag as partial replacement of fine aggregates.
- To study the strength properties of SCC mixes containing iron slag.
- To study the durability properties of SCC mixes containing iron slag.
- SEM & XRD characterization of SCC mixes Containing iron slag.
- To carry out comparative study of strength and durability properties for the selected concrete mixes.

1.7 METHODOLOGY

To achieve the above objectives research was undertaken in four stages: -

First Step, review the mix design procedures of SCC and find the easiest way for the concrete production. Self-compacting concrete (SCC) mixes of varying strengths and performances were developed to meet the flow-ability, passing ability and segregation resistance criteria. The design of SCC mixes making of new recipes is done mainly by trial and error approach using the slump cone, L-box, U-box and V-funnel tests on trial

mixes, until the mix was found that met the flow-ability and passing ability criteria and had no visible signs of segregation.

Second step, review the existing accelerated test for strength and durability properties of self-compacting concrete and choose the appropriate methods. Then conduct the tests for strength and durability properties and comparing the results with existing literature.

Third Step, SEM and XRD analysis were conducted on SCC mixes to characterize the pore structure of self-compacting concrete at all stages of age (7, 28, 91 and 365 days) and all replacement levels (10, 25 and 40%) of sand with iron slag.

Fourth Step, statically analysis was done for strength and durability properties.

1.8 ORGANIZATION OF THE THESIS

The thesis is presented in the five chapters as detailed below:

Chapter-1 Introduces about self-compacting concrete, applications of self-compacting concrete, iron slag, applications of iron slag, fly ash, applications of fly ash.

Chapter-2 Presents literature review and presents the work done by various researchers on self-compacting concrete with different mineral admixtures.

Chapter-3 Gives the details of experimental programme, materials used, techniques adopted for casting, curing, heating and testing of the specimens.

Chapter- 4 Deals with the discussion of results obtained from experimental data. The results are presented both in tabular as well as graphical form.

Chapter -5 Gives the major conclusions of the study.

A list of references referred to in this research work is presented after Chapter-5.

CHAPTER-2

LITERATURE REVIEW

This chapter details the review of published literature on self-compacting concrete, and use of industrial by products in self-compacting concrete.

2.1. REVIEW OF LITETARUTRE ON SELF-COMPACTING CONCRETE

Malathy et al. (2006) studied the development of mix design values for different grades of self-compacting concrete (SCC). A mix design of SCC had been developed following European Federation for Specialist Construction Chemicals and Concrete system (EFNARC) specifications. The mix design of SCC for different grades, M20 to M60 was developed and their flow parameters and strength properties were studied. Compressive strength of SCC was investigated after 7 and 28 days curing period and also the splitting tensile strength was got after 28 days curing. The grades had been developed for obtaining quantity of cement, fly ash and coarse aggregate required for different grades. From research it was concluded that flow properties of developed SCC for various grades were satisfying the recommended values. Also the quantity of cement required for SCC was about 5-20% less than that of normal concrete.

Sivarama et al. (2006) discussed the novel method of placing SCC by bottom up pumping in their study. It was the first innovative attempt in India, that L & T had developed a mechanism to pump the concrete from bottom up. An experimental trial had been made with M50 grade concrete and experimental data proved that concreting could be done by the novel method of bottom up which sets a new trend in construction practices in near future.

Domone (2006) analyzed the case study of eleven years of self-compacting concrete. The author analyzed the case studies of 68 applications of SCC, published from 1993 to 2003, the period of increasing widespread use of SCC in worldwide. The range of properties, component materials and mixture proportions indicated the diverse nature of SCC, and confirmed that it should be considered as a family of mixtures suitable for a wide range of applications to widely varying requirements.

Domone (2007) reviewed the hardened mechanical properties of SCC. Data from more than 70 recent studies on the hardened mechanical properties of SCC had been analyzed and correlated to produce comparisons with the properties of equivalent strength normally vibrated concrete (NVC). The significant scatter obtained in much of the data was a consequence of the wide range of materials and mixes used for SCC, but clear relationships had been obtained between cylinder and cube compressive strength, tensile and compressive strengths, and elastic modulus and compressive strength. It was also clear that limestone powder, a common addition to SCC mixes, made a substantial contribution to strength gain.

Aggarwal et al. (2008) evolved a procedure for mix design of the SCC. Their study presented an experimental procedure for the design of the SCC mixes. The test results for acceptance characteristics of the SCC such as slump flow, J-ring, V-funnel and L-Box were presented. Further, compressive strength at the ages of 7, 28, and 90 days were also determined and the results concluded that the SCC could be developed without using viscosity modifying admixtures and by using the OPC 43 grade, normal strength of 25 MPa to 33 MPa at 28 days was obtained, provided the cement content was kept around 350 kg/m^3 to 414 kg/m^3.

Aggarwal et al. (2008) predicted the compressive strength of the SCC with fuzzy logic. In the present research comparisons of fuzzy logic and neural network techniques for predicting the compressive strength for SCC mixtures was done. The authors concluded that the fuzzy logic model showed better performance than neural network model.

Peter et al. (2009) used SCC for under-reamed piles. An experimental study conducted at the Structural Engineering Research Centre (SERC), Chennai, clearly demonstrated the control on geometry of self-compacting concrete under reamed piles when cast against soil form work. Three piles made of SCC and three of conventional vibrated concrete having similar strength, were cast and tested to evaluate their dynamic and static behavior. The authors had observed the similar performance of SCC and conventional vibrated concrete piles under dynamic action.

Sengupta et al. (2009) studied the influence of aggregate characteristic on the uniformity of SCC. According to the author the property that was affected by the aggregate characteristics was passing ability. The size and gradation of coarse aggregate, along with the presence of flaky and elongated particles, were factors that affect passing ability, and thus the uniformity of SCC. In the present research an attempt was made to analyze the influence of aggregate characteristics on the passing ability through a probabilistic model. The probabilistic model developed in this study allowed the mix designer to decide on the maximum allowable coarse aggregate content of a specific maximum size and gradation for a given blocking tolerance. The results of the experimental study showed that the fraction of large sized and longer aggregates decreased considerably as the SCC flowed through successive set of barriers.

Singh et al. (2012) carried out the investigation on fatigue analysis of plain and fiber reinforced SCC. The findings of the research showed significantly increased fatigue performance of self-compacting fiber reinforced concrete with enhanced sensitivity of fatigue lives to the change of applied stress.

Niewiadomski et al. (2015) studied the influence of additives (Nano-particles) on the physical and mechanical properties of self-compacting concrete. SCC concrete modified with different amounts of SiO_2, TiO_2 and Al_2O_3 additions. With the addition of SiO_2 and Al_2O_3 fluidity of SCC mixtures deteriorated and contrast and SiO_2 also beneficial for 28-days compressive of SCC as compared with reference concrete.

2.1.1 Properties of self-compacting concrete made with furnace slag

Boukendakdji et al. (2009) examined the fresh and strength properties of self-compacted concrete using Algerian furnace slag. In this research up to 25% of cement by weight was replaced by slag with 5% increment. Slump flow, V-funnel, U-box, J-ring test and 5mm sieve test were performed to access the fresh properties of SCC. Compressive test were done to access the strength of SCC. The result indicates that use of Algerian furnace slag in replacement with cement is good for fresh properties (workability) and compressive strength decreases with the increase of slag content.

Wang and Lin (2013) carried out an investigation on fresh and engineering properties of self-compacting concrete by the utilization of furnace slag with constant water cement ratio of 0.37 in which the part of cement replaced by furnace slag in mass ratio of 0, 15 and 30% and indicates that fresh concrete properties and compressive strength of self-compacting high strength concrete (SCHSC) made with 15% furnace slag is higher than control mix. Slag group has maximum shrinkage at 30% replacement and ultrasonic pulse velocity (UPV) of control group is close to that of 15% furnace slag group at the age of 28days and UPV of 30% furnace slag group is slightly lower.UPV increases with passage of time.

Valcuende et al. (2015) studied the performance of self-compacting concrete containing blast furnace slag as fine aggregates. A seven type of mixtures were made with constant water/cement ratio of 0.55 and different slag contents 0 to 60% with 10% increment. It was observed from the study that at early ages the compressive strength of SCC using granulated blast furnace slag as fine aggregates is similar to the SCC made with fine aggregates, but at 90 and 365 days, the strength is higher. Furthermore, SCCs with slag high autogenously shrinkage

2.1.2 Properties of self-compacting concrete made with ladle furnace slag

Anastasiou et al. (2014) carried out the investigations on ladle furnace slag (LFS) as filler and steel fiber as reinforcement and studied their effects on self-compacting concrete. Different dosage of ladle furnace slag, ranging from 60 to 120 kg/m3, and steel fiber, ranging from 0 to 7% were incorporated. Tests were conducted on different mixtures in fresh state, filling abilities, passing abilities and resistance to segregation and in hardened state for compressive strength, fracture toughness, freeze thawing, chloride penetration resistance. Test result indicates that LFS can be used to increase powder content in fiber reinforced SCC without compromising the self-compactability, strength and durability properties.

Sideris et al. (2015) studied the strength and durability properties of self-compacting concrete using ladle furnace slag as filler material. Different dosages of ladle furnace slag ranging 45 to 92.5 kg/m^3 were added. The durability properties were examined through

the measurement of chloride penetration resistance and carbonation depth. The depth was measured by spaying the fresh broken surfaces of concrete with phenolopthalcin indicator. Result indicated that use of ladle furnace slag improved the carbonation resistance up to 28% as compared with reference SCC mixtures and incorporating ladle furnace slag in SCC also improve the compressive strength and some extent.

2.1.3 Properties of self-compacting concrete made with copper slag

Soya et. al.(1999) carried out a study on self-compacting concrete properties with slag (ferronickel slag and copper slag) as fine aggregates replacement. In this research, the self compact-ability of fresh, mechanical and durability properties were test to conduct passing, filling ability test, compressive strength and splitting tensile strength, static modulus of elasticity, permeability, carbonation and shrinkage tests. It was observed that water demand increased as the slag content increases in SCC mixes but all fresh properties almost similar or bit higher than control SCC mix and furthermore it was concluded that copper slag as fine aggregates gives the promising results in the production of high performance self-compacting concrete.

Afshoon and sharifi (2014) examined the consequences of ground copper slag as substitutes of cement on fresh properties (slump flow, V-funnel, J-ring, L-box, air content, screen stability, segregation index, wet density and setting time) of SCC. A total of seven mixes were made with fix water-powder ratio at replacements of 0-30% with 5% increment by weight of cement. The author had observed with increasing the ground copper slag dose as cement replacement, slump flow increases, viscosity was decreased, passing ability was decreased, air content decreased and setting time increased. Copper slag can be used beneficially as cementing material in self-compacting concrete.

Fadaee et al. (2015) investigated the fresh and strength properties of self-compacting concrete incorporating copper slag at 20, 25, 30, 35 and 40% replacement of cement by weight. Tests were conducted at 7, 14, 28 and 42 days to evaluate compressive strength at all replacement levels. The fresh properties of SCC were studied through the measurement of J-ring and V-funnel. The results show that copper slag is better in case of workability parameters and study also show that by using copper slag, the 28 days

compressive strength of SCC samples was almost same as the samples without copper slag but replacement of copper slag instead of cement causes reduction of compressive strength for the percentage above 20% at different ages.

2.1.4 Properties of self-compacting concrete made with steel slag

Yoo et al. (2005) carried out the investigation on the fresh and strength properties of self-compacting fabricated with atomized steel slag as fine aggregates replaced with sand and compared with control self-compacting concrete. In this research slum flow, U-box, time of slump flow tests was conducted to evaluate the fresh properties and compressive strength for hardened properties. Result shows that SCC incorporating atomized steel slag has good workability parameters due to its spherical shape and approximately same or more compressive strength as compared with conventional SCC.

Pen and Hwang (2010) study the performance of self-compacting concrete incorporating carbon steel slag (5, 7.7, 10% replacement) as partial replacement of Portland cement. SCC mixtures were made with different water cement ratio of 0.28, 0.32 and 0.40 and different super-plasticizer dosage. The test results for acceptance characteristics of SCC as slump flow and setting time were presented in this study. Furthermore, compressive strength, ultrasonic pulse velocity and micro-structure were also conducted. Test results indicates that concrete using carbon steel slag has higher compressive strength that using Portland cement, at 0.32 and 0.40 water/cement ratio compressive strength improved by 21%at 90 days. The SEM images indicated that the hydration rate of carbon steel slag SCC is lower that SCC made with Portland cement. The results of this research showed that carbon steel slag can potentially used as cementitious material in SCC.

Kothai and Malathy (2012) investigated SCC with levels up to 40% of fine aggregate replacement by steel slag in mixtures adjusted to grade M20 to M40. The fresh and mechanical properties of self-compacting concrete and relationship between hardened properties were then studied. To study the behavior of SCC in fresh state slump flow, V-funnel and L-ox test were performed and found the satisfactory results. Furthermore, hardened properties of SCC were investigated with or without the use of steel slag by conducting compressive strength, tensile strength and flexural strength tests. The test

results showed that significantly increased the strength properties up to 40% replacement of steel slag with fine aggregates.

Sheen et al. (2015) investigated that the properties SCC made with stainless steel reducing slag (SSRS). Two different kinds of SSRS, being in the different surface area 1766cm^2/g and 7979cm^2/g were incorporated as filler and cement substitution respectively. Six mixture proportions by replacing ordinary Portland cement varying from 0% to 50% with 10% increment were made for research work. The passing and filling ability of fresh mixture were observed by conducting slump flow, V-funnel and box filling tests and the hardening and durability parameters such as compressive strength, ultra-sonic pulse velocity, water absorption , rebound hammer and sulphate resistance were estimated. As SRSS incorporation in SCC for OPC of 20% or less, the slump flow were found more than the control group with 0% SRSS, afterwards inclusion of SRSS more than 20% giver lower values as compared with control group in case of slump flow. V-funnel and box filling height were mostly achieved the requirements of SCC incorporating with SRSS replacing for OPC up to 50%. The ultra-sonic pulse velocity values for 28 days (4500 m/s) indicates the excellent quality of SCC up to 30% incorporation of SRSS with replacement of OPC and furthermore, water absorption at all replacement levels meets the acceptance range after seven days of curing and absorption was lowest for mix with 30% SRSS. More than 40% incorporation of ultra-fine SRSS in SCC mixtures was effects the setting time.

Sheen et al. (2016) examined the effect of utilizing oxidizing and reducing slag obtained from stainless steel making as sand on the engineering concrete properties. The oxidizing slag was used as fine and coarse aggregates substituting of natural material with up to 100% replacement and reducing slag partially replaces Portland cement up to 30% with 10% increment. In this research all engineering properties (compressive strength, sulphate resistance, ultra-sonic pulse velocity and rebound hammer) were comparable with control mix and it could save cost up to 43% with 100% substitution of stainless steel oxidizing slag as coarse aggregates and 30% part of stainless steel reducing slag substitutes to Portland cement in SCC.

2.1.5 Properties of self-compacting concrete made with electric arc furnace slag (EAF)

Tomasiello and Felitti (2010) examined the fresh and hardened properties of self-compacting concrete incorporating eclectic arc furnace (EAF) slag. EAF slag replaced 30% of the crushed lime stone aggregate with size 4-8mm. Five mixes (SSC1, SCC2, SCC3, SCC4 and SCC5) with approximate constant water and super-plasticizer dosage (150-160 liters water and 6-8 liters of super plasticized by weight of cement) were prepared to evaluate the properties of SCC with or without the replacement of EAF. SCC1 and SCC2 do not contain EAF slag they contain limestone and fly ash. The results indicated that no segregation and bleeding for the mixtures. Slump flow and J-ring tests were conducted to evaluate the fresh properties of SCC all values shows satisfactory results (600-750mm). Whereas a decline in compressive strength at all ages is observed in this study after addition of EAF slag in SCC.

Santamaria (2015) reviewed the properties of SCC containing electric arc furnace slag as fine aggregates and concluded that concrete fabricated with EAFS as an aggregate has at least the same mechanical properties and durability as concrete with natural aggregates. Self-compacting mixes have been successfully performed using EAFS as a heavy aggregate. Even the use of LF slag in low proportions can be admissible, producing a delay in the increase of mechanical strength. The global results in terms of mechanical strength are promising. The use of EAFS aggregate contributes little to drying shrinkage.

2.1.6 Properties of self-compacting concrete with waste glass

Kou and Poon (2009*)* investigated the effects of recycled glass (RG) cullet on fresh and hardened properties of self-compacting concrete A total of four SCC mixes were produced, these included one control mix, and three mixes made with RG to replace 10mm granite (at 5%, 10% and 15% levels), and river sand (at 10%, 20% and 30% levels), respectively. From each concrete mix, fifteen 100 mm cubes were cast for the determination of compressive strength. The compression testing machine was used with a loading capacity of 3000 KN. The loading rates applied for the compressive and tensile

splitting tests were 200 KN/min and 57 KN/min, respectively. The compressive strength test was carried out at the ages of 1, 4, 7, 28 and 90 days and found satisfactory results.

Shakhmenko et al. (2010) observed that the concrete mixes containing ground glass has more tacky consistency in comparison with conventional concrete mix. Mixtures with glass require little bit more water for obtaining the similar workability. Glass powder additionally was ground 15, 30, 45 and 60 minutes in planetary ball mill. Prepared material was used for mix making in amount 80 kg in cubic meter Produced samples were tested after 7 and 28 days, compressive strength results. The first laboratory mix (SCC1) Self-compacting concrete is filled with traditional micro filler dolomite powder. In second mix (SCC2) traditional micro filler is completely replaced by glass powder. Third mix contains additionally ground (60 min.) glass powder. Micro filler content 190 kg in cubic meter is constant for all 3 mixtures. It must be emphasized, that traditional concrete mix consistency determination methods (for example cone slump method) are inapplicable for Self-compacting concrete. In this case new consistency determination methods are used: cone flow test and L-box test. These methods indicate mix flowing and self-leveling capacity, these methods are approved as future European standards. Concrete mixes with glass powder are characterized with good flow ability, high homogeneity and reduced segregation risk. SCC2 concrete containing raw glass powder has 11% lower compressive strength then concrete SCC1 with dolomite powder. Additionally, ground glass powder increases strength by 11 % comparing to standard mix.

Wang and Huang (2010) investigated the properties of self-compacting glass concrete (SCGC), where liquid crystal glass sand (0%, 10%, 20%, and 30%) is used in place of aggregates. The unit cementing material can be obtained by W/B and the mixing water content. The amount of cementing material in this study was 661 kg/m3, with the cement partially replaced by fly ash and slag. The mixing water content was adjusted to 185 kg/m3, according to the test results. Because the waste LCD glass is hydrophobic with a smooth surface, a large amount of adhesive paste is required to promote the waste LCD glass sand. The SCGC compressive strengths of each group increased with time. Compressive strength increased similarly at 7 days and 28 days. At 90 days, with a glass replacement of 30%, the compressive strength reached 98.4% of the control group's

compressive strength; the smooth surface of the glass sand allowed more cement paste to participate in adhering the glass to the cement mortar, thereby enhancing the concrete strength. The compressive strength of the concretes containing waste LCD glass aggregates decreased with an increase in LCD glass content. The concrete containing 20% waste glass aggregates resulted in the highest strength properties.

Liu (2011) observed that with an increase of glass content in self-compacting concrete, the weight of concrete mixes decrease because the specific gravity of glass is lower than that of cement and sand. The influence of inclusion of glass as both cement and sand's substitute in SCCs that an increase in the glass content and the water/powder ratio lead to the decrease in all hardened properties from early to late ages, with greater reductions for the higher replacement ratios. Depending on the water/powder ratio, glass types and glass content, the 28-d compressive strength obtained varies from 58 to 75 MPa.

Ling et al. (2012) studied the effects of recycled glass on the fresh and hardened properties of self-compacting concrete. The self compacting glass concrete (SCGC) mixtures prepared with 0% to 100% of recycled glass (RG) and were maintained within the specific limit of 750 ± 50 mm by adjusting the dosage of super-plasticizer Furthermore, the increase in RG content tended to decrease the slump loss rate. This implies that the RG would be able to maintain the consistency of the fresh SCGC mixtures. As regards the blocking ratio, it was observed that without any difficulties, all the fresh SCGC mixtures were able to flow through the confined gaps and narrow opening areas of the L-box, and all the height ratios measured satisfied the minimum acceptance value of 0.80. For the GTM screen stability test, it was observed that the control SCC mixture without using RG tended to have higher resistance to segregation. As the RG content increased, the resistance to segregation reduced. This might be related to the impermeable property and smooth surface of RG which was prone to segregation. When the replacement of RG content reached 100%, a segregation ratio of 16.08% was obtained which was slightly higher than the maximum limit of 15% suggested by EFNARC.

Tersawy and Ali (2012) used recycled glass waste as partial replacement of fine aggregates in self-compacting concrete. Total eighteen concrete mixes were produced with different cement contents (350, 400 and 450 kg/m^3) at W/C ratio of 0.4. Recycled glass was used to replace fine aggregate in proportions of 0%, 10%, 20%, 30%, 40%, and 50%. The experimental results showed that the slump flow increased with the increase of recycled glass content. On the other hand, the compressive strength, splitting tensile strength, flexural strength and static modulus of elasticity of recycled glass of SCC mixtures were decreased with the increase in the recycled glass content. The results showed that recycled glass aggregate can successfully be used for producing self-compacting concrete

Vanjare and Mahure (2012) used glass powder to replace the cement content by three various percentages (5, 10 and 15%). The partial replacement with glass powder was carried out for three grades of concrete. All the ingredients were first mixed in dry condition. Then, 70% of the calculated amount of water was added to the dry mix and mixed thoroughly. Then, 30% of water was mixed with the super plasticizer. The results that the addition of glass powder in SCC mixes reduce the filling ability, passing ability and segregation resistance. The flow value is seen to decrease by an average of 1.30%, 2.5% and 5.36% for glass powder replacements of 5%, 10% and 15% respectively. Hence, the relative flow area reduced with increase in glass powder content, which is an indicator of a decrease in deformability of the mix. The V-funnel time, which is a representative of the filling ability of the mix, was observed to increase by an average of 6.21%, 15% and 22.54% for glass powder contents of 5%, 10% and 15% respectively. This increase in the V-funnel time indicates decreased values of relative flow time and thereby the higher viscosity (resistance to flow) for the mixes. The L-box value was also observed to follow a decreasing trend with an average variation of 1.5%, 3.20% and 5% for glass powder contents of 5%, 10% and 15% respectively

Sharifi et. al. (2013) carried out the research to investigate the effect of waste glass replacement with fine aggregates on self-compacting concrete properties. In the research, fine aggregates have been replaced with waste glass in six different mass ratios ranging 0% to 50%. Result indicates that the flow ability and passing ability parameters have

increased as the replacement of waste glass increases but strength properties (compressive strength, split tensile strength and flexural strength) of SCC mixtures containing waste glass content shown to decrease when replacement level increases.

2.1.7 Properties of self-compacting concrete made with coal bottom ash

Siddique (2013) studied the fresh, hardened and durability properties of self-compacting concrete incorporating coal bottom ash as fine aggregates. In reference SCC mixture sand was replaced with coal bottom ash at various percentages such as 10%, 20% and 30%. Slump flow, j-ring, V-funnel, L-box and U-box tests were conducted to evaluate fresh properties, compressive strength for strength properties, abrasion resistance, rapid chloride permeability, water absorption and sorptivity tests were conducted to evaluate the durability parameters. Fresh properties were in the range at all replacement levels, compressive strength decrease with the increase of coal bottom ash content and rapid chloride permeability and abrasion resistance decreases with coal bottom ash inclusion but, water absorption and sorptivity of SCC mixes increase with the increase of coal bottom ash content.

Ibrahim et. al. (2015) carried out the investigation on split tensile strength and fresh properties of self-compacting concrete containing coal bottom ash as fine aggregates. In control SCC sand was replaced with 10%, 20% and 30% of coal bottom ash with variation of water-cement ratio 0.34, 0.40 and 0.45. Results indicate that replacement of coal bottom ash with sand average of slum flow, L-box ratio and percentage of segregation resistance decreased while coal bottom ash content increases and also splitting tensile strength decrease with the increase of coal bottom ash dose.

Siddique and Kunal (2015) conducted experimental program to examine the properties of self-compacting concrete (SCC) containing coal bottom ash (CBA). SCC mixtures were made with CBA as partial replacement of fine aggregates. Tests were conducted for slump flow, J-ring, V-funnel, L-box and U-box, compressive strength, splitting tensile strength, deicing salt surface scaling, carbonation and rapid chloride penetration resistance. Results indicated that, compressive and splitting tensile strength increased with the increase in age. Carbonation depth and deicing salt surface scaling weight loss

increased with the increase in CBA. SCC mixes made with CBA shows very low chloride permeability.

Awasthi and Mathews (2015) performed a experimental study to know the behavior of self-compacting concrete containing coal bottom ash at various replacement levels with fine aggregates to find the optimum dose of coal bottom ash. The various tests of fresh and hardened properties were conducted like compressive strength, flexural strength, splitting tensile strength and modulus of elasticity. It was observed from the results slump flow and L-box ratio decreased with the increase of coal bottom ash dose and same as in case of strength properties and concluded that 10% replacement of coal bottom ash with fine aggregates gives the maximum strength as compared with reference mix.

2.1.8 Properties of self-compacting concrete made with foundry sand

Sahmaran et al., (2011) reported the fresh properties such as flow ability, passing ability, segregation resistance of self-compacting concrete using spent foundry sand (SFS) and fly ash (FA). Sixteen self-compacting concrete mixtures were made. The Portland cement in the mixtures was replaced with Fly ash at 0, 30, 50 and 70% by mass. For each FA replacement level, about 0, 25, 50 and 100% of sand by volume was replaced with SFS. For all mixtures, the total amount of binder (PC + FA) and the water to binder ratio (w/b) were kept constant at 450 kg/m^3 and 0.40, respectively. Super-plasticizer dose was to secure the concrete be SCC considering the specifications of The European Guidelines for Self-compacting concrete. The results for slump flow diameter, slump flow time, V-funnel flow time, and rheological parameters (yield stress and relative viscosity) of the SCC mixtures satisfy the The European Guidelines for Self-compacting concrete. Moreover, no visible segregation or bleeding was observed in the fresh mixtures. Spread of 50FA-50SFS mixture which was a typical example of the uniform spread of SCC mixtures. Generally, for a given FA content, the super plasticizer requirement increases with SFS content for fresh properties like slump flow diameter .The conclusion, therefore, is that SCC with proper fresh properties can successfully be produced with SFS and FA.

Pathak and Siddique (2012) reported the results of laboratory findings of self-compacting concrete at elevated temperature made with spent foundry sand and fly ash. The influence of spent foundry sand as partial replacement with sand and influence of fly ash as replacement with cement was investigated. Results show that SCC produced adequate fresh properties with spent foundry sand and fly ash. Although spent foundry sand fly ash reduces the strength but it is possible to produces SCC with compressive strength ranging 30.69MPa at 28 days.

2.1.9 Properties of self-compacting concrete made with marble and tiles waste

Hameed et. al. (2012) investigate the strength and durability properties of SCC incorporating marble sludge powder and crushed rock dust as filler material replaced with fine aggregates. It was observed that utilization marble sludge dust (MSD) and crushed rock dust (CRD) wastes in SCC gives positive results. The inclusion of these wastes improves the physical and mechanical properties.

Tennich (2015) studied the fresh properties, mechanical prosperities and ultra-sonic pulse velocity of SCC with inclusion of fillers from marble and tile waste. Eight SCC mixtures were prepared with different water-cement, super-plasticizer dosage and various fillers like limestone, marble waste, marble tile waste. It was observed all fresh properties parameters (slump flow, L-box and V-funnel) are in range and the inclusion of marble filler positively affects the mechanical properties of SCC and also the combination of waste filler from marble industries improved the compactness of SCC.

CHAPTER-3

EXPERIMENTAL PROGRAM

This unit gives the detailed descriptions of laboratory tests for the measurements of fresh properties (slump flow, L-box, U-box, V –funnel), strength properties (compressive strength, splitting tensile strength, flexural strength and modulus of elasticity) and durability properties such as water absorption, rapid chloride permeability, sulphate resistance, sorptivity, ultra-sonic pulse velocity of self-compacting concrete mixtures prepared with varying percentages of iron slag as partial replacement of fine aggregates.

3.1. MATERIALS USED

3.1.1. Cement

Portland pozzolana 43 grade (fly ash based) cement was used. It was checked as per Indian standard specification (BIS: 8112:1989). Consistency, setting time (Initial and final), specific gravity, soundness and compressive strength were determined and shown in Table 3.1, SEM and EDS images are shown in Figs 3.1 and 3.2.

Table 3.1: Physical Properties of Portland Pozzolana Cement

Properties	BIS-8112-1989	Test Result
Compressive Strength (N/mm^2)		
7 day	22	25.2
28 day	33	44.8
Setting time (minutes)		
Initial	30 Min	79
Final	600 Max	273
Specific gravity	_	3.09
Standard Consistency (%)	_	34%
Soundness	10.0 Max	1.7

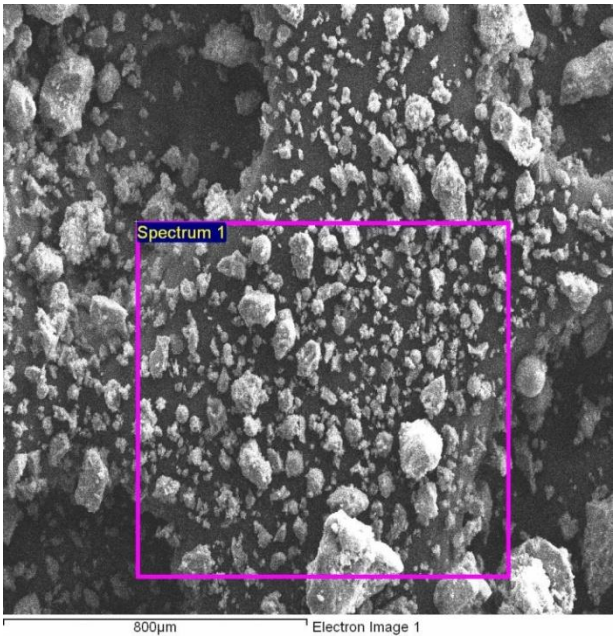

Fig 3.1: SEM morphology of ordinary Portland cement

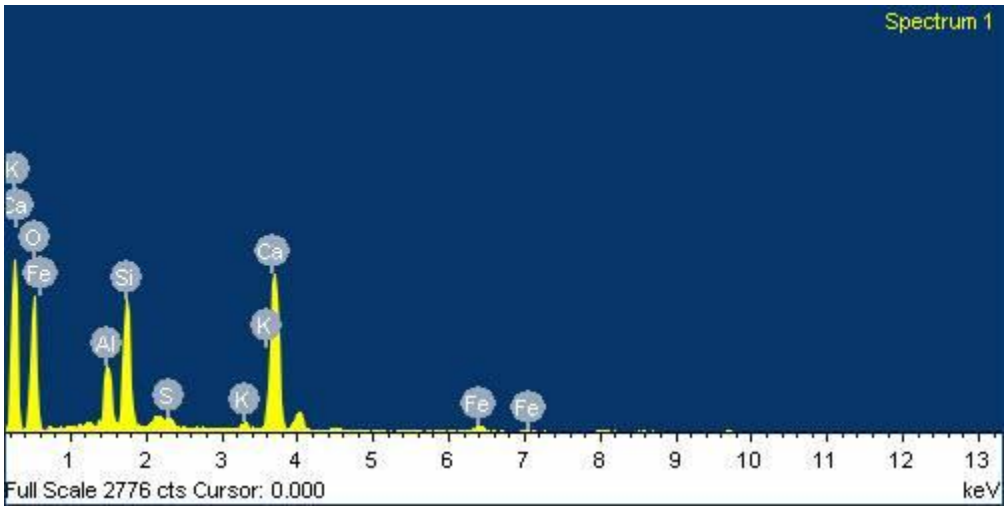

Fig 3.2: EDS spectrum of ordinary Portland Cement

3.1.2. Fine Aggregates

Locally available natural sand with 4.75mm maximum size was used as fine aggregate. Its physical properties and sieve analysis are given in Table 3.2 and 3.3 respectively.

Table 3.2: Physical properties of fine aggregate

Properties	Observed values
Bulk Density (Loose), kg/m^3	1670
Bulk Density (Compacted), kg/m^3	1875
Specific Gravity	2.57
Moisture content (%)	0.18
Material finer than 75µ (%)	0.6
Water absorption by mass (%)	3.65
Appearance	Light gray

Table: 3.3 Sieve analysis of fine aggregates

Weight of the sample taken = 1.0 kg

I.S. Sieve Size	Weight retained in grams	Percentage weight retained in grams	Cumulative percentage of weight retained	Percentage passing	IS: 383-1970 Requirement for Zone II
10mm	00	00	00	100	100
4.75mm	10	1.0	1.0	99	90-100
2.36mm	62	6.2	7.2	92.8	75-100
1.18mm	235	23.5	30.7	69.3	55-90
600µm	170	17	47.7	52.3	35-59
300µm	338	33.8	81.5	18.8	8-30
150µm	145	14.5	96.0	4.0	0-10
Pan	36	3.6	100	00	--

Fineness modulus of fine aggregate = 2.64

Sand conforms to grading zone II as per BIS: 383-1970

3.1.3. Coarse Aggregates

Crushed stone with maximum 12.5mm graded aggregates (nominal size) were used. Physical properties and sieve analysis results are given in Table 3.4and 3.5 respectively.

Table 3.4: Physical properties of coarse aggregates

Properties	Observed values
Maximum size (mm)	12.5
Bulk Density (kg/m^3)	1710
Specific Gravity	2.66
Total Water Absorption (%)	1.31
Moisture content (%)	Nil

Table: 3.5 Sieve analyses of coarse aggregates

Weight of the sample taken = 2.0 kg.

I.S. Sieve Size	Weight retained in grams	Percentage weight retained in grams	Cumulative percentage of weight retained	Percentage passing	BIS: 383-1970 Requirement
20mm	00	00	00	100	----
12.5mm	0.98	4.8	4.8	95.2	90-100
10mm	641	32.1	36.9	63.1	40-85
4.75mm	1183	59.2	96.1	3.9	0-10
Pan	78	3.85	100	00	----

Fineness modulus of coarse aggregate = 6.35

Coarse aggregates conformed to BIS: 383- 1970.

3.1.4. Fly Ash

Fly ash Class – F used as mineral admixture in this research work collected from Guru Har-Gobind Singh thermal power plant Lehar Gaga, Bathinda, Punjab, India. Fly ash is grey in color, particle size less than 45 micron. Physical and chemical properties are given in Table 3.6 and 3.7 respectively and SEM, EDS spectrum shown in Figs 3.3 and 3.4 respectively. The incorporation of fly ash reduces the need of super plasticizer necessary to obtain a similar slump flow compared with the concrete containing only cement as binder (Khatib, 2007). There is a need to replace cement in order to reduce global carbon dioxide emissions (Smarzewski and Hunek, 2016).

Table 3.6: Physical properties of fly ash

Physical properties	Value
Color	Grey
Specific gravity	2.13

Table 3.7: Chemical composition of fly ash (BIS: 3812-2003)

Constituents	% age by weight
Silica (SiO_2)	58.55
Iron oxide (Fe_2O_3)	3.44
Alumina (Al_2O_3)	28.20
Calcium oxide (CaO)	2.23
Magnesium oxide (MgO)	0.32
Total sulphur (SO_3)	0.07

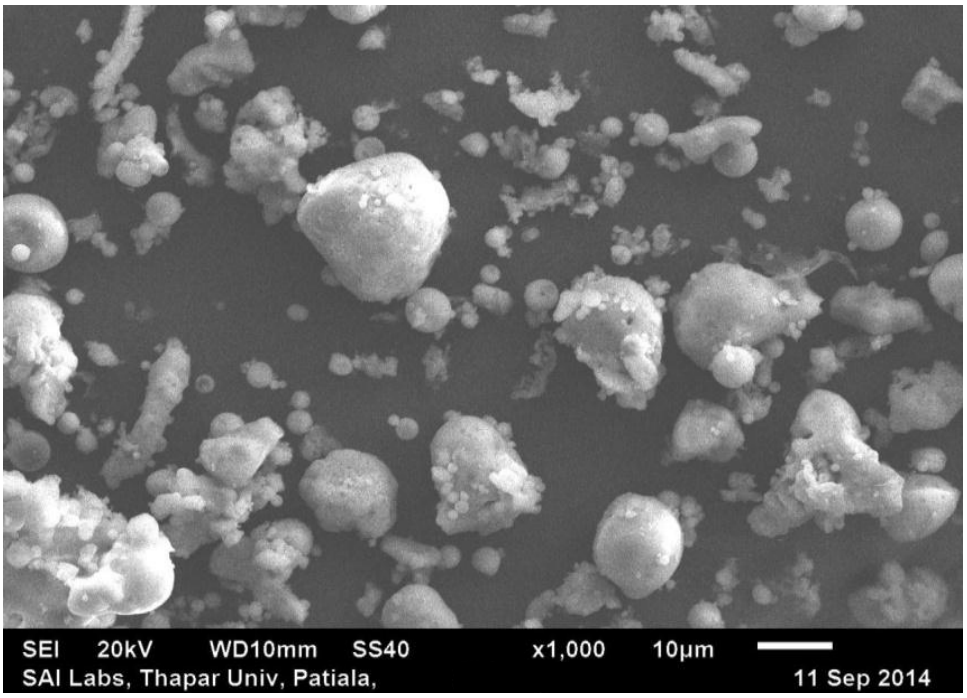

Fig 3.3: SEM morphology of fly ash

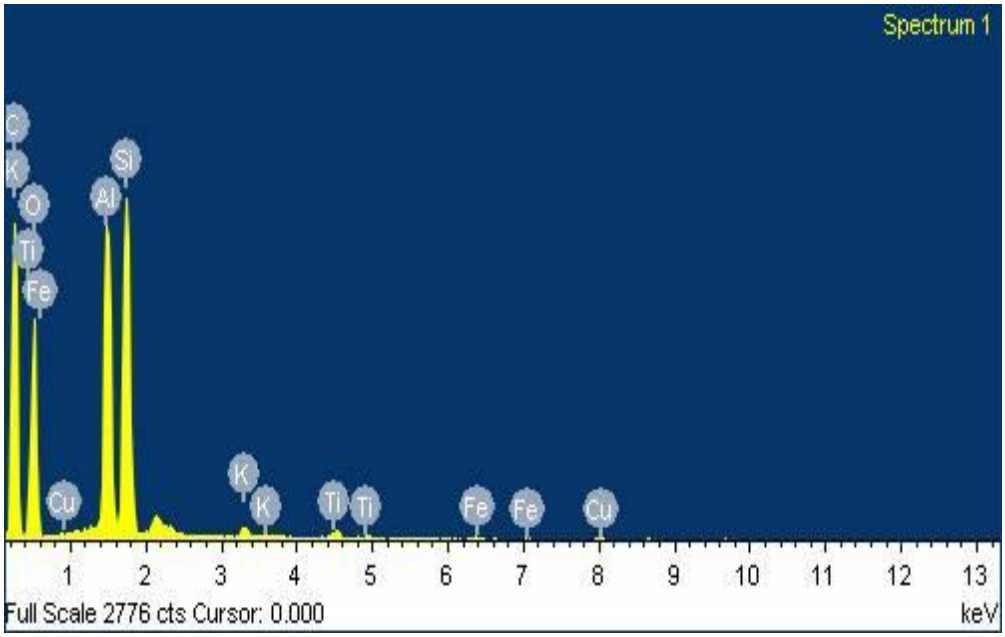

Fig 3.4: EDS spectrum of fly ash

3.1.5. Iron Slag

Iron slag was collected from Dhiman iron and steel rolling mills, Mandi-Gobindgarh, Fatehgarh Sahib, Punjab, India. Iron slag was screened to remove the oversized particle and material passing through 4.75mm sieve was used in manufacturing of concrete.

The major chemical compounds in iron slag are Fe_2O_3 (66.88%), SiO_2 (6.98%), Al_2O_3 (2.94%), CaO (0.8%), CO_2 (22.40%) and physical properties and sieve analysis of iron slag used in this research shown in Table 3.8 and 3.9. Iron slag is brittle and lighter than river sand. River sand and iron slag were dried in oven at 100° C for 24 hrs and then cooled down to room temperature before using in concrete. EDS spectrum shown in Fig 3.5 and grading of sand and iron slag particle shown in Fig 3.6

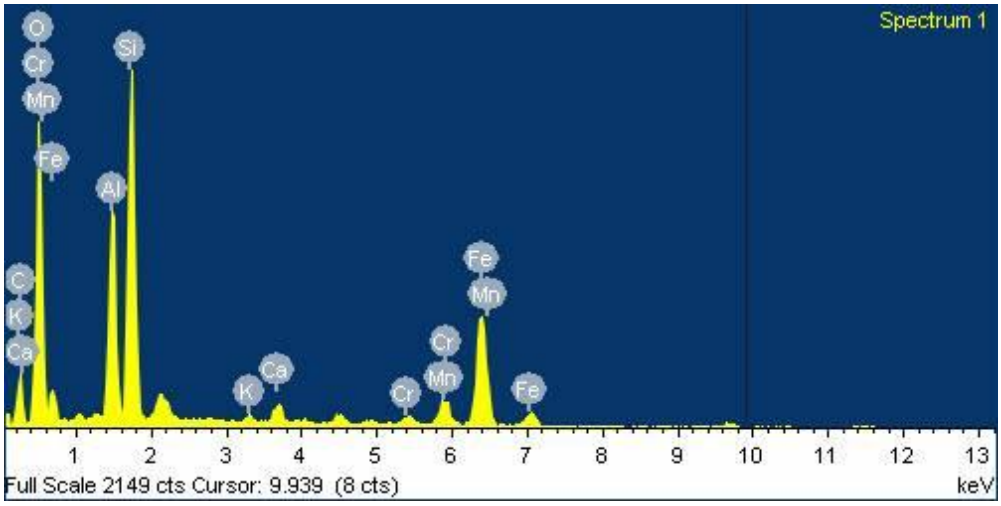

Fig. 3.5: EDS spectrum of iron slag

Table 3.8: Physical properties of iron slag

Property	Iron Slag
Specific gravity	2.49
Water absorption by mass (%)	18.54
Fineness modulus	2.41
Unit Weight (kg/m^3)	2000
Appearance	Black, glassy more vesicular when granulated

Table 3.9: Sieve analysis of iron slag

I.S. Sieve Size	Weight retained in grams	Percentage weight retained in grams	Cumulative percentage of weight retained	Percentage passing
10mm	00	00	00	100
4.75mm	00	00	00	100
2.36mm	52	5.2	5.2	94.8
1.18mm	197	19.7	24.9	75.1
600µm	149	14.9	39.8	60.2
300µm	360	36.0	75.8	24.2
150µm	195	19.5	95.3	4.7
Pan	47	4.7	100	00

Fineness modulus of iron slag 2.41

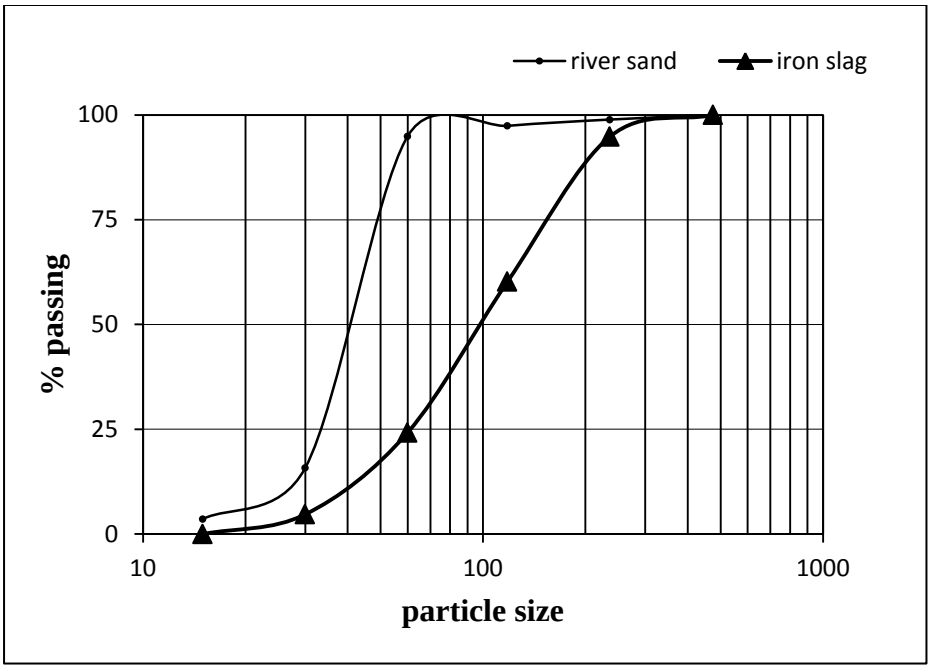

Fig. 3.6: Grading of sand and iron slag

3.1.6. Admixture

Auramix-400 low viscosity high performance super-plasticizer based on polycarboxylic technology used where high water reduction and long workability retention are required and it has been developed for use in SCC, pumper concrete and high performance concrete etc. it is light yellow colored liquid with 6.0 pH (min.) value and 0% chloride content.

3.1.7. Water

Potable tap water was used for casting and for curing of concrete specimens conforming to the requirements of BIS: 456-2000.

3.2. MIX DESIGN

Since its inception in 1980, self-compacting concrete was used for a variety of applications worldwide and not just due to its properties but also due to the possibility of usage in its composition of local materials. The composition of self-compacting concrete successfully incorporated material used for the production of conventional vibrated concrete, making it an attractive solution in the construction industry. It is indeed clear

that there is a big difference between the modes used for designing vibrated concrete and self-compacting concrete mixtures. While VC features a well organized methodology which renders robust mixtures, this is quite difficult to achieve for self-compacting concrete. The major difference is that self-compacting concrete accepts more combinations of material and reaches the same properties, yet these combinations oftentimes contain several variables. In order to properly obtain SCC, considerations such as the following must be taken into account:

1. Obtaining a universal SCC mixture is impossible due to the variation of properties for material used.

2. Obtaining a unique method to include all characteristics and requirements imposed by the use of local material for each individual application is also impossible;

3. Due to the increased number of variables compared to VC, self-compacting concrete requires higher attention for designing the mixtures.

Mix design in this research made by European Guidelines.

3.2.1. The European Guide for Self-Compacting Concrete [EFNARC, 2005]

The Guidelines were developed under a European project for promoting new types of concrete. This project was conducted from 1998 and included representatives of organizations such as: BIBM – The European Precast Concrete Organization; CEMBUREAU – The European Cement Association; ERMCO – The European Readymix Concrete Organization; EFCA – The European Federation of Concrete Admixture Associations and EFNARC – The European Federation of Specialist Construction Chemicals and Concrete Systems. This guide does not provide an actual sizing method for SCC mixtures rather presenting minimum and maximum values for the materials used (Table 3.10). However, the guidelines contain certain steps to be followed in order to achieve a quality self-compacting concrete. The values contained therein are not limitative but informative, with the possibility of also producing SCC mixtures by using quantities and percentages not falling exactly within the values provided by the guide.

Table 3.10: Optimum SCC quantities, [EFNARC, 2005]

Contituents	**Mass (kg/m^3)**	**Volume(litres/m^3)**
Fine part (addition)	360-600	-
Paste content	-	300-380
Water	150-210	150-210
Coarse aggregate	750-1000	270-360
Fine aggregate	The fine aggregate content depends on other materials, usually using 48-55% of the total aggregate weigh	
Water/fine part ratio	-	0.85-1.0

a. Selection of necessary specified performances.

b. Selection of materials to be used in the production of concrete - evaluation of the water content and optimizing paste slump and stability; - determination of suitable aggregate and additions proportions so the concrete provides and adequate robustness.

c. Mixture production - testing of concrete sensitivity to small variations and quantities used; - testing of fresh and hardened concrete properties.

d. Verifying and adjusting performances obtained in the laboratory. e. Evaluation for observing beneficiary needs a. If such are met, only a few concrete verifications are conducted on site;

e. If such are not met, a fundamental redesign of mixtures must be performed.

f. Depending on the problem occurred, one of the following measures may be taken into consideration:

i Modifying the cement/powder ratio and of the water/binder ratio;

ii. Changing the type of addition used;

iii. Modifying the proportion of fine aggregated and of the super-plasticizer dosage;

iv. The use of viscosity admixtures may be taken into account to reduce mixture sensitivity;

v. Modifying the quality of coarse aggregate used.

3.2.2. Mixture Proportions

SCC mixtures finalized on the bases of EFNARC guidelines. The control mixture was designed to achieve strength 36.25 N/mm^2 at the age of 28 days. Rivers sand was replaced with iron slag (10, 25 and 40%) by mass in SCC and 10% of fly ash replaced by cement. Fixed quantities of cement, fly ash and coarse aggregates i.e., 455 kg/m^3, 45 kg/m^3, 760 kg/m^3 respectively were used in concrete samples. Fixed water powder ratio of 0.44 and admixture of 1.2% by weight of powder were applied in all SCC mixes. Mix proportions of self-compacting concrete are given in Table 3.11.

Table 3.11: Mixture proportion of SCC

Mixture	Cement (kg/m^3)	Fly Ash (kg/m^3)	W/P ratio	Sand (kg/m^3)	IS (kg/m^3)	IS (%)	CA (kg/m^3)	Admixture (%)
SCC-CM	455	45	0.44	960	0	0	760	1.2
SCC-IS10	455	45	0.44	864	96	10	760	1.2
SCC-IS25	455	45	0.44	720	240	25	760	1.2
SCC-IS40	455	45	0.44	576	384	40	760	1.2
IS-Iron Slag (10, 25, 40 are the percentage replacement of iron slag with river sand), CM- control mix, CA-coarse aggregates,								

3.3. PREPARATION, CASTING AND TESTING OF SPECIMENS

Before casting, the entire test specimen were cleaned and oiled properly. These were firmly tightened to correct dimensions before casting. Care was taken that there is no gaps left from where there is any possibility of escape of slurry. The ingredients of concrete were mixed in 0.08cu-m capacity mixer. Immediately after casting of SCC mixtures were examined for fresh concrete properties by slump test, V-funnel test, U-box and L-Box. Besides measuring the fresh properties hardened state of SCC were tested on various properties mentioned in Table 3.12.

Table 3.12: Various properties with size of specimen and age of testing

Property	Reference Code	Age (days)
Properties of Fresh SCC		
Slump flow	EFNARC, 2005	Just after casting
L-box	EFNARC, 2005	Just after casting
U-box	EFNARC, 2005	Just after casting
V-funnel	EFNARC, 2005	Just after casting
Strength Properties		
Compressive strength	(BIS:516:1959)	7, 28, 91 and 365 days
Splitting tensile strength	(BIS:5816:1999)	7, 28, 91 and 365 days
Flexural strength	(BIS:516:1959)	7, 28, 91 and 365 days
Modulus of elasticity	(BIS:516:1959)	7, 28, 91 and 365 days
Microstructure & XRD phase identification	-	28, 91 and 365 days
Durability Properties		
Water absorption	ASTM C 642-06	7, 28, 91 and 365 days
Sorptivity	ASTM C 1585-04	7, 28, 91 and 365 days
Sulphate resistance Mass loss Compressive strength	ASTM C1012-10	28, 91 and 365 days
Rapid chloride permeability	ASTM C1202-10	7, 28, 91 and 365 days
Abrasion resistance	BIS-1237-2012	7, 28, 91 and 365 days
Ultra-sonic pulse velocity	ASTM C 597-02.	7, 28, 91 and 365 days

Fig. 3.7: Curing of SCC specimens

3.4. FRESH SCC PROPERTIES

3.4.1. Slump Flow Test

The slump flow spread, which is the diameter of the concrete after a standard slump test is the simplest and most popular test for the assessment of concrete flowability (or fluidity). For SCC, because of its good filling capacity, no tamping of the concrete is required. It is very important to know the factors influencing the slump flow spread. The super-plasticizer dosage, in relation to the water/powder ratio and powder content is the dominant factor, followed by the paste volume. Fig 3.8 shows that at constant super-plasticizer dosage the slump flow increases with reducing coarse aggregate content, and when both super-plasticizer dosage and coarse aggregate content are kept constant, slump flow increases with the reducing fine aggregate content. As a result of combining these two effects, slump flow increases with the paste volume. Other influencing factors include the maximum size and the shape and texture of the aggregate.

This method is the among the most popular methods used for assessing the properties of self-compacting concrete due to the relatively simple procedure and equipment, deriving from the slump flow test for conventional concretes described in the EN 12350-2 standard. This method covers issues concerning the deformability of fresh concrete by observing the flow rate and size under its own weight. It is recommended for use in testing concretes with an increased fluidity, whose components include super-plasticizers. It is not applicable to concretes prepared with aggregates with a maximum size exceeding 40mm [EFNARC, 2005].

Equipment s

The equipment used must comply with EN 12350-2: - Base bed with minimum sizes of 900 x 900mm and a minimum thickness of 2mm, made from a waterproof and rigid material (preferably steel); - Abrams Cone with inner diameters 100/200mm and a height of 300mm, according to ISO 4190.

Recorded parameters and interpretation

Slump (S) is determined as the arithmetic mean of the maximum diameter reached by concrete and the diameter perpendicular to it.

$$S = (d_{max} + d_{perp})/ 2$$

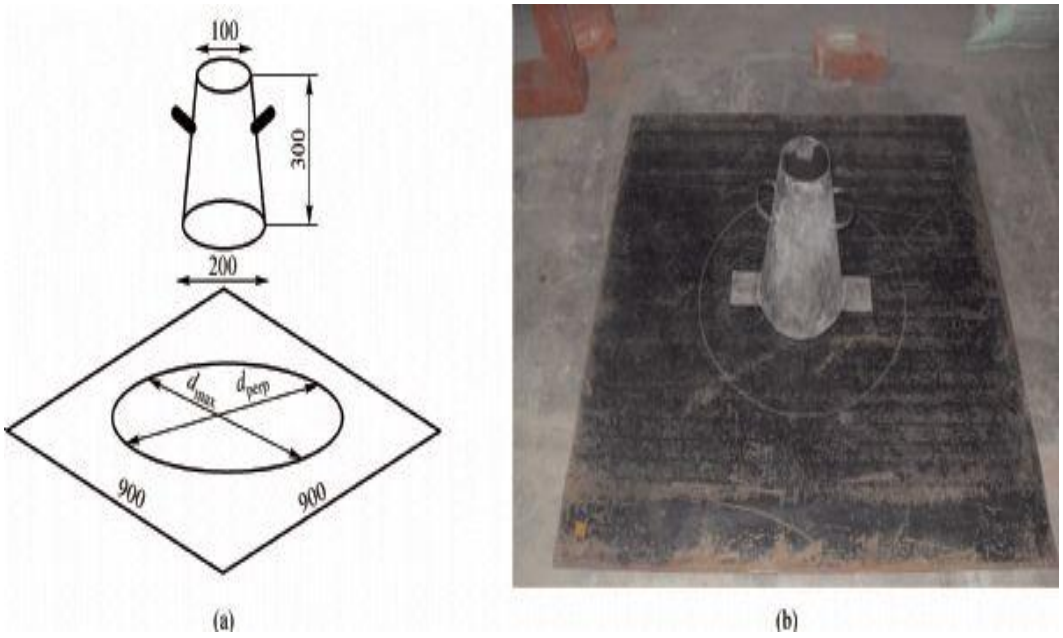

Fig. 3.8: Slump flow test setup

Classification of self-compacting concretes according to slump capacity.

The EFNARC European guidelines followed by the Eurocode 206-9. classify self-compacting concrete into 3 classes (SF1, SF2 and SF3) depending on the "S" parameter value which describes the slump of self-compacting concrete.

Table 3.13: SCC classifications depending on slump distance (EFNARC, 2005)

Class	Dia. (mm)	Applications
SF-1	550	Filling ability is low, oftentimes a concrete with values
	650	Unreinforced and poorly reinforced elements.
SF-2	660	Unreinforced and poorly reinforced elements.
	750	
SF-3	760	Is recommended for performance only if the maximum size of the aggregate used is 16 mm and is generally used for vertical applications in structures with reduced spacing between reinforcements and with complex formwork shapes
	850	It is recommended for prefabricated plants, having a greater flow rate and filling capacity, thus the element casting times can be reduced.
	>850	Values exceeding 850mm may only be achieved in special cases, however, the risk of concrete segregation and the maximum aggregate diameter must not exceed 12mm.

3.4.2. L-Box Test

This test was initially used in Japan to determine the characteristics of concretes about to be cast under water but is also applicable to concretes with high flow rate values such as SCC, thus becoming a typical method for self-compacting concrete. This test determines properties such as flow rate, ability to pass through tight spaces, the observation of a dynamic segregation is also possible.

Main parameters observed:

• Flow distance (maximum distance reached by concrete in the box) • Time necessary to reach a set distance (flow rate)

• Ultimate flow time • Segregation level (visual observation)

Equipment

Comprising of an L shaped box as described in Fig 3.9 two sizes may be used for the free spaces between reinforcements by variation of the reinforcement number, 2 bars for 59mm and 3 bars for 41mm.

Recorded parameters and interpretation

Passing ratio - is determined between two heights: H1 is the height of concrete at the tail end of the box, while H2 is the height of concrete at the opposite end. The ratio of these two parameters renders the ratio of concrete pass through described by equation

$$PR = H2/H1$$

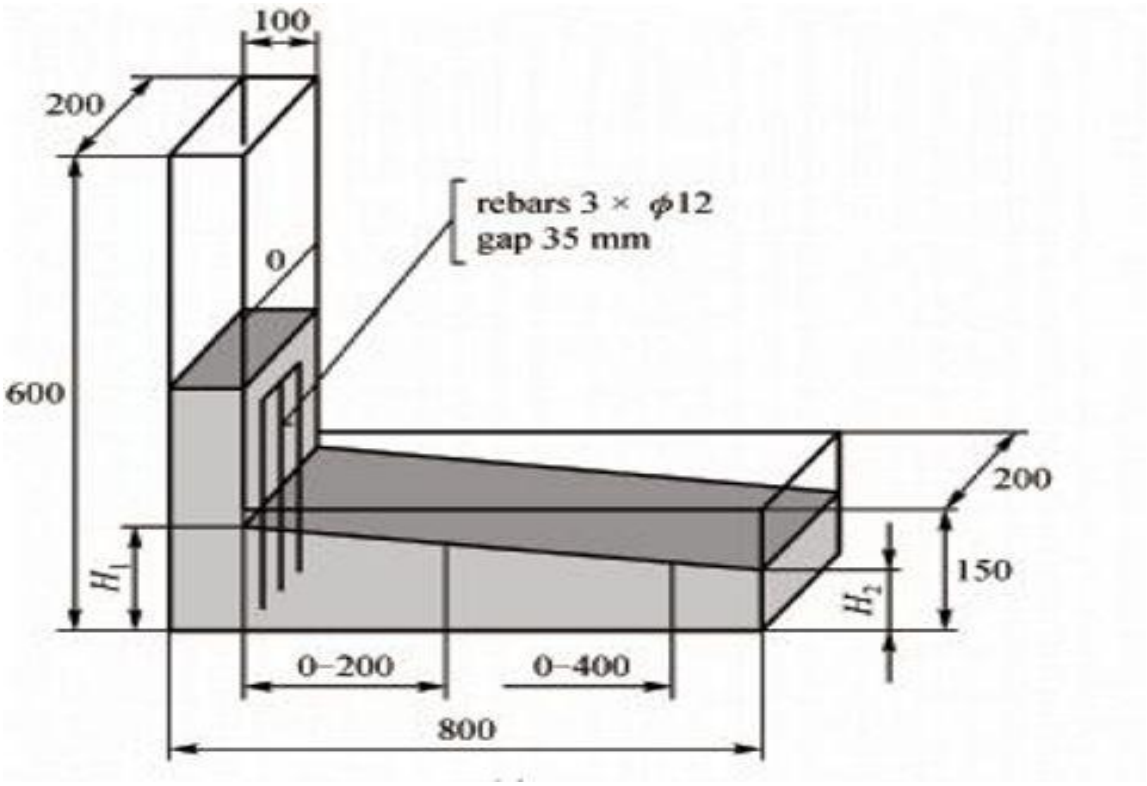

Fig. 3.9: L-box test

3.4.3. U-Box Test

U-box test is used for determine the flow ability of SCC through hurdles with coarse aggregates having the maximum size of less than 20 mm. The time and height to be

filled in the chamber band and the amount of aggregate passing through the obstacles are measured for self-compactability. The apparatus consists of a vessel that is divided by a middle wall into two compartments as shown in Fig 3.10. For performing the U-box test, one compartment of the apparatus was filled with the SCC sample and the filled concrete was left to stand for one minute. Then the sliding door was lifted up to allow the SCC to flow out into the other compartment. After the concrete comes to rest, the height of the concrete in the compartment that had been filled was measured in two places and the mean height (H1) was calculated. Also the height in the other compartment (H2) was Experimental Program 63 measured. The filling height was then calculated as H1-H2. The whole test had to be performed within five minutes. If the concrete flows as freely as water, at rest it will be horizontal, so H1- H2 = 0. Therefore, the nearer this test value, i.e., the 'filling height (H_f)', is zero, the better the flow ability and passing ability of SCC (EFNARC, 2005).

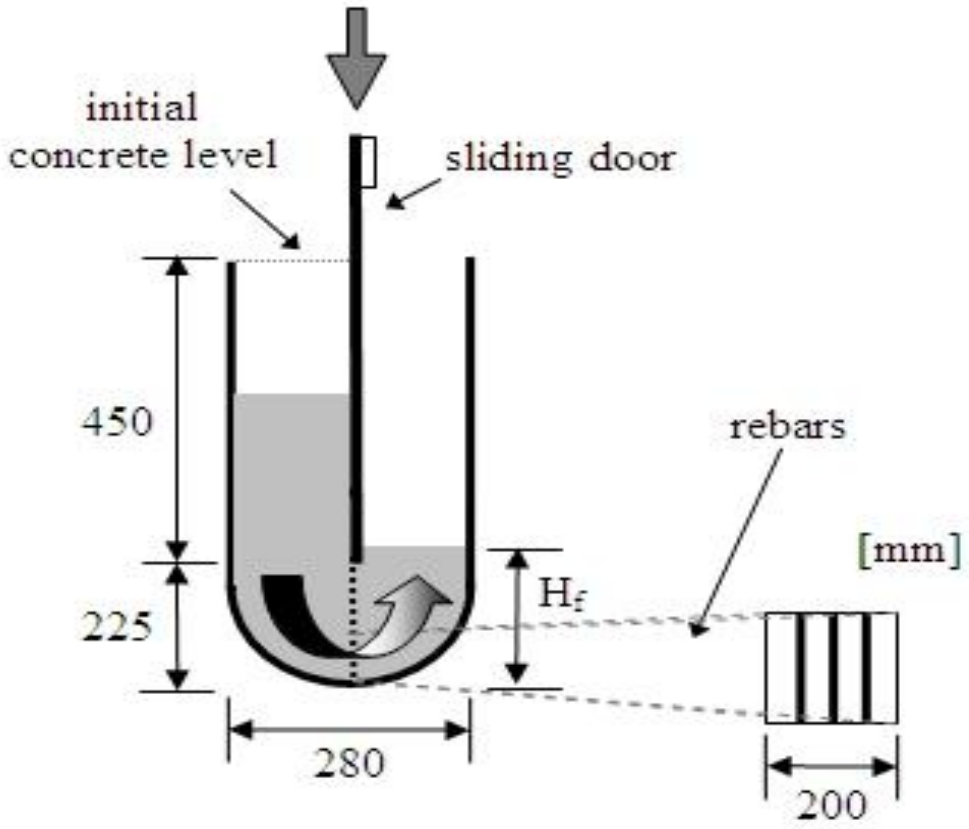

Fig. 3.10: U-box test setup

3.4.4. V- Funnel Test

The method is used to determine the viscosity and filling ability of self-compacting concrete. The test renders information concerning mixture viscosity by measuring the flow rate under its own weight and also rendering information regarding static segregation resistance by increasing the waiting time between filling the container with concrete and the actual commencement of the test. The application of such test for concretes with a greater flow capacity which comprise of super-plasticizers is recommended. The test cannot be performed on concretes comprising of aggregates with a maximum diameter exceeding 20mm [EFNARC, 2005].

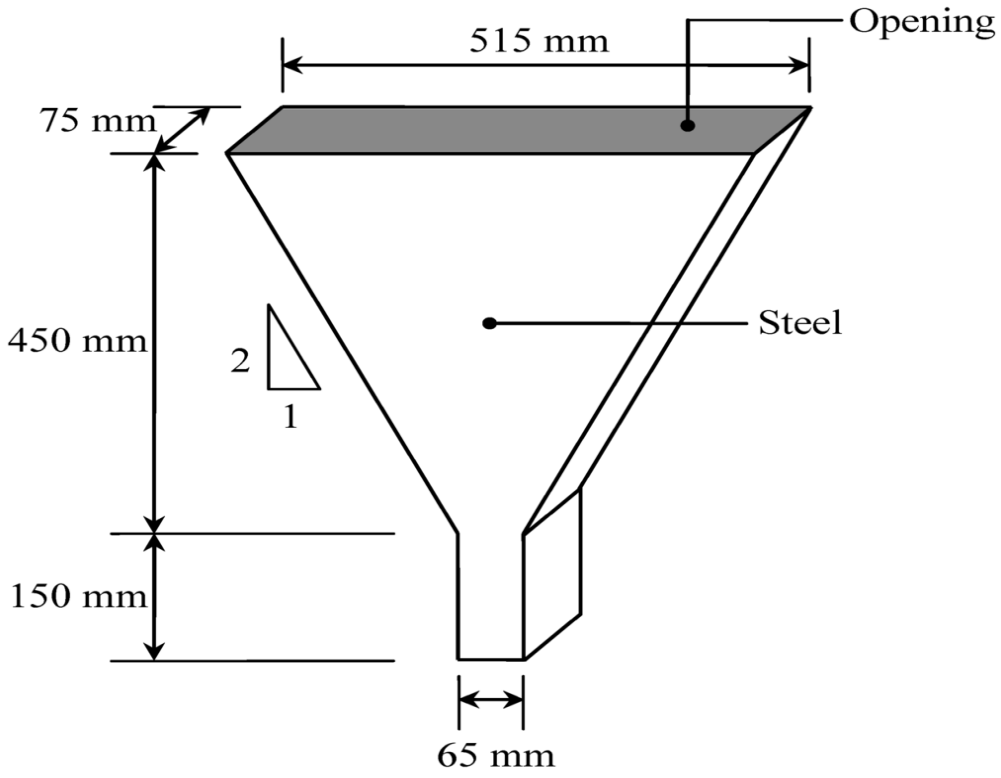

Fig 3.11: V-funnel

Equipment – consists of a funnel with the shape and sizes shown in Fig 3.11. A steel construction and the placement on a vertical support are recommended, while the lower side must be fitted with a mobile cap to allow opening during the test.

Recorded parameters and interpretation- The determined parameters are influenced by concrete deformability, a concrete with a higher flow capacity tending to render a shorter time for passing through the funnel even if viscosity is constant (Schutter et. al. (2008)). The flow time as well as the rate may be used as viscosity indicators regardless of concrete deformability. In certain cases, viscosity may be assessed if is possibly to produce a concrete with constant flow capacity values. In this case, a longer time for passing through the funnel represents a high viscosity, being directly proportional and providing a high segregation resistance.

3.5. STRENGTH PROPERTIES

3.5.1. Compressive Strength

A significant portion of this research focused on the behaviors of self-compacting concrete incorporating iron slag cube specimens under compressive loading. The compressive tests discussed in this section were all completed nominally according to (BIS: 516-1959) standard test method for cubes. Numerous trial mixtures were made. For each batch of SCC made, 150x150x150 mm cube specimens were prepared, as shown in Fig 3.12. The cubes were filled with fresh concrete in one layer without any compaction, after preparing the specimens inside the cube were covered with plastic sheets for about 24 hours to prevent moisture loss. Cubes stored in water until the time of the test. The cubes are placed in the testing machine so that the load is applied to opposite sides as cast and not to the top and bottom as cast. Therefore, the bearing faces of the specimen are sufficiently plane as to require no capping. If there is appreciable curvature, the face is grinded to plane surface because, much lower results than the true strength are obtained by loading faces of the cube specimens that are not truly plane surfaces.

All the cube specimens of size 150 mm were tested in an automated CTM. The compressive strength was than calculated according to the formula:

$$Cs = P / A$$

Where,

Cs = Compressive Strength (N/mm^2)

P = Maximum load (N),

A = Cross sectional area of cube (mm^2)

Fig. 3.12 Compressive strength testing machine and specimens

3.5.2. Splitting Tensile Strength

The splitting tensile strength of SCC was measured based on (BIS: 5816-1999) Methods of test for strength of concrete. This test often referred to as the split cylinder test, indirectly measures the tensile strength of concrete by compressing a cylinder through a line load applied along its length. The tensile strength of concrete is most often is evaluated using a split cylinder test, in which a cylindrical specimen (150mm x 300mm) is placed on its side and loaded in diametrical compression, so to induce transverse

tension. Practically, the load applied on the cylindrical concrete specimen induces tensile stresses on the plane containing the load and relatively high compressive stresses in the area immediately around it. When the cylinder is compressed by the two plane-parallel faceplates, situated at two diametrically opposite points on the cylinder surface then, along the diameter passing through the two points, the major tensile stresses are developed which, at their limit, reach the fracture strength value. Fig. 3.13 shows the samples for splitting tensile strength..

Fig 3.13: Samples of splitting tensile test

The magnitude of this tensile stress acting in a direction perpendicular to the line of action of applied compression is given by:

$$Ts = 2P/ \Pi dl$$

Where,

Ts = Tensile Stress (N/mm^2), P = Applied load at failure (N)

D = Diameter of cylinder (mm), L = Length of cylinder (mm)

3.5.3. Flexural Strength

The flexural strengths of concrete specimens are determined by the use of simple beam with two points loading in accordance with (BIS: 516-1959) The spacemen is a beam 100 x 100 x 500 mm. the mold is filled in one layer, without any compacting or rodding, the

beam casting and then immersing in water. The cast beam specimens are tested turned on their sides with respect to their position as molded as shown in Fig.3.14 This should provide smooth, plane and parallel faces for loading if any loose sand grains or incrustations are removed from the faces that will be in contact with the bearing surfaces of the points of support and the load application. Because the flexural strengths of the prisms are quickly affected by drying which produces skin tension, they are tested immediately after they are removed from the curing basin. The flexural strength of the specimen is expressed as the modulus of rupture. The flexural strength of the beam, F_b (in MPa), is calculated as follows:

$$f_b = P \times L/b \times d^2$$

Where,

b = measured width in cm of the specimen,

d = measured depth in cm of the specimen was supported, and

P = maximum load in kg applied on the specimen.

Fig. 3.14: Beams for flexural strength test

3.5.4. Modulus of Elasticity

Elastic modulus of concrete is a crucial parameter reflecting the ability of the concrete to deform elasticity. The modulus of elasticity is defined as the slope of the stress-strain

curve with the proportional limit of a material. Before conducting the modulus of elasticity test, three cubic specimens were tested first to determine the compressive strength of concrete. Extensometer was used for finding the change in length of concrete specimens on compressive loading. The extensometer consists of two frames for clamping the specimens by means of five adjusting screws with a hardened and tapered end. The spacers hold the two frames in position. The dial gauge was attached with the compresso-meter. Least count of dial gauge was 0.025 mm. On the specimens, load was applied according to BIS 516:1959. The rate of loading was 15N/mm^2/min. The modulus of elasticity was obtained according to the following formula:

$$Cs = P/A,\ A = \pi / 4\ d^2,\ Є = \Delta L / L,\ E = Cs / Є$$

Cs = Compressive stress (N/mm^2)

P = Compressive load (N)

A = Area of cylindrical specimen (mm^2)

D = Diameter of cylinder (mm)

Є = strain, ΔL = Change in length (mm)

L = Length of cylinder,

E = Modulus of elasticity (N/mm^2)

Fig. 3.15: Modulus of elasticity testing machine

3.6. DURABILITY PROPERITIES

3.6.1. Water Absorption

The water absorption of concrete was measured in accordance to ASTM C 642-06. Measure the mass of each specimen, then cubes were oven dried at 105 ºC for 24 hours and such that each one is not less than 25mm from any heating surface or from each other. If the concrete specimen was comparatively dry when its mass was first determined, and the second mass agrees with the first within 0.5%, consider it dry. If the concrete specimen was wet when its mass was first determined, keep it in the oven for a second drying treatment of 24 hours and again measure the mass. If the difference between measured values obtained from two successive values of mass exceeds 0.5% of the lesser value, return the specimens to the oven for an additional 24 hour drying period, and repeat the procedure until the difference between any two successive values is less that 0.5 % of the lowest value obtained. Designate this last value A.

Immerse the specimen water at 22 ±3°C. Continue soaking the concrete specimen in water for not less than 48 hours and until two successive values of mass of the surface-dried sample at intervals of 24 hours show an increase in mass of less than 0.5% of the larger value. Surface-dry the specimen by removing surface moisture with a cloth, and measure the mass. Designate the final surface-dry mass after immersion B. Place the specimen in the boiling water. Boil the specimen completely submersed for a minimum of 5 hours then allow it to cool by natural loss of heat for not less than 14 hours to a final temperature of 22 ± 3°C. Continue to store the samples on their edge in the boiled water until the final two steps are completed. Suspend the concrete specimen in the bucket at a constant water level and measure the apparent mass of the concrete sample in water 25 ± 1 °C. Designate this apparent mass D. Remove concrete sample from the water. Immediately damp dry the sample with a damp cloth and measure the mass of the specimen. Designate the soaked, boiled, surface-dried mass C. Then calculate the percentage of water absorbed by the concrete specimen according to this formula;

$$\text{Absorption after immersion, \%} = [(B-A)/A] \times 100$$

$$\text{Absorption after immersion and boiling, \%} = [(C-A)/A] \times 100$$

Bulk density, dry = $[A/(C-D)]\cdot\rho = g1$

Bulk density after immersion = $[B/(C-D)]\cdot\rho$

Bulk density after immersion and boiling = $[C/(C-D)]\cdot\rho$

Apparent density = $[A / (A-D)]\cdot\rho = g2$

Volume of permeable pore space (voids), % = (g2-g1)/g2 x 100 or [(C-A)/(C-D)] x 100

Where;

A = Mass of oven dried sample in air

B = Mass of surface-dry sample in air after immersion

C = Mass of surface-dry sample in air after immersion and boiling

D = Apparent mass of sample in water after immersion and boiling

g1 = Bulk density, dry

g2 = Apparent density

ρ = Density of water

Fig. 3.16: Specimens in oven for drying and in water for absorption

3.6.2. Sorptivity

ASTM C1585 was developed based on Hall's (1989) investigations and became a Standard in 2004. This test defines the rate of water absorbed by concrete samples due to capillary forces in unsaturated conditions. This rate, is called sorptivity

According to the ASTM C1585 Standard, the test should be done using disc concrete specimens of 100 ±6 mm diameter with length of 50±3 mm. These samples may be obtained from either molded cylinders or drilled cores of concrete elements. Samples should be conditioned in an environment with temperature of 50 ± 2 □ C and Relative Humidity of 80 ± 3 % for 3 days. Next, each sample is placed in a sealed container at 23 ± 2 □ C for at least 15 days. This step provides enough time for moisture to be well distributed throughout the specimen. This avoids a moisture gradient in concrete depth which can cause misleading sorptivity values (Bentz et al., 2001). After the conditioning steps, the samples are removed from containers and the mass determined. The side surfaces of the samples are sealed and a plastic sheet is used to cover the top surface of the specimens to prevent water evaporation of concrete. Lastly, the sealed concrete sample is placed in pan which filled with water

The specimens are removed from the pan and their mass recorded at intervals up to 9 days. In this study 15 different time interval were choose to measure the mass of specimen those time interval were 0, 1800, 3600, 5400, 7200, 9000, 10800, 21600, 92220, 193200, 268500, 432000, 527580, 622200, 691200 seconds. Equation presents the calculation of the absorption, I, which is the change in specimen's mass divided by the product of the cross-sectional area of the sample and the density of water which is considered as 0.001 g/mm^3.

$$I = m(t)/a.d$$

Where: I = absorption (mm),

m(t) = specimen mass in grams at time t (g)

a = exposed area of the sample (mm^2)

3.6.3. Sulphate Resistance

The length change of concrete prism specimens immersed in sulphate solution was calculated as per ASTM C1012-10. The loss of strength from sulfate resistance was measured by immersing the specimen in sulfate solution ($MgSo_4$) after demoulding. The loss in mass and compressive strength of specimen was recorded over a period of 7, 28, 91 and 365 days age of curing and then compared with the compressive strength of those specimens that were immersed in simple water for curing at similar ages.

$$\text{Change in Compressive Strength (\%)} = [(C_1 - C_2)/C_1] \times 100$$

Where;

C_1 = 28 days compressive strength of concrete specimen

C_2 = Average compressive strength of concrete specimen after immersion in solution at the age of test.

Fig. 3.17: SCC specimen after 365 days period of immersion in 10% magnesium sulphate solution

3.6.4. Rapid Chloride Permeability

The rapid chloride permeability test was performed as per ASTM C 1202-10. Total electric charge in coulombs passed through 50 mm thick and100 mm diameter size piece of concrete during 6h time span. A potential difference of 60 V DC was maintained across the ends of the specimen. One end of the specimen was immersed in sodium chloride solution and other end was immersed in sodium hydroxide solution. The total charges in coulombs passed through the specimens were related to its resistance to chloride ion penetration. The resistance to chloride ion penetration of concrete was rated negligible, very low, low, moderate, and high as per Table 3.14 The chloride permeability test for the present research was conducted to assess the concrete quality at the ages of 7, 28, 91, and 365 days.

Table 3.14: Chloride ion penetration based on charged passed (ASTM C 1202-10)

Charged Passed (C)	Chloride ion penetration
> 4000	High
2000-4000	Moderate
1000-2000	Low
100-1000	Very low
<100	Negligible

Fig. 3.18: Experimental set up for measuring chloride ion penetration

3.6.5. Abrasion Resistance

Abrasion resistance of concrete calculated according to procedure given in BIS: 1237-2012. Specimens were weighed accurately on a digital balance (0.1 g.). After initial drying, the thickness of the specimens was measured at five points (i.e. center and four corners). The grinding path of the disc of the abrasion-testing machine was evenly distributed with 20-gram of abrasive (aluminum) powder. The specimens were fixed in the holding device of the abrasion machine, and a load of 300 N was applied. The abrasive powder was continuously fed back in to the grinding path so that it remained uniformly distributed in the track corresponding to the width of the test specimen. The thickness and weight of specimens were taken. The extent of abrasion was determined from the difference in values of thickness measured before and after the abrasion test. Loss in thickness of specimens was also confirmed by the measurement of average loss in thickness of the specimens according to formula:

$$T = \frac{W_1 - W_2}{W_1} \times \frac{V_1}{A}$$

Where;

T = average loss in thickness in mm

W_1 = the initial weight of the specimen in gram

W_2 = the mass of the specimen after abrasion in gram

` V_1 = the initial volume of the specimens in mm^3

A = the surface area of the specimens in mm^2

Abrasion resistance of SCC mixtures was measured at 7, 28, 91 and 365 days of curing period.

3.7. NON DESTRUCTIVE TESTING

3.7.1. Ultra-sonic Pulse Velocity (UPV)

Ultrasonic pulse velocity was conducted as per ASTM C 597-02. Ultrasonic scanning is non-destructive evaluation test for to assess the homogeneity and integrity of concrete. This test consists of measuring travel time, T of ultrasonic pulse of 50 to 54 KHz, produced by an transducer held in contact with one surface of the concrete sample under

test and receiving the same by a similar transducer in contact with the surface at the other end. With the path length L, (i.e the distance between the two probes) and the time travel T,

The Pulse velocity, V=L/T

The general guidelines for concrete quality based on UPV given in Table 3.15. Battery operated fully portable digitized unit PUNDIT (Portable Ultrasonic Non-destructive Digital Indicating Tester) was used shown in Fig.3.19 The Direct transmission way was used for measuring pulse velocity through concrete. . UPV test results were measured at 7, 28, 91 and 365 days curing age.

Table 3.15: General guidelines for concrete quality based on UPV [ASTM C 597-02]

PULSE VELOCITY	CONCRETE QUALITY
>4000 m/s	Very good to excellent
3500 – 4000 m/s	Good to very good, slight porosity may exist
3000 – 3500 m/s	Satisfactory but loss of integrity is suspected
<3000 m/s	Poor and los of integrity exist.

Fig. 3.19: Ultra-sonic pulse velocity set up

3.8. MICROSCOPY (SCANNING ELECTRON MICROSCOPY-SEM)

Scanning electron microscope (SEM) plays crucial role for the analysis concrete surfaces. The SEM images give the information regarding the particle morphology, texture, porosity, and agglomeration of the powder. SEM exhibits properties of very high resolution, extensive magnification range and high depth of field. The sample for SEM analysis is mounted on a conductive substrate such as aluminum stub and gold plated in vacuum. The gold coated samples are kept at the sample stage of the microscope. The samples can be moved in X-axis, Y-axis, and Z-axis directions, tilted as well as rotated. Further, the data signal is released due to interaction between bombarding electrons and atoms of the specimens. These data signal arise due to elastic or inelastic collisions of beam electrons with the atoms of the specimens. The elastic (electron nucleus) collisions produce back scattered electrons (BSE) and inelastic (electron-electron) produce secondary electrons. The back scattered electrons provide topographic as well as compositional information about the specimens. In other words, SEM micrographs could be taken in two modes i.e., secondary emission and back scattered; both the modes were used in this study. . In this research broken pieces of concrete generated by crushing were mounted on the SEM stub and images were obtained using SE image mode and back scattered mode.

3.9. X-RAY DIFFRACTION

X-ray diffraction is one of the most powerful tools for identifying unknown crystalline phases. By comparing the positions and intensities of the diffraction peaks against a library of known crystalline phases, the target material can be recognized. In addition, multiple phases in sample can be identified and quantified. XRD analyses were conducted to identify the components of SCC mixtures and material used. The XRD was done using a Panalytical X'Pert pro, with Cu Kα, radiation (Fig.3.20) at SAI labs, Thapar University, Patiala. The X'Pert High Score Plus software was used to identify the phases. The cement paste was separated from concrete samples and was sieved through 90μm sieve. The XRD were conducted for diffraction angle 2 Theta range between 10^0 and 90^0. XRD diffractograms of powder cement paste of SCC control mixture.

3.9.1 Procedure for Deduction of Minerals

(i) For a given sample, XRD graphs are obtained with intensities on Y-axis and 2θ on X-axis.

(ii) Match the d values and intensities of peaks of respective minerals with the fundamental peaks of X-ray powder diffraction files given in the software.

(iii) For any mineral to be present, all the strong peaks should be present in the XRD graph, else the mineral is not present.

Fig 3.20: X-ray diffractometer (XRD)

CHAPTER – 4

RESULTS AND DISCUSSION

This chapter deals with the results of experimental investigations. Various tests were performed to investigate the effect of iron slag on fresh properties (slump flow, L-box, U-box and V-funnel), strength properties (compressive strength, splitting tensile strength, flexural strength and modulus of elasticity), durability properties (water absorption, sorptivity, sulphate resistance, rapid chloride permeability and abrasion resistance), non destructive testing (ultra-sonic pulse velocity) on SCC designated mixes incorporating various percentage of fine aggregates replaced with iron slag (10, 25 and 40%). SEM and XRD analysis was done to analyze the microstructure and phase identification of SCC.

4.1. FRESH PROPERTIES OF SCC

4.1.1. Slump Flow

The results of slump flow test for different iron slag contents (10, 25 and 40%) are given in Table 4.1 and results have also been plotted in Fig 4.1.

Behavior of self-compacting concrete with or without replacement of iron was studied by performing slump flow test and results indicate that, flow of self-compacting concrete decreased with increase of iron slag content. Fig 4.2 show the various slump flows.

All mixes of SCC shows slump flow are in the range of 788-673 mm and lies within the limits (650-800mm) given by EFNARC. However, slump flow decreased with the increase of iron slag content as compared to the SCC mix prepared without iron slag. The slump flow was calculated as average of five SCC fresh mixes. At 0% replacement the value of slump flow was 788 mm and this flow value was 7, 11 and 15% more than the values obtained by replacing fine aggregates with iron slag at 10, 25 and 40%, respectively.

Table 4.1: Slump flow (mm) result value of SCC

Mix ID	Slump Flow (mm)	Average Slump flow (mm)	EFNARC Recommendations
SCC (CM)	774	788	650-800 mm
SCC (CM)	790		
SCC (CM)	810		
SCC (CM)	800		
SCC (CM)	770		
SCC (IS-10)	733	735	650-800 mm
SCC (IS-10)	745		
SCC (IS-10)	735		
SCC (IS-10)	720		
SCC (IS-10)	740		
SCC (IS-25)	723	705	650-800 mm
SCC (IS-25)	720		
SCC (IS-25)	700		
SCC (IS-25)	690		
SCC (IS-25)	695		
SCC (IS-40)	687	673	650-800 mm
SCC (IS-40)	677		
SCC (IS-40)	670		
SCC (IS-40	665		
SCC (IS-40)	670		

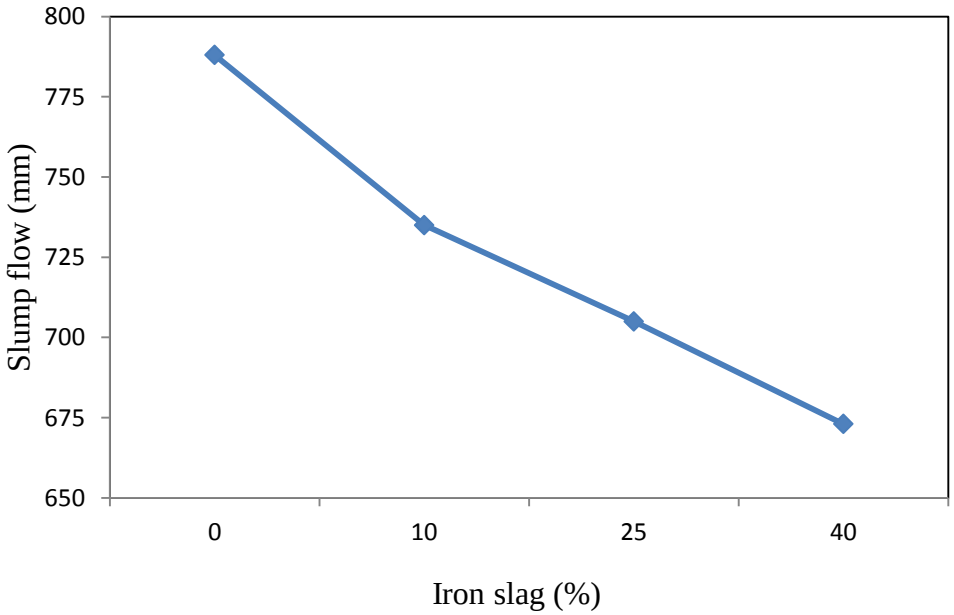

Fig 4.1: Effect of iron slag on slump values

Fig 4.2: Slump flow during testing

4.1.2. L-Box

The L-box ratio for all the SCC mixes was between 0.825-0.91 and it lies within boundaries of EFNARC range (0.8-1.0). The result shows (Fig 4.3 and Table 4.2) that blocking ratio decreased with the increase in replacement percentage of iron slag. Fig 4.4 shows the L-box test.

Table 4.2: Results of L-box values of SCC

Mix ID	L-box ratio (H2/H1)	Average L-box ratio (H2/H1)	EFNARC Recommendations
SCC-CM	0.91	0.91	0.8-1.0
SCC-CM	0.93		
SCC-CM	0.90		
SCC-CM	0.89		
SCC-IS10	0.88	0.88	0.8-1.0
SCC-IS10	0.88		
SCC-IS-10	0.89		
SCC-IS10	0.87		
SCC-IS25	0.87	0.86	0.8-1.0
SCC-IS25	0.85		
SCC-IS25	0.86		
SCC-IS25	0.85		
SCC-IS40	0.80	0.825	0.8-1.0
SCC-IS40	0.84		
SCC-IS40	0.82		
SCC-IS40	0.84		

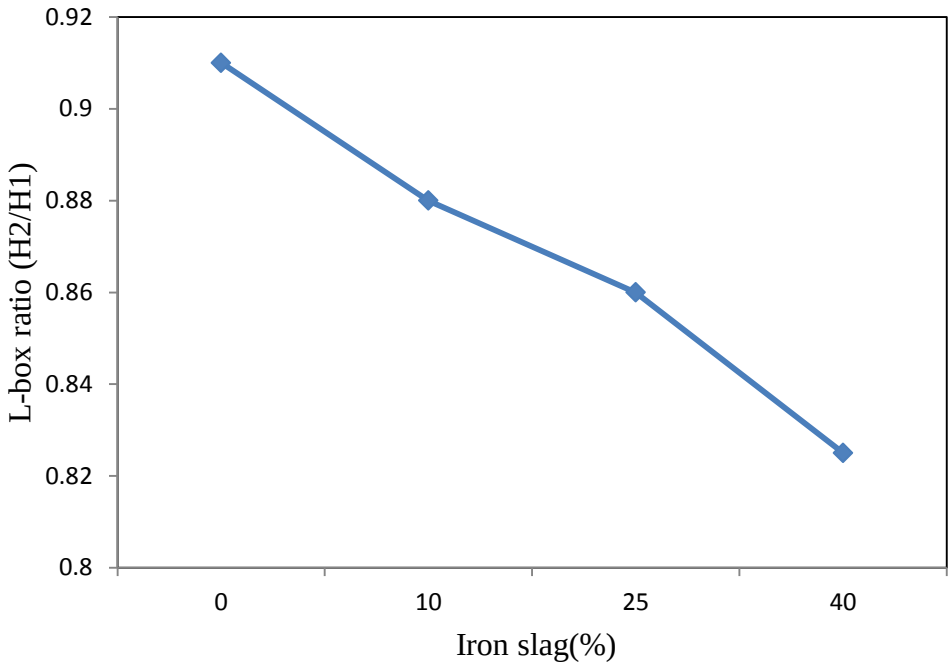

Fig 4.3: Effect of iron slag on L-box values

Fig 4.4: Images L-box during testing

Results of L-box test exhibited that blocking ratio decreased with the increase of iron slag content as compared to the SCC mix prepared without iron slag. The L-box was calculated as average of four SCC fresh mixes. At 0% replacement the average ratio of L-box ratio is 0.91, and this ratio was 3, 6 and 10% more than the values obtained by replacing fine aggregates with iron slag at 10, 25 and 40%, respectively.

4.1.3. U-Box

The variation on height of concrete in two compartments of U-box was found in the range of 31-35 mm. The results of U-box were inside the limits of EFNARC. The U-box test results are given in Table 4.3 and shown in Fig 4.5. It can be observed that values of U-box increased with the increase of replacement percentage of fine aggregates with iron slag. Fig 4.6 shows the U-box test.

Table 4.3: Results of U-box values of SCC

Mix ID	U-box (H2-H1) in mm	Average U-box (H2-H1) in mm	EFNARC Recommendations
SCC-CM	31	31	Not more than 35 mm
SCC-CM	29		
SCC-CM	31		
SCC-CM	32		
SCC-IS10	32	32	Not more than 35 mm
SCC-IS10	33		
SCC-IS-10	31		
SCC-IS10	32		
SCC-IS25	33	34	Not more than 35 mm
SCC-IS25	34		
SCC-IS25	34		
SCC-IS25	35		
SCC-IS40	36	35	Not more than 35 mm
SCC-IS40	35		
SCC-IS40	35		
SCC-IS40	35		

Results of U-box test indicated that difference of level between two compartments were increased with the increase in iron slag content as compared to the SCC mix prepared without iron slag. The U-box was calculated as average of four SCC fresh mixes. At 0% replacement the average value of U-box was 31 mm. Further, at 10, 25 and 40% replacements, U-box values were increased to 4, 9 and 12%, respectively. According to EFNARC lesser difference of level between two compartments after opening the blocking gates shows good filling ability of SCC.

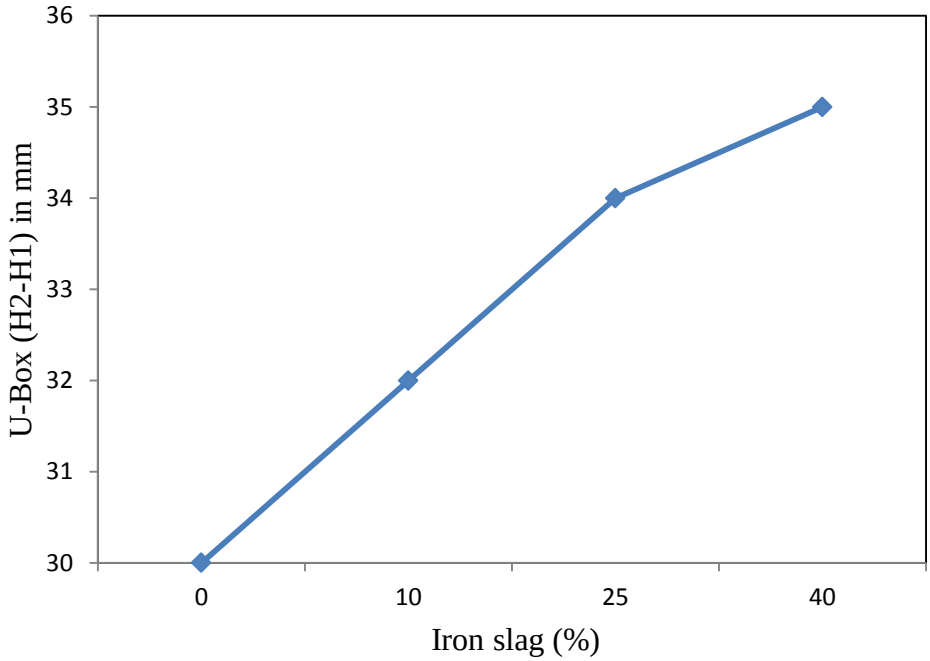

Fig. 4.5: Effect of iron slag on U-box values

Fig 4.6: Images of U-box during testing

4.1.4. V-funnel

Time in V-funnel test increased as iron slag content increases. The test results are given in Table 4.4 and plotted in Fig. 4.7 It shows that time ranges between 9- 13 sec. The results of V-funnel test of SCC mixes were inside the limits as per mentioned in EFNARC. Fig 4.8 shows the V-funnel test.

Table 4.4: Results of V-funnel values of SCC

Mix ID	V-funnel time (Sec.)	V-funnel time (sec.)	EFNARC Recommendations
SCC-CM	09	9	Not more than 12 seconds
SCC-CM	09		
SCC-CM	10		
SCC-CM	09		
SCC-IS10	11	11	Not more than 12 seconds
SCC-IS10	12		
SCC-IS-10	11		
SCC-IS10	10		
SCC-IS25	11	12	Not more than 12 seconds
SCC-IS25	12		
SCC-IS25	12		
SCC-IS25	12		
SCC-IS40	13	13	Not more than 12 seconds
SCC-IS40	13		
SCC-IS40	12		
SCC-IS40	13		

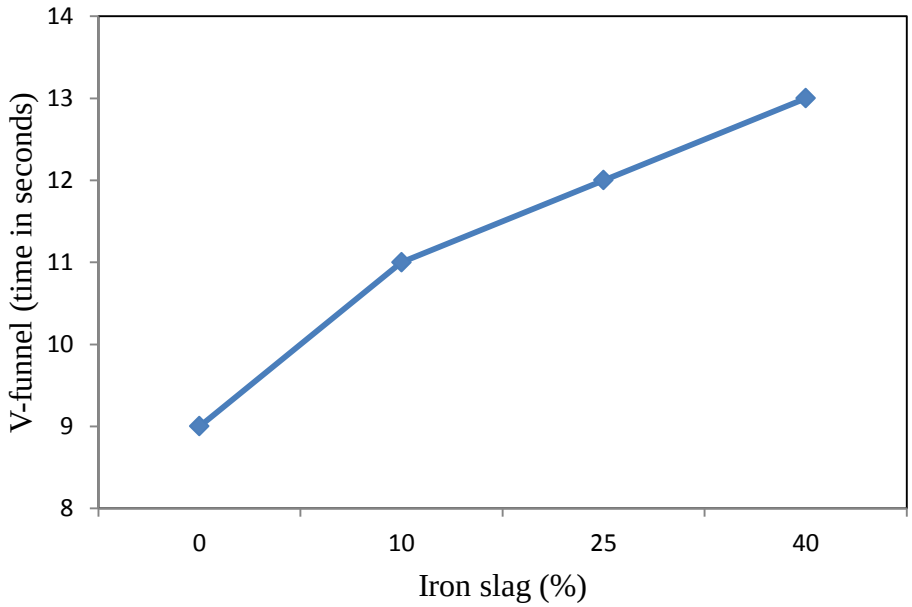

Fig 4.7: Effect of iron slag on V-funnel values

Results of V-funnel test were exhibited that passing time increased with the increase of iron slag content as compared with control SCC mix. The V-funnel was calculated as average of four SCC fresh mixes. At 0% replacement the average value of V-funnel was 9 seconds. Further, at 10, 25 and 40% replacements, the V-funnel values were increased by 18, 25 and 30%, respectively.

Slump flow, L-box, U-box and V-funnel results indicate that inclusion of iron slag as partial replacement of fine aggregates fulfills the requirements of SCC as per EFNARC. However, the values of slump flow, L-box decreased and the values of U-box, V-funnel increased with the increase of iron slag content.

Iron slag particles are more granulated and sharp edged as compared to fine aggregates (sand). The rough texture and complicated shape of iron slag particles plays a significant role in increasing the inter-particle friction causing jamming of concrete particles. The test results of this study are in good agreement with those reported in previous studies given in Table 4.5.

Fig 4.8: Images of V-funnel during testing

Table 4.5: Comparison of fresh properties of SCC

	Present Research	Anastasiou et al.,(2014)	Afshoon and Sharifi, (2014)	Sideris et al., (2015)	Boukendakdj et al., (2009)	Tomasiello and Felitti, (2010)	EFNARC, (2005)
Replaced material	Iron slag with sand	LFS with sand	GCS with cement	LFS with sand	Algerian Slag with cement	EAF with sand	-
Replacement (%)	Up to 40	Up to 35	Up to 30	Up to 25	Up to 25	Up to 30	-
Slump flow (mm)	690-790	500-800	640-710	695-780	630-790	700-750	650-800
L-box (H2/H1)	0.84-0.92	0.78-0.83	0.84-0.97	0.84-1.0	-	0.7-0.86	0.8-1.0
U-box (H2-H1) (mm)	28-31	-	-		30-90	-	0-30
V-funnel (sec.)	11-12.5	-	5.52-8.15	6.4-10.4	7-14.8	8-12	6-12

4.2. STRENGTH PROPERTIES OF SCC

4.2.1. Compressive strength

The compressive strength test results are presented in Fig 4.9. Compressive strength result demonstrates that strength of SCC with iron slag increased with all percentages of iron slag, as well as at all ages.

At 7 days, compressive strength of SCC mixes containing 10, 25, and 40% iron slag as fine aggregates gained 3, 8.5 and 18%, respectively, in comparison with SCC without iron slag (25.1 MPa). 28-day compressive strength of SCC made with 10, 25 and 40% iron slag achieved 4, 15 and 26% higher strength as compared with SCC with 0% slag (35.7 MPa). At 91 and 365 days, a similar trend in strength was observed with increase in iron slag from 0-40%. At 91 days, SCC mixes containing 10, 25 and 40% iron slag as fine aggregates gained 5, 14 and 28%, compressive strength respectively, as compared to 38.5 MPa of control SCC. At 365 days, SCC mixes containing 10, 25 and 40% iron slag as fine aggregates gained 5, 16 and 26%, compressive strength respectively, as compared to 47.3 MPa, of control SCC.

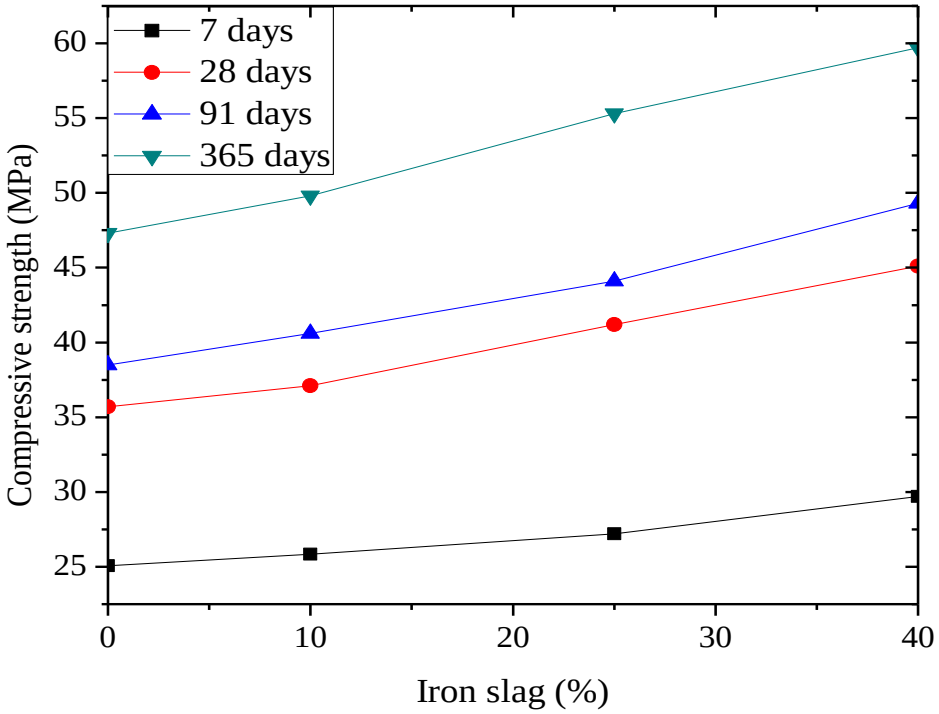

Fig. 4.9: Effect of iron slag on compressive Strength of SCC

In control SCC, compressive strength result value at 7 days was 25.1 MPa, and at 28, 91 and 365 days, the result values increased about 42.23, 53.38 and 88.40%, respectively. With 10% iron slag in SCC mix (SCC-IS10), compressive strength result value at 7 days was 25.8. Further at 28, 91 and 365 days, strength value was increased about 43.7, 57.36 and 93.02%, respectively. When the iron slag content increased from 10 to 25% in SCC (SCC-IS25), compressive strength result value at 7 days was 27.2 MPa and same SCC mix measured at 28, 91 and 365 days, the results value increased about 51.47, 62.13 and 92.27%, respectively. Furthermore, at 40% replacement of iron slag content in SCC (SCC-IS40), compressive strength result value at 7-day was 29.7 MPa. Strength at 28, 91 and 365 days, increased about 51.85, 65.69 and 101%, respectively.

The test results exhibited that inclusion of iron slag as fine aggregates in SCC improved the compressive strength of SCC at all ages as presented in Fig 4.10. The reason for enhancement in compressive strength is silica in iron slag that reacts with calcium hydroxide and forms calcium silicates and aluminates hydrates, which fill the voids and

improves the micro-structure of SCC, thereby enhancing its strength. As it can be predicted from SEM results the micro-structure get denser after the incorporation of iron slag in SCC mix as compared with control SCC. The test results of this experimental are similar to those reported in previous researches by Sideris et al., 2015, Peng and Hwang, 2010 and Soya et. al.,1999.

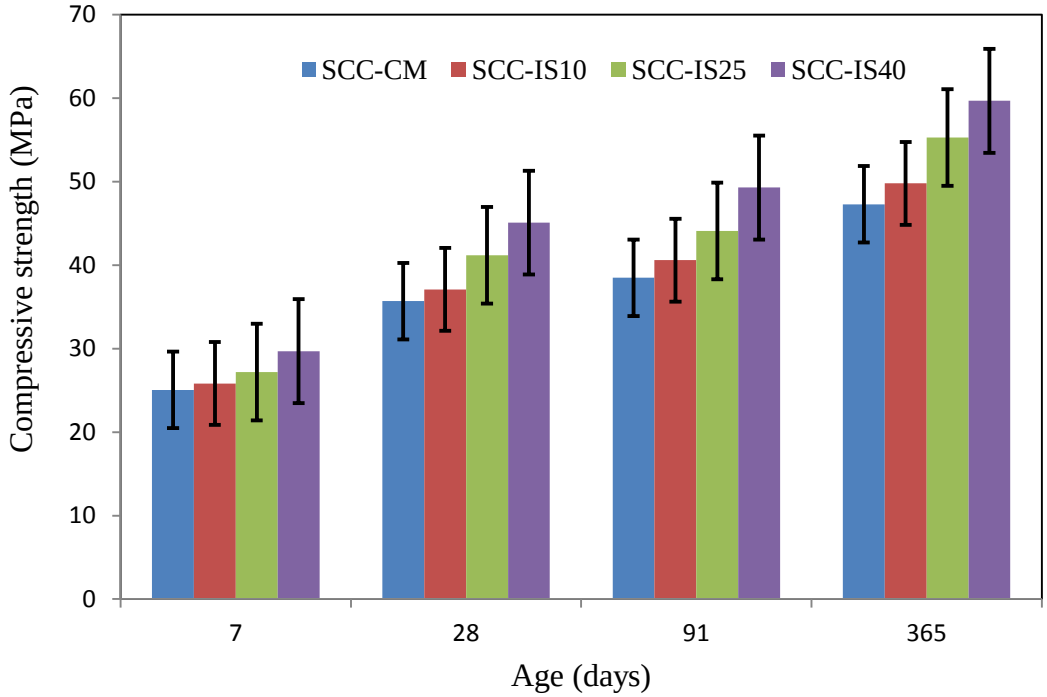

Fig. 4.10: Compressive strength versus age

4.2.2. Splitting Tensile Strength

Splitting tensile strength results of SCC mixes with iron slag is shown in Fig 4.11. The splitting tensile strength of SCC increased with increase in iron slag content. At all ages, iron slag SCC mixes exhibited higher splitting tensile strength than Control SCC. At 7 days, SCC containing 10, 25 and 40% iron slag attained 23.23, 39.43 and 52.11% higher splitting tensile strength than control SCC(1.42 MPa). The improvement in splitting tensile strength of SCC at 28 days containing 10, 25 and 40% iron slag was 3.70, 18.51 and 25.90% higher than control SCC (2.70 MPa). At 91 days, SCC containing 10, 25 and 40% iron slag attained 3.3, 25 and 30% higher splitting tensile strength than control SCC(3.0 MPa). Furthermore, at 365 days age, SCC containing 10, 25 and 40% iron slag

as fine aggregates attained 7.5, 17.5 and 29.7% more splitting tensile strength than control SCC(3.70 MPa).

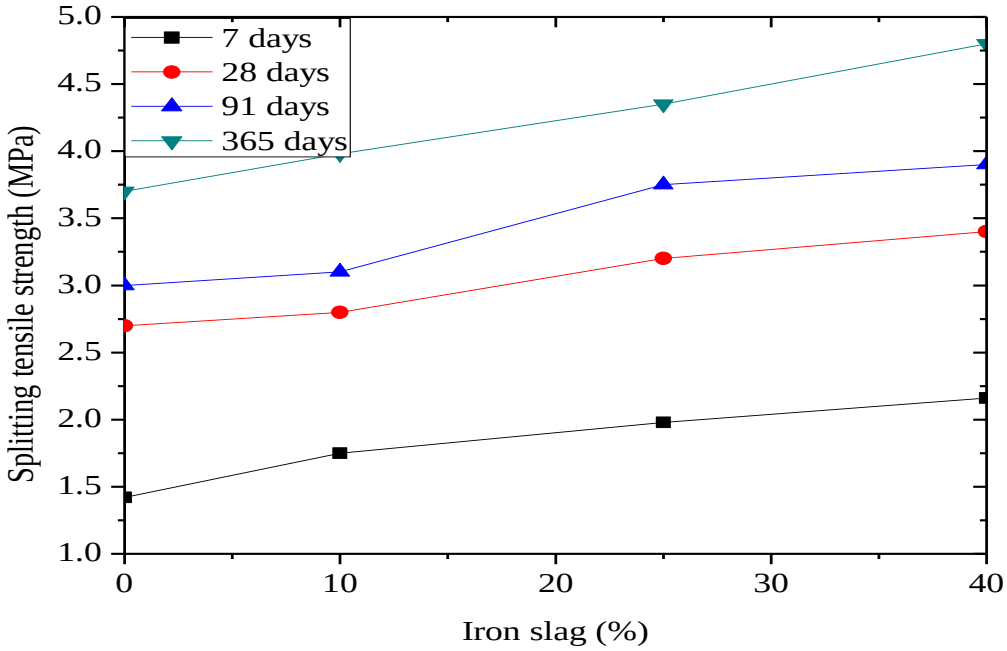

Fig. 4.11: Effect of iron slag on splitting tensile strength of SCC

Effect of age on splitting tensile strength of SCC is presented in Fig 4.12. Splitting tensile strength of self-compacting concrete at 7 days was 1.42 MPa and at 28, 91 and 365 days, results value increased about 90.14, 111.26 and 160.56%, respectively. With 10% iron slag in SCC mix (SCC-IS-10), at 7 days value was 1.75 MPa, and at 28, 91 and 365 days, the results value increased about 60, 77.14 and 127.42%, respectively. When the iron slag content increased from 10% to 25% in SCC (SCC-IS25), at 7 days, splitting tensile strength test result value was 1.98 MPa, the same SCC mix measured at 28, 91 and 365 days the results value increased about 61.61, 89.39 and 119.69% respectively. Furthermore, with 40% replacement in SCC, at 7 days splitting tensile strength value was 2.16 MPa and at 28, 91 and 365 days, results value increased about 57.40, 80.55 and 122.22%, respectively.

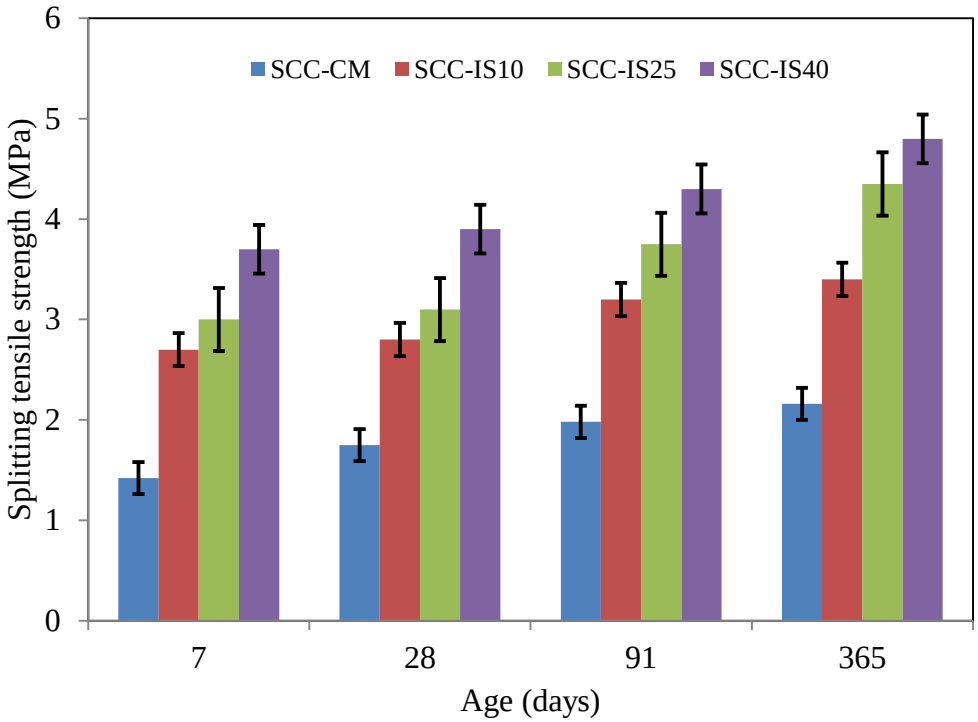

Fig. 4.12: Splitting tensile strength versus age

Splitting tensile strength and compressive strength ratios are given in Table 4.6. All the parameters of fine and coarse aggregates, curing age, water cement ratio and mixing affect the relationship of splitting tensile and compressive strength. Splitting tensile strength/compressive strength ratios were increased with the increase of iron slag percentage in SCC at all replacement percentages of iron slag with fine aggregates. At 7 days age, the ratio increased from 5.7 to 7.3 on 0 to 40% replacement of iron slag with fine aggregates. At 28, 91 and 365 days, the average ratio (%) of iron slag SCC mix were 7.6, 7.9 and 8.8 respectively

Table 4.6: Ratios of splitting tensile strength and compressive strength

SCC Mix	**Age**			
	7 days	28 days	91 days	365 days
SCC-CM	5.7	7.6	7.8	7.8
SCC-IS10	6.8	7.5	7.6	8.0
SCC-IS25	7.3	7.8	8.5	7.9
SCC-IS40	7.3	7.5	7.9	8.0

4.2.3. Flexural Strength

Flexural strength results of SCC mixes incorporating iron slag are shown in Fig 4.13. The results indicate that replacement of fine aggregates with iron slag in SCC enhanced the flexural strength at all replacement levels as well as at all ages. Iron slag as fine aggregates in SCC affects the flexural strength of SCC in a similar way as in the case of compressive strength and splitting tensile strength. At 7 days, flexural strength of control SCC was 2.43 MPa, whereas, at 10, 25 and 40% fine aggregates replacement, flexural strength attained was 2.46, 13.99 and 22.63%. At 28 days, flexural strength of control SCC was 3.46 MPa and at 10, 25 and 40% fine aggregates replacement, flexural strength attained was 2.02, 17.63 and 21.96%. Further, at 91 days, SCC containing 10, 25 and 40% iron slag achieved 4.0, 11.00 and 18.25% more flexural strength than control SCC(4.0 MPa). Lastly, at 365 days, SCC containing 10, 25 and 40% iron slag attained 2.51, 13.69 and 17.12% more flexural strength than control SCC(4.38 MPa).

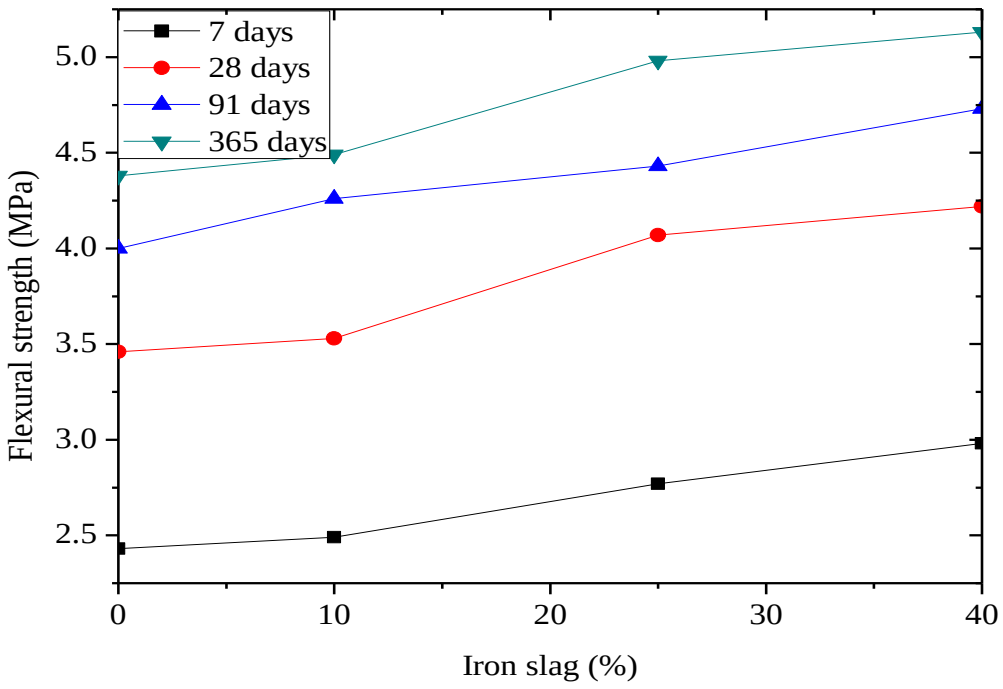

Fig. 4.13: Effect of iron slag on flexural strength of SCC

Effect of age on flexural strength of SCC is presented in Fig 4.14. At 7 days, the flexural strength of control SCC was 2.43 MPa, and at 28, 91 and 365 days, flexural strength

increased about 42.38, 64.60 and 80.24%, respectively. With 10% iron slag in SCC mix (SCC-IS10), at 7 days, flexural strength was 2.49 MPa. Further, at 28, 91 and 365 days the results value increased about 41.76, 67.07 and 80.32%, respectively. From 10 to 25% replacement in SCC, flexural strength at 7 days was 2.77 MPa and at 28, 91 and 365 days, flexural strength value was increased about 46.94, 59.93 and 79.89%. With the further increase in iron slag content from 25 to 40% in SCC (SCC-IS40), flexural strength at 7 days was 2.98 MPa, which increased about 41.61, 58.72 and 72.14% at 28, 91 and 365 days respectively. The results of present research are in good agreement with those reported by Kothai and Malathi, 2012.

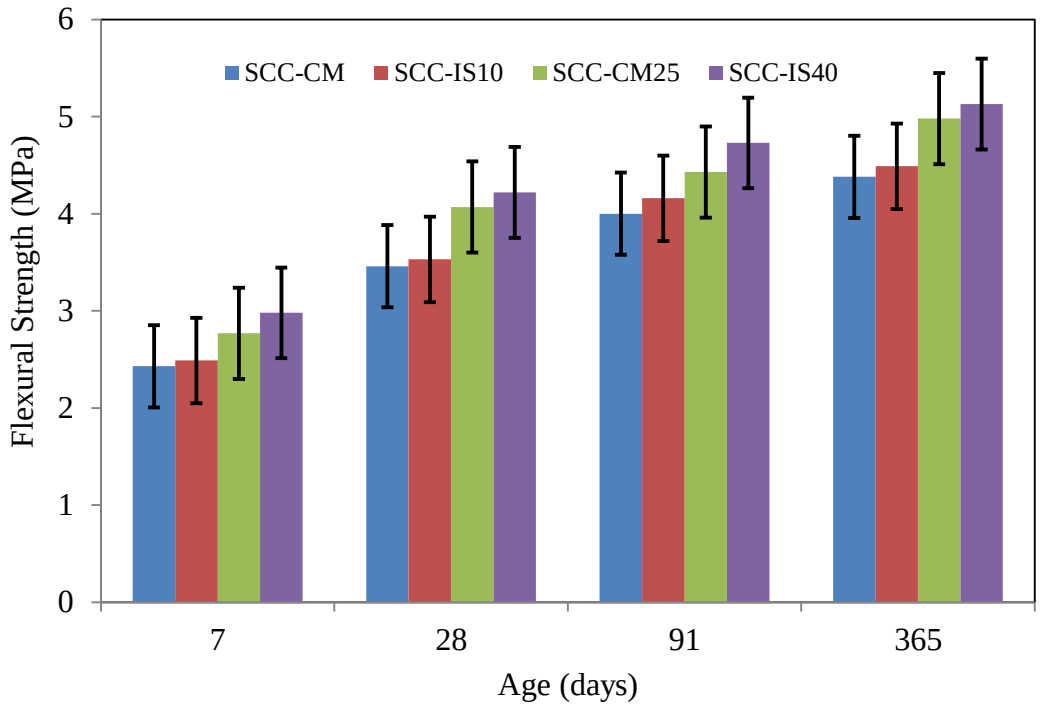

Fig 4.14: Flexural strength versus age

4.2.4. Modulus of Elasticity

In this experimental study, modulus of elasticity which is also known as secant modulus, is taken as the slope of the chord from the origin to some arbitrary point on the stress-strain curve. The test results of modulus of elasticity are evaluated for the different iron slag contents in SCC (0, 10, 25 and 40%) at the end of age (7, 28, 91 and 365 days) are given in Table 4.7. Modulus of elasticity results of SCC mixes has been plotted in Fig

4.15 and Fig 4.16. Modulus of elasticity increased linearly by replacement of fine aggregates with iron slag in SCC. At 7 days, modulus of elasticity of control SCC was 25.51GPa. However, with 10, 25 and 40% iron slag, modulus of elasticity of SCC mixes was observed as 25.62, 26.07 and 26.17GPa respectively. At 28 days, modulus of elasticity of control SCC was 27.9 GPa and with 10, 25 and 40% iron slag, modulus of elasticity was 28.19, 28.71 and 28.87 GPa. Further, at 91 days, modulus of elasticity of control SCC mix was 28.19GPa and approximate same value was observed at 10% replacement. Then with 25% replacement, modulus of elasticity of SCC mixes gained 4.4% higher value than control SCC, and at 40% replacement of fine aggregates with iron slag, modulus of elasticity of SCC increased by 5.7%. At 365 days, modulus of elasticity of control SCC mix was 29.6GPa. Further, with 10% iron slag in SCC mixes was gives almost similar results. Furthermore, 5% increment was observed in modulus of elasticity value after replacing 25% and 40% replacement of fine aggregates with iron slag as compared with control SCC.

Table: 4.7 Modulus of elasticity of SCC mixes

Mix ID	7 days	28 days	91 days	365 days
SCC-CM	25.51	27.9	28.19	29.6
SCC-IS10	25.62	28.19	28.78	30.23
SCC-IS25	26.07	28.71	29.43	30.76
SCC-IS40	26.17	28.87	29.79	31.06

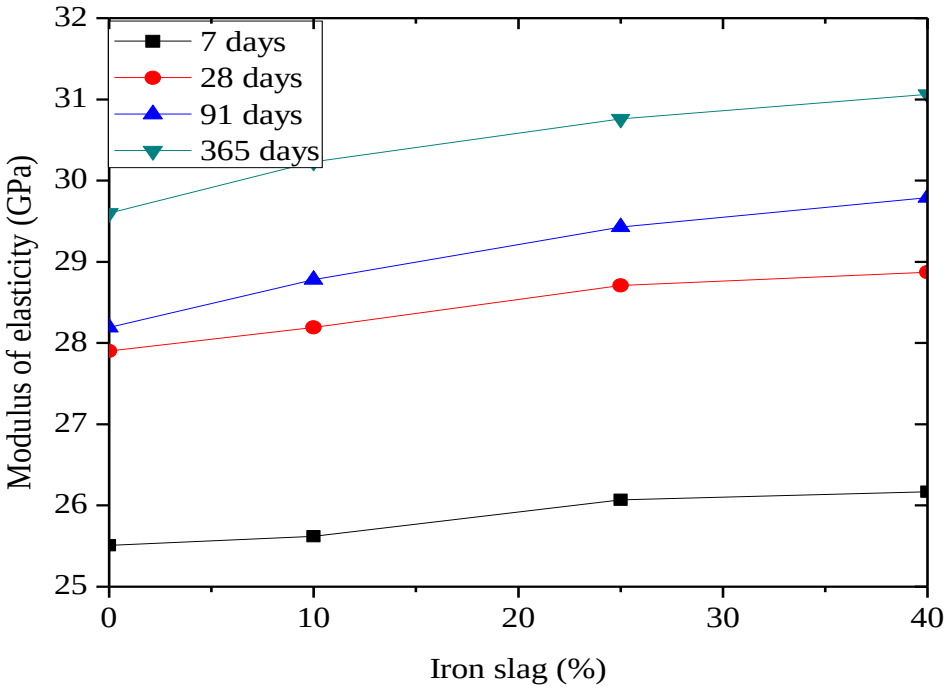

Fig 4.15: Effect of iron slag on modulus of elasticity of SCC

SCC mixes with iron slag content shows higher modulus of elasticity than control SCC at all ages. Modulus of elasticity of control SCC (SCC-CM) at 7 days was 25.51GPa. Further, at 28, 91 and 365 days, modulus of elasticity increased about 9.37, 10.51 and 16.04%, respectively. With 10% replacement of fine aggregates with iron slag in SCC mix (SCC-IS10), at 7 days, the observed value of modulus of elasticity was 25.62GPa. At 28, 91 and 365 days the results value increased of 10.03, 12.33 and 18%, respectively. When the iron slag content increased from 10 to 25% (SCC-IS25), the modulus of elasticity value was 26.07GPa at 7 days, the same SCC mix value increased to 10.12, 12.88 and 18% at 28, 91 and 365 days, respectively. With further increase in iron slag content from 25 to 40% (SCC-IS40), modulus of elasticity increased about 10.31, 13.84 and 18.70% at 28, 91 and 365 days as compared to 7 days modulus of elasticity value 26.17 GPa at same replacement level.

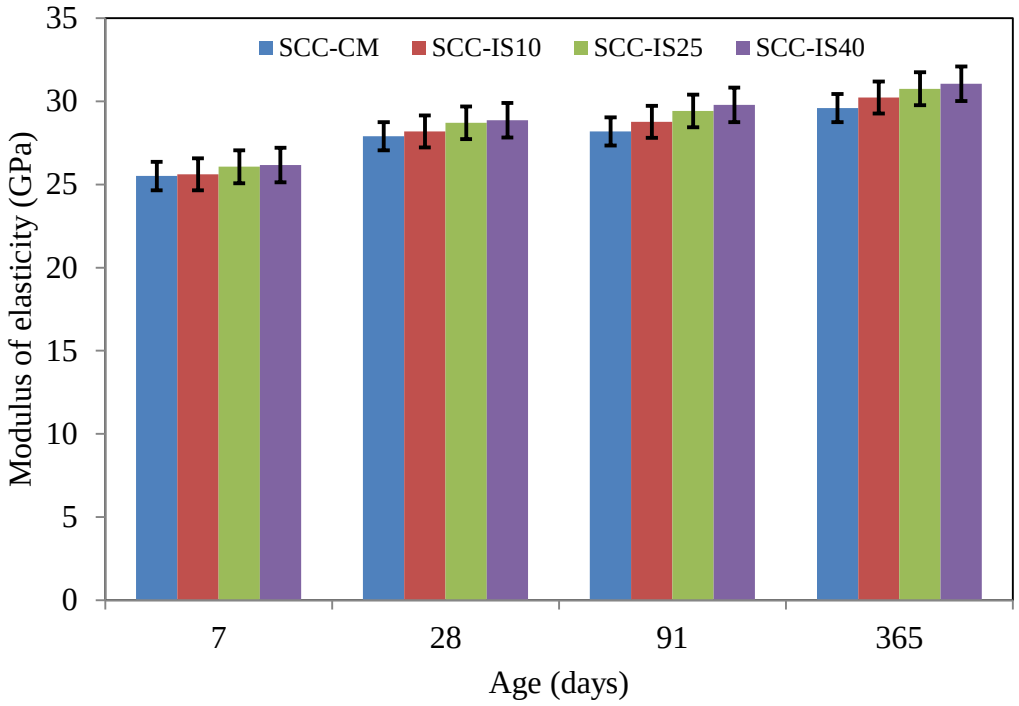

Fig 4.16: Modulus of elasticity of SCC verses age

4.3. DURABILITY PROPERTIES OF SCC

Concrete durability is generally defined as ability to resist weathering action, chemical attack, abrasion, or any process of concrete deterioration. Durability is largely dependent on the transport properties which are highly influenced by the pore system. In order to increase the sustainability and to decrease the repair costs of concrete structures during their service life, it is mandatory to use durable materials in construction.

4.3.1 Water Absorption

Water absorption results of iron slag in SCC mixes up to 365 days are shown in Fig 4.17. Test results of water absorption indicate that as the percentage of iron slag increases, the percentage of water absorption decreased in all SCC mixes and as well as at all ages. At 7 days, water absorption of control SCC was 5%. At the same age, with 10, 25 and 40% iron slag, water absorption of SCC mixes were observed 1, 4 and 13%, respectively, which was less than the control SCC. Further at 28 days, water absorption of control SCC was 4.81%, and at 10, 25 and 40% iron slag, water absorption decreased about 1.45, 13.72 and 16.83%, respectively. At 91 days, SCC with 10, 25 and 40% iron slag as fine

aggregates attained 1, 4.2 and 15% lower water absorption than control SCC (4.12%). Lastly, at 365 days, SCC containing 10, 25 and 40% iron slag as fine aggregates absorbs 5.7, 10 and 11.5% less water than control SCC (3.5%).

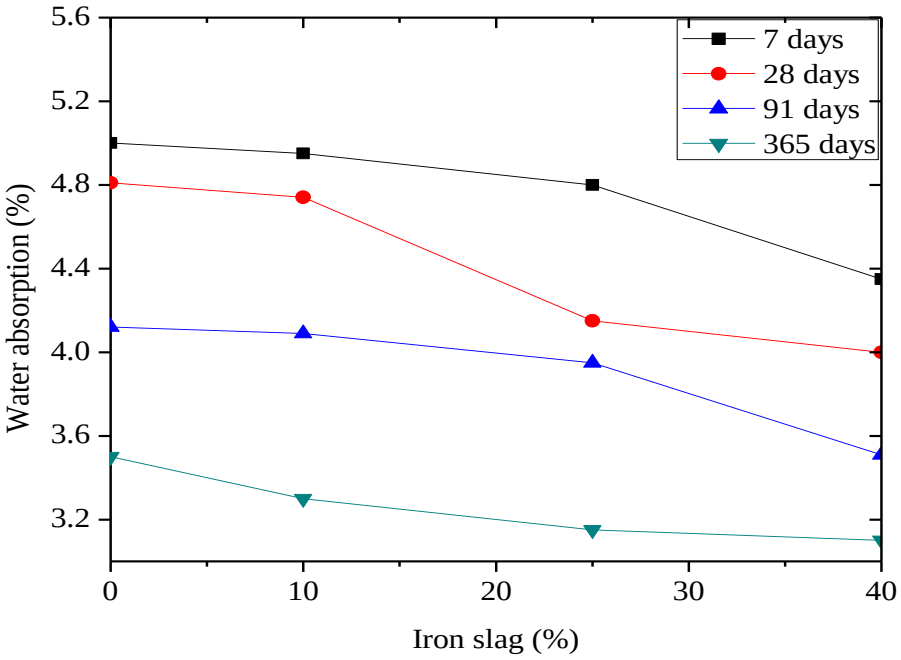

Fig 4.17: Effect of iron slag on water absorption of SCC

SCC mixes with iron slag content shows lower water absorption rate than control SCC at all ages. Results of water absorption versus age are presented in Fig 4.18. Water absorption of control SCC, at 7 days was 5%. Further, at 28, 91 and 365 days the results value decreased about 3.8, 17.6 and 30% respectively. With 10% replacement of iron slag in SCC (SCC-IS10), at 7 days, the observed value of water absorption was 4.95%, and the same SCC mix at 28, 91 and 365 days the results value decreased about 4.24, 17.37 and 33.33%, respectively. When the iron slag content increased from 10 to 25%, at 7 days, absorption value was 4.8%. Further, at 28, 91 and 365 days absorption decreased about 13.54, 17.7 and 34.37%, respectively. With the further increase in iron slag content from 25 to 40% in SCC, the decrease of absorption value was about 8.04, 19.31 and 28.73% at 28, 91 and 365 days, respectively, as compared to 7 days water absorption value of 4.35%.

Water absorption generally related to the structural pores (inter-layer C-S-H) and porous paste, aggregate interface zone, especially more at initial stage (Mehta and Monteito 2006). As seen in the results, water absorption decreases with increase of iron slag content. With iron slag content, internal structure gets denser and reduces void spaces due to early formation of ettringites in SCC with iron slag content. The results of present research are good agreement with those results reported by Sheen et al., 2015.

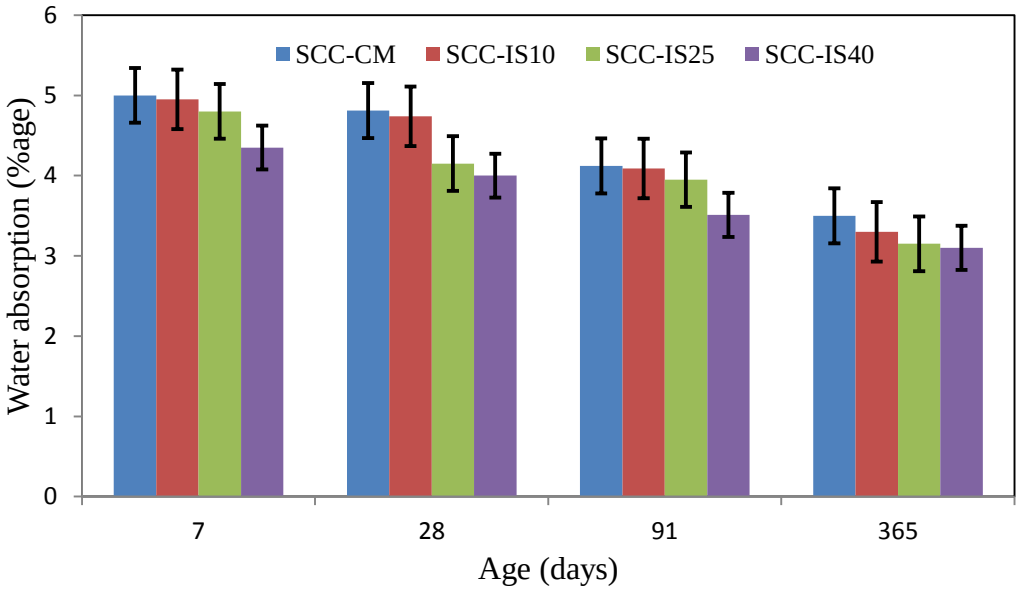

Fig 4.18: Percentage of water absorption verses age of SCC

4.3.2. Sorptivity

Sorptivity measurements were performed on SCC mixes at four different replacements of fine aggregates with iron slag. Three samples were taken from each replacement. Figs 4.19 to 4.22 shows test results of the measurements for each SCC mix with iron slag replacement (0, 10, 25 and 40%). It can be observed from the results that water absorption (Capillary rise) decreased as the iron slag percentage increases. At 7 days, SCC mix containing 10, 25, 40% iron slag as fine aggregates absorbed 10.04, 15.97 and 21.86%, respectively, less water as compared to 7 days absorption value of control SCC. Absorption (sorptivity) of SCC mixes at 28 days made with 10, 25 and 40% iron slag as fine aggregates absorbed 9.05, 22.39 and 29.34%, respectively, less water in comparison to 28-day absorption of control SCC. At 91 days, SCC mixes containing 10, 25 and 40%

iron slag absorbed (capillary rise) 10, 15.97 and 21.86%, respectively, less water as compared to control SCC. At 365 days, SCC mixes containing 10, 25 and 40% iron absorbed 4.67, 8.45 and 13.18% respectively, less water as compared to absorption of control SCC. These percentage values were calculated on the basis of the mean of 15 values observed during the test.

Water absorption and sorptivity are generally related to the structural pores (inter-layer C-S-H), porous paste and aggregate interface zone, especially more at the initial stage. It has been concluded from SEM images, matrix gets denser after the inclusion of iron slag, which may be a cause to reduce the absorption of water after the inclusion of iron slag content.

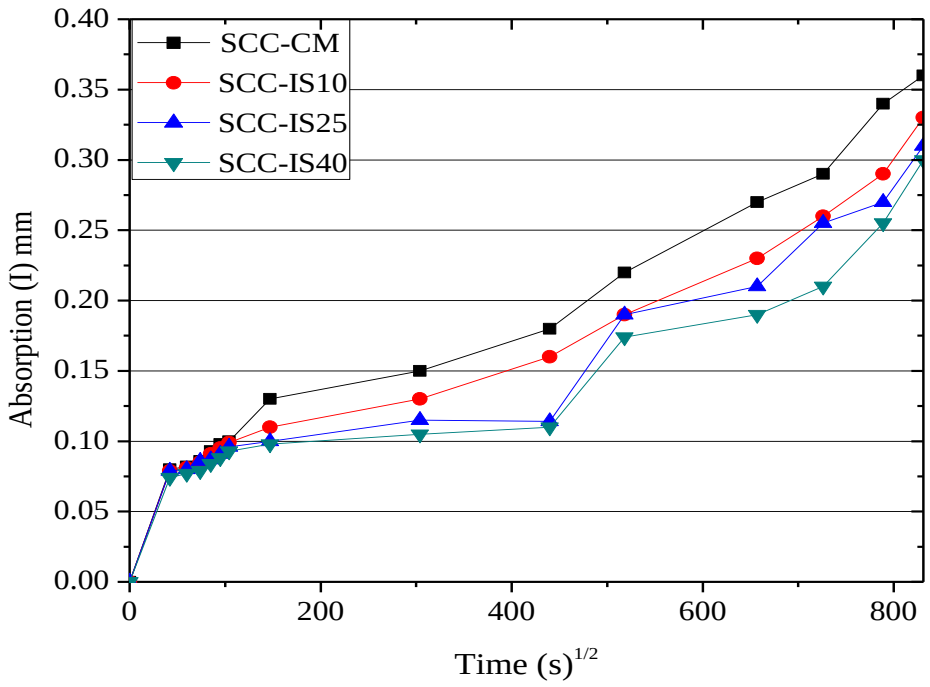

Fig 4.19: Effect of iron slag on sorptivity in SCC at 7 days curing age

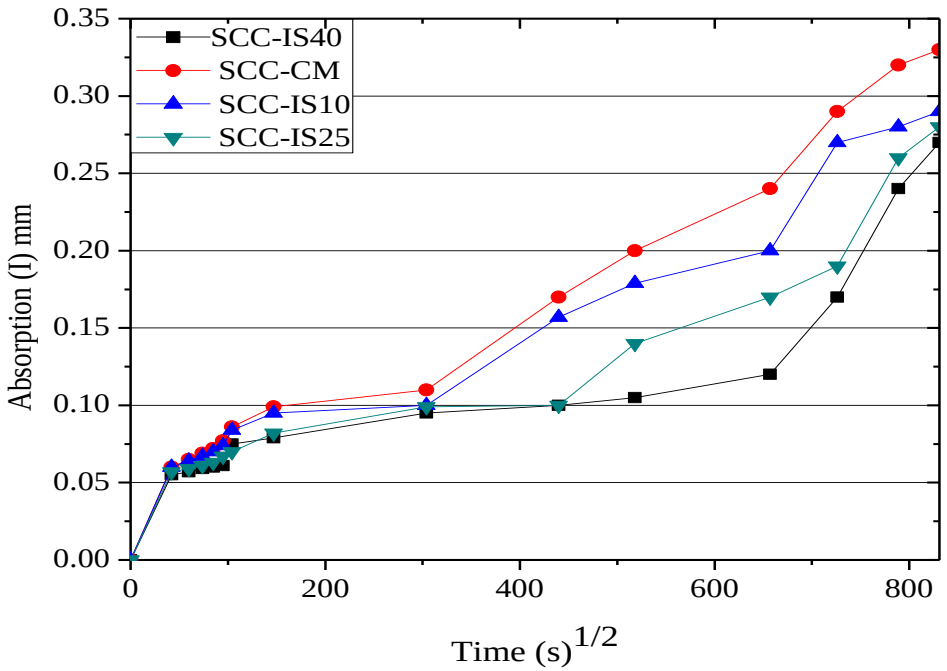

Fig 4.20: Effect of iron slag on sorptivity in SCC at 28 days curing age

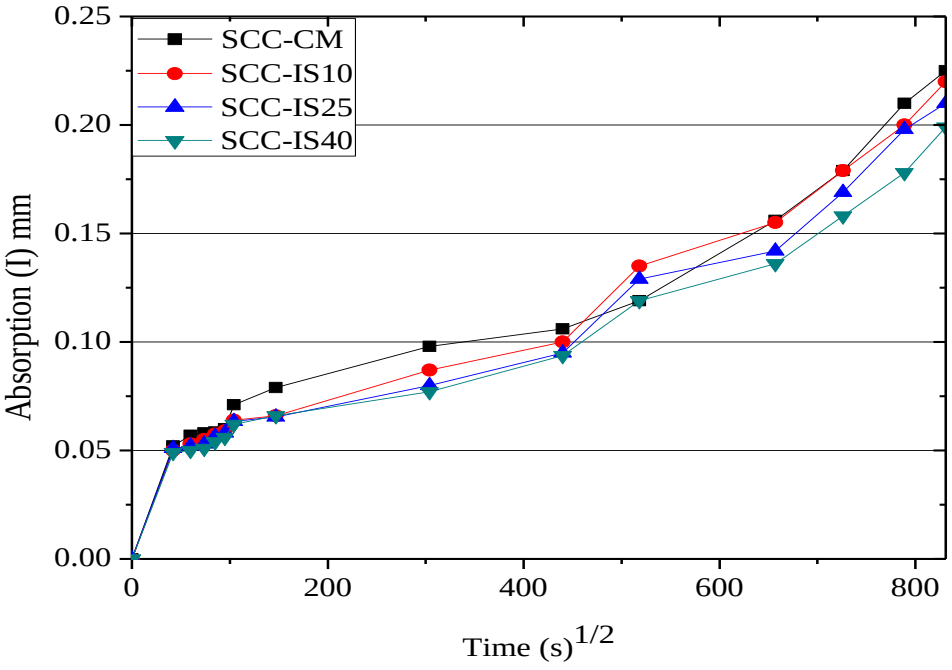

Fig 4.21: Effect of iron slag on sorptivity in SCC at 91 days curing age

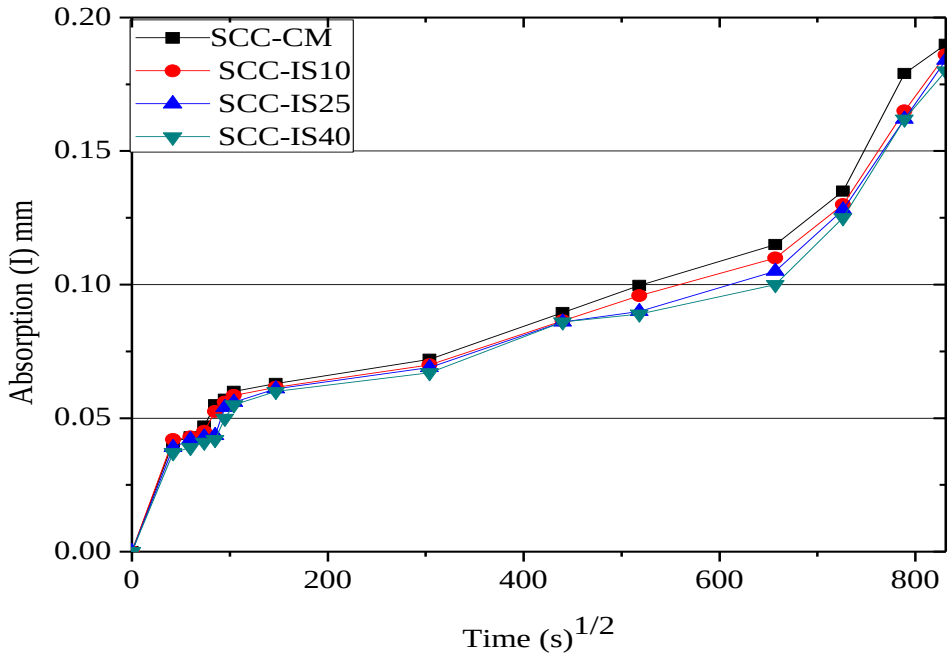

Fig 4.22: Effect of iron slag on sorptivity in SCC at 365 days curing age

As Figs 4.23 to 4.26 depicts that in all SCC mixes, sorptivity (absorption) value decreases as age increases. At 7 days, water absorption (by capillary rise) average value of control SCC was 0.165mm (average of all 15 value measured at different time intervals). Further, at 28, 91 and 365 days sorptivity values decrease of about 11.73, 37.33 and 49.79%, respectively. With 10% replacement, at 7 days, the observed value of absorption was 0.148 mm. At 28, 91 and 365 days the results value decreased about 10.76, 33.60 and 46.10%, respectively. When the iron slag content increased from 10 to 25% in SCC (SCC-IS25), it can be observed from the results, 7 days, water absorption test result value was 0.139 mm. Further, at 28, 91 and 365 days the absorption value decrease of about 18.48, 31.72 and 44.19%, respectively. With the increase in iron slag content from 25 to 40% in SCC (SCC-IS40), the decrease in absorption was about 20.18, 30.37 and 41.50% at 28, 91 and 365 days respectively, as compared to 7 days absorption value of 0.129 mm. Thus, sorptivity (absorption) value decreases with the increase of age.

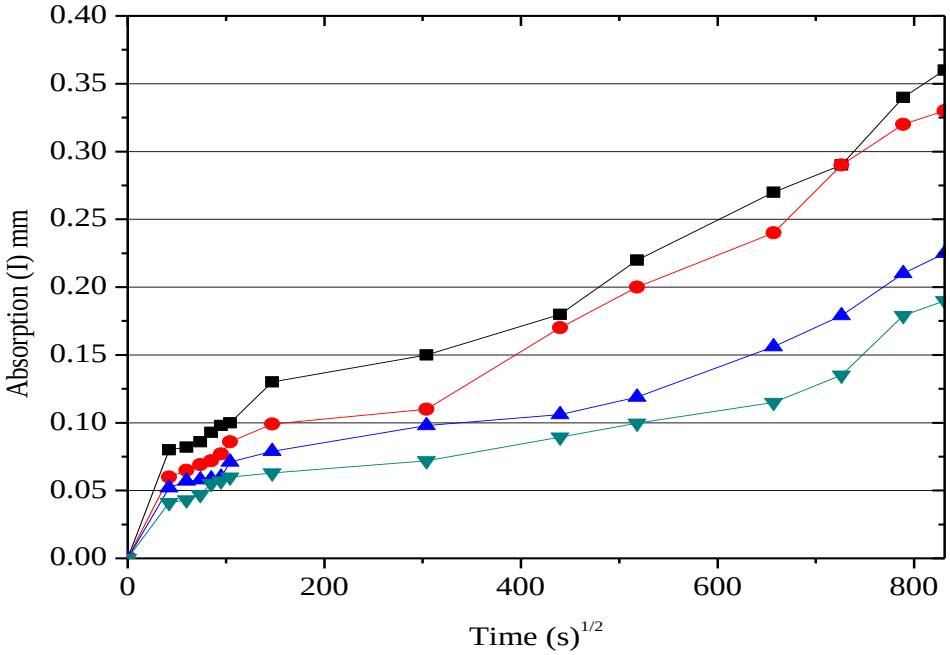

Fig 4.23: Effect of iron slag on sorptivity of SCC without iron slag

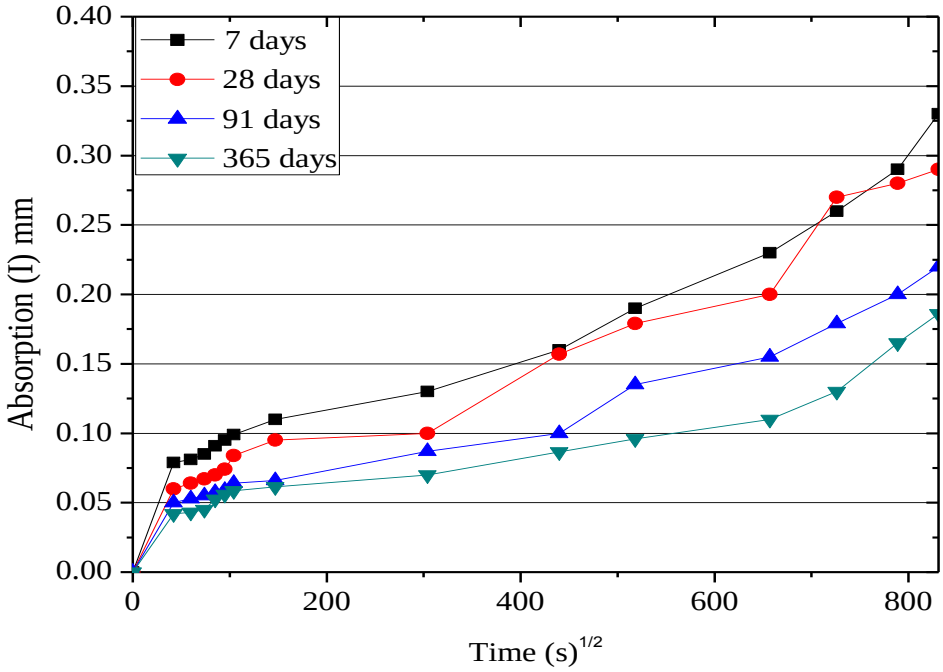

Fig 4.24: Effect of iron slag on sorptivity of SCC with 10% iron slag

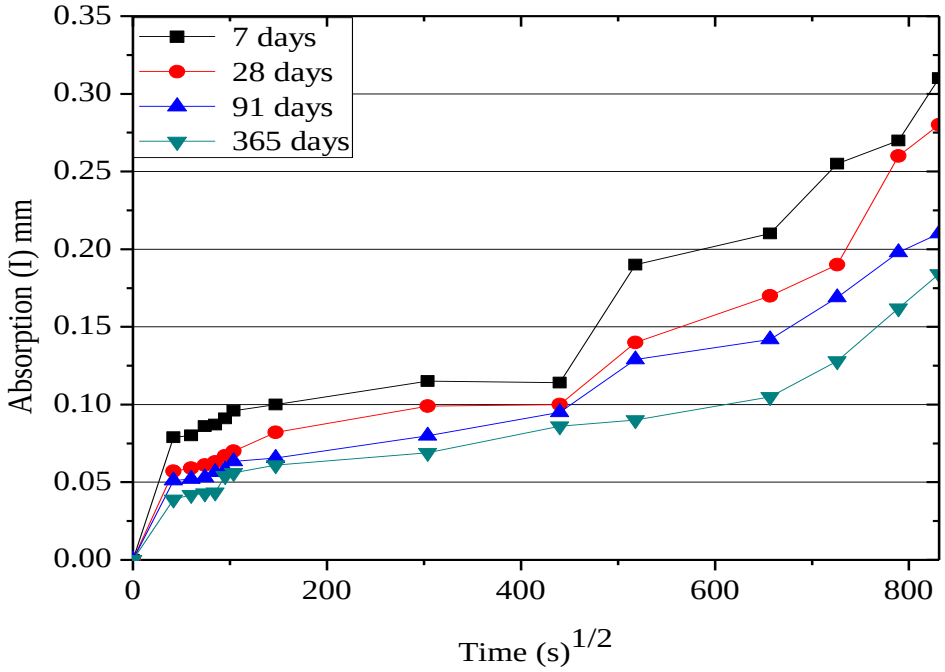

Fig. 4.25 Effect of iron slag on sorptivity of SCC with 25% iron slag

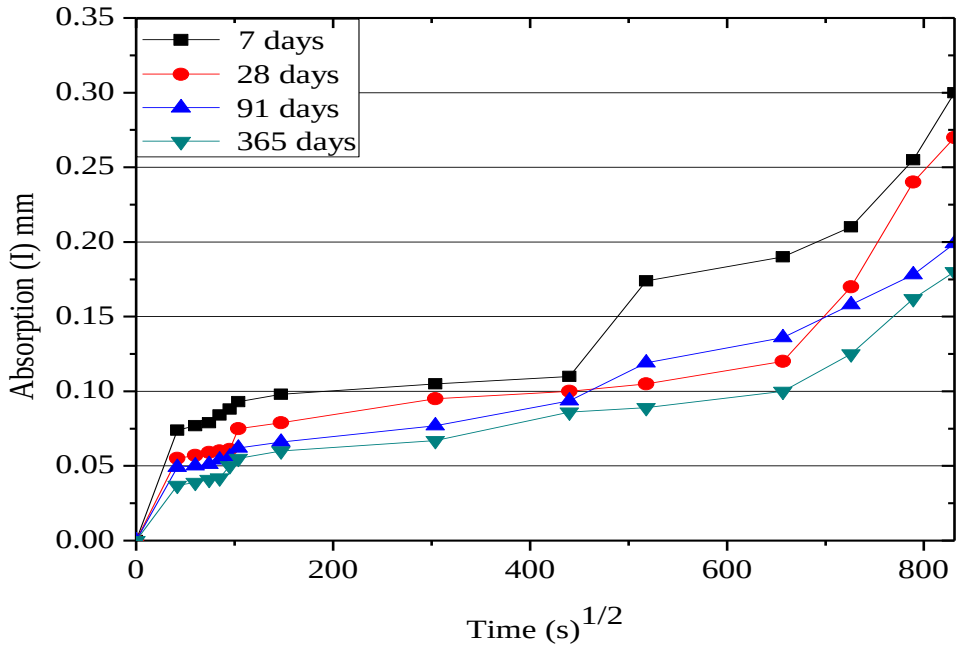

Fig. 4.26 Effect of iron slag on sorptivity of SCC with 40% iron slag

4.3.3. Sulphate Resistance

Concrete is often attacked by sulphates external environment. Sulphate reacts with cement compounds and forms expensive products such as gypsum and ettringites. The formation of ettringites and gypsum due to sulphate reactions results in loss of weight and compressive strength. SCC mixes of various iron slag replacements were tested for sulphate attacks at 28, 91 and 365 days. Mass loss and loss of compressive strength of all the SCC specimens were measured after immersing the specimen in Mg_2SO_4 solution. Results are presented in Fig 4.27. It can be observed from the test results, control SCC performs slightly better than SCC with iron slag content at all replacement levels.

4.3.3.1. Mass Loss

After the immersion in Mg_2SO_4, SCC specimens were measured for mass loss. Findings show that no spalling and cracks were observed in all the SCC specimens during the entire duration of the test. Even after 365 days of immersion in 10% magnesium sulphate solution, no loss in mass at all replacement levels of SCC specimens was observed. However, signs of white deposits were observed after 150 days of immersion period.

4.3.3.2. Change in Compressive Strength

The results of compressive strength after immersion in magnesium sulphate solution are displayed in Fig.4.27. The result shows that in control SCC at 28, 91 and 365 days, compressive strength of water cured specimens was 35.7, 38.5 and 47.3MPa and compressive strength of magnesium sulphate cured specimens was 34.7, 34.2 and 40.2 MPa. With 10% iron slag, at 28, 91 and 365 days, compressive strength of water cured specimens were 37.1, 40.6 and 49.8 MPa and compressive strength of magnesium sulphate cured specimens was 35.9, 35.3 and 41.7 MPa, respectively.

Further, with 25% iron slag, at 28, 91 and 365 days, compressive strength of water cured specimens was 41.2, 44.1 and 55.3 MPa and compressive strength of magnesium cured samples was 40.5, 38.2 and 46.27 MPa, respectively.

Lastly, with 40% replacement of iron slag in SCC, at 28, 91 and 365 days, compressive strength of water cured specimens was 45.1, 49.3 and 59.7 MPa respectively and

compressive strength of magnesium sulphate cured samples was 43.7, 42.6 and 50 MPa, respectively.

Thus it was concluded, the decrease in compressive strength was observed as the SCC mixes immersed in magnesium sulphate solution.

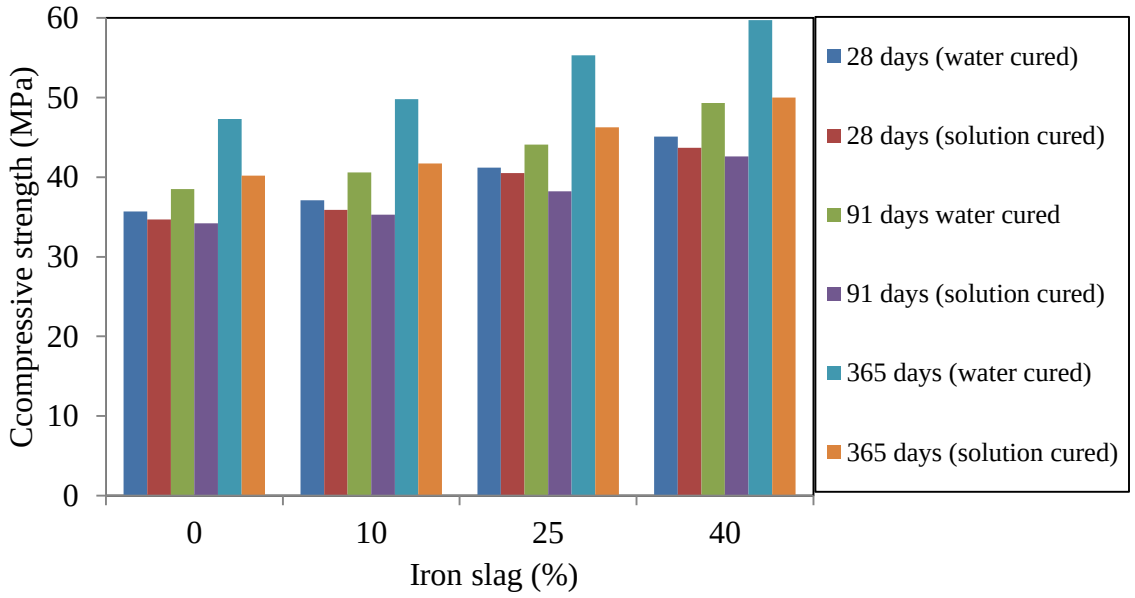

Fig. 4.27: Comparison of compressive strength of water cured and 10% magnesium sulphate solution cured specimens of SCC mixes

Percentage loss in compressive strength after immersion in 10% magnesium sulphate solution is presented in Fig.4.28. In control SCC at 28 days, loss of compressive strength of magnesium sulphate solution specimens was 2.8% more than normal water cured samples. Furthermore, at 91 and 365 days, loss of compressive strength increased up to 11.16 and 15.01%, respectively, with magnesium sulphate solution.

With 10% iron slag at 28 days, loss of compressive strength of magnesium sulphate solution specimens was 3.23% more than normal water cured samples. Furthermore, at 91 and 365 days, loss of compressive strength increased up to 13.05 and 16.26%, respectively, with magnesium sulphate solution.

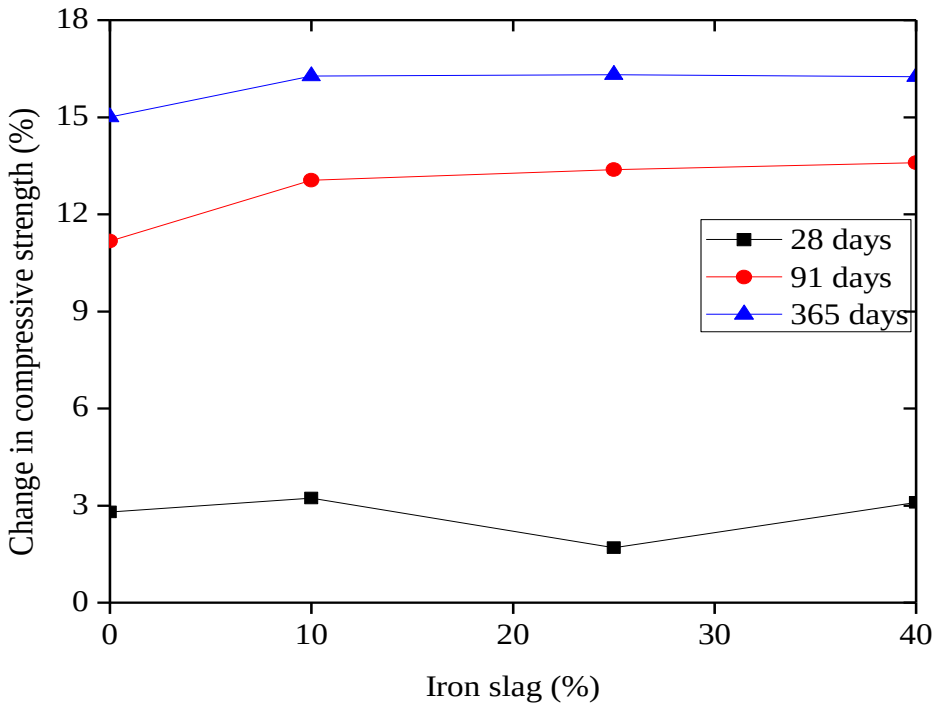

Fig 4.28: Loss of compressive strength of SCC specimens after immersion in 10% magnesium sulphate solution

When the iron slag content was 25% at 28 days, loss of compressive strength of magnesium sulphate solution specimens was 1.69% more than normal water cured samples. Further, at 91 and 365 days, loss of compressive strength increased about 13.37 and 16.32%, respectively.

With the further increase in iron slag content from 25 to 40% in SCC (SCC-IS40), loss in compressive strength was about 3.10, 13.59 and 16.25 % at 28, 91 and 365 days strength respectively, as compared to water cured SCC specimens.

Hence, it was observed from the results, as the immersion time of magnesium sulphate cured specimens increased, the loss of compressive strength also increases and control SCC performed better under the sulphate attack as compared to SCC with iron slag.

4.3.4 Rapid Chloride Permeability

Rapid chloride permeability test results of SCC with and without iron slag content are given in Table 4.8 and shown in Fig 4.29. It depicts the results that, lesser reduction in permeability at all levels of fine aggregates replacement with iron slag and exhibited that permeability decreased with increase in age at all replacement levels. At 7-day, permeability values with 0, 10, 25 and 40% iron slag were 1522, 1493, 1431 and 1366 coulombs, respectively. At 28 days, permeability values with 0, 10, 25 and 40% iron slag were 1268, 1200, 1185 and 1085 coulombs, respectively. Furthermore, at 91 days the result values were 1081, 1056, 1037 and 1017 coulombs at 0, 10, 25 and 40% replacements of fine aggregates with iron slag. Moreover, at 365 days, at all iron slag replacements, SCC mixes exhibited 'very low' permeability values which was lesser than 1000 coulombs. Thus, the percentage decreased in permeability was more at 40% replacement at 28 and 365 days as compared with other replacement levels.

The effect of age on chloride permeability of SCC is presented in Fig 4.30. In control SCC, at 7 days, chloride permeability was 1522 coulombs and at, 28, 91 and 365 days the permeable pore spaces were decreased about 16.68, 28.97 and 40.86%, respectively. With 10% iron slag, at 7 days, chloride permeability was 1493 coulombs. Further, at 28, 91 and 365 days the permeable pore spaces decreased about 19.62, 29.27 and 42.39%, respectively. When the iron slag content increased from 10 to 25% in SCC, it can be observed at 7 days, chloride permeability value was 1431 coulombs, same SCC when at 28, 91 and 365 days, decrease in permeability value was observed about 17.19, 27.53 and 43.39% respectively. With the further increase in iron slag content up to 40% in SCC, decrease in chloride permeability value was about 20.57, 25.54 and 44.36% at 28, 91 and 365 days respectively as compared to 7 days chloride permeability (1366 coulombs).

The decrease in permeability results is good indication for concrete as the void spaces filled by the formation of ettringites. The void space decreases with the increase of age. The permeability results co-relate with the strength results of SCC mixes as compressive strength increases and chloride permeability decreases.

Table: 4.8 Charge passed through SCC specimens

SCC Mix	Coulombs passed at curing age (days)			
	7	**28**	**91**	**365**
SCC-CM	1522	1268	1081	900
SCC-IS10	1493	1200	1056	860
SCC-IS25	1431	1185	1037	810
SCC-IS40	1366	1085	1017	760

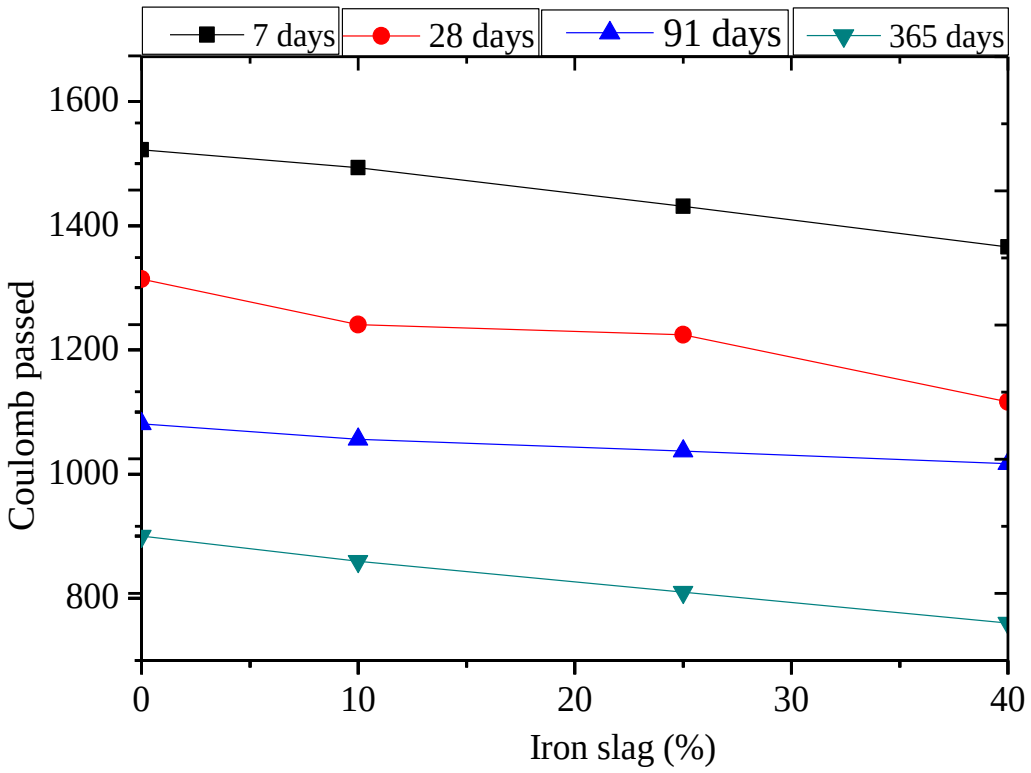

Fig 4.29: Effect of iron slag on chloride ion penetration in SCC

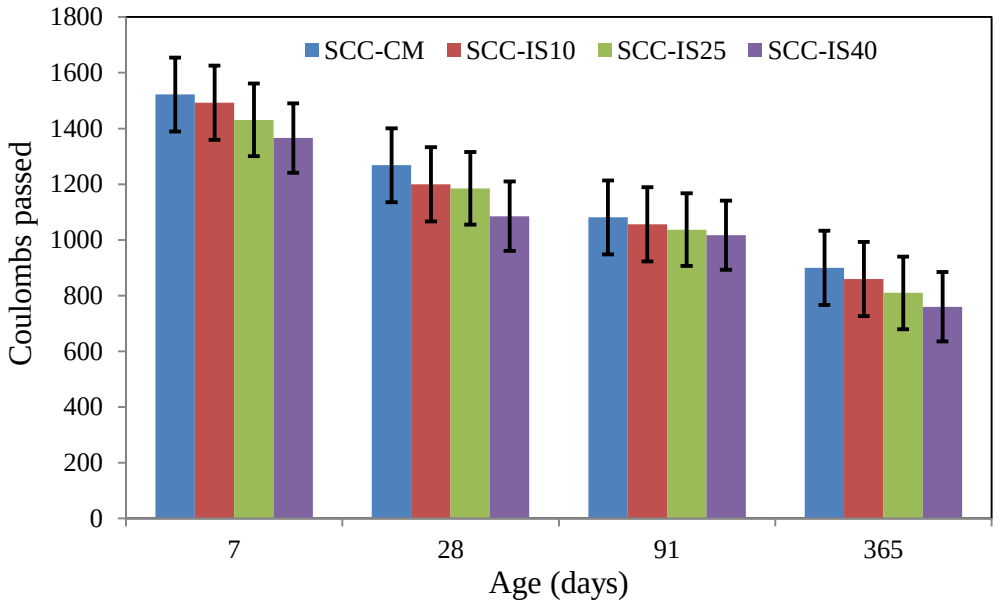

Fig 4.30: Chloride ion penetration of SCC verses age

4.3.5 Abrasion Resistance

Abrasion of the concrete occurs due to scraping, rubbing, skidding or sliding of objects on its surface**.** Abrasion resistance is measured in terms of depth of wear. Reduction in depth of wear indicated enhanced (increased) abrasion resistance and vice-versa.

The test results of wear depth of iron slag SCC and control SCC are shown in Figs 4.31-4.34. Test results show that average depth of wear increased with increase in abrasion time. A research finding indicates that average depth of control SCC mix was higher than SCC with varying iron slag percentages. As iron slag content increased, the depth of wear decreased and also the depth of wear decreased with increase of age. The continued matrix densification of SCC matrix with increasing age may be a possible cause of decrease in average depth. At 7 days, the average depth of wear with 10, 25 and 40% iron slag for 15 minutes of wear time was 3.35, 5.71 and 12.26%, respectively, lower than the control SCC (0.648 mm average depth of wear). At 28 days, average depth of wear was 1.1, 10.00 and 14%, respectively, lower than that of control SCC (0.53 mm average depth of wear). At 91 days, average depth of wear of SCC mixes with iron slag was 2, 8.16 and 12.61%, respectively, lower than the control SCC (0.50 mm average wear of depth of control SCC). In control SCC, average depth of wear at 365 days was 0.39mm. Further, at 10, 25 and 40% iron slag, depth of wear value reduced to 3.11, 8.35 and 13.39%,

respectively. Average depth of wear after 7.5 minutes of wear time of SCC control mix was 0.596 mm against 2 mm mentioned in BIS: 1237-1980 for heavy load tiles. When iron slag content increased from 0 to 10%, no major difference was observed in the depth of wear at all ages and maximum percentage decrease was 3.1%. Further with increase in iron slag content 13% decrease in wear of depth was observed.

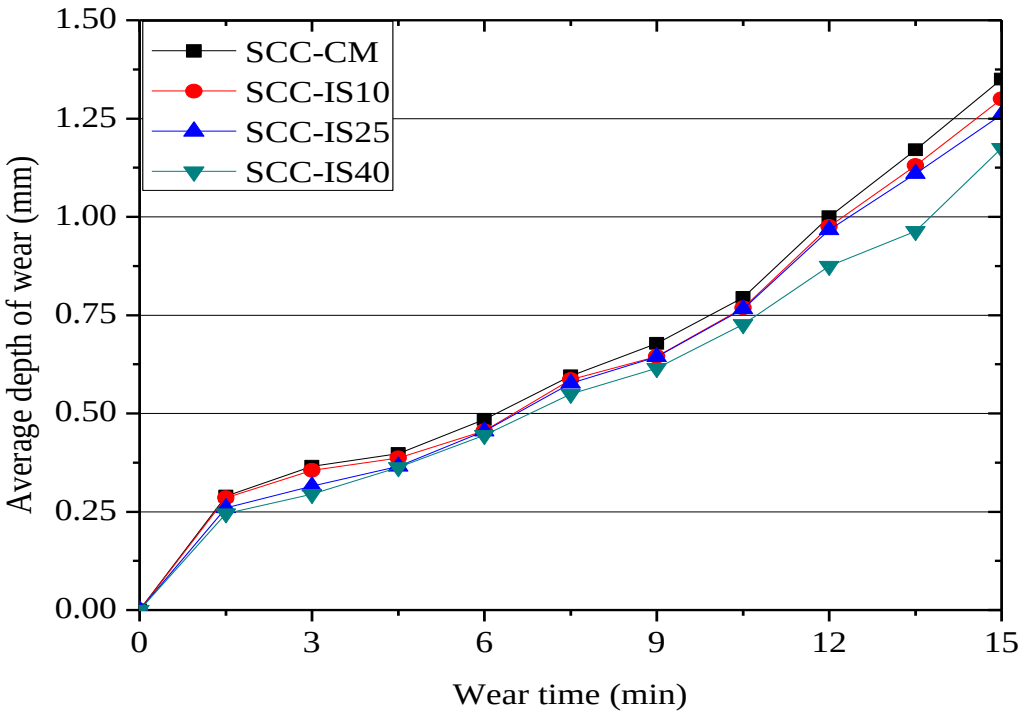

Fig 4.31: Variation in depth of wear with iron slag content in SCC at 7 days of curing age

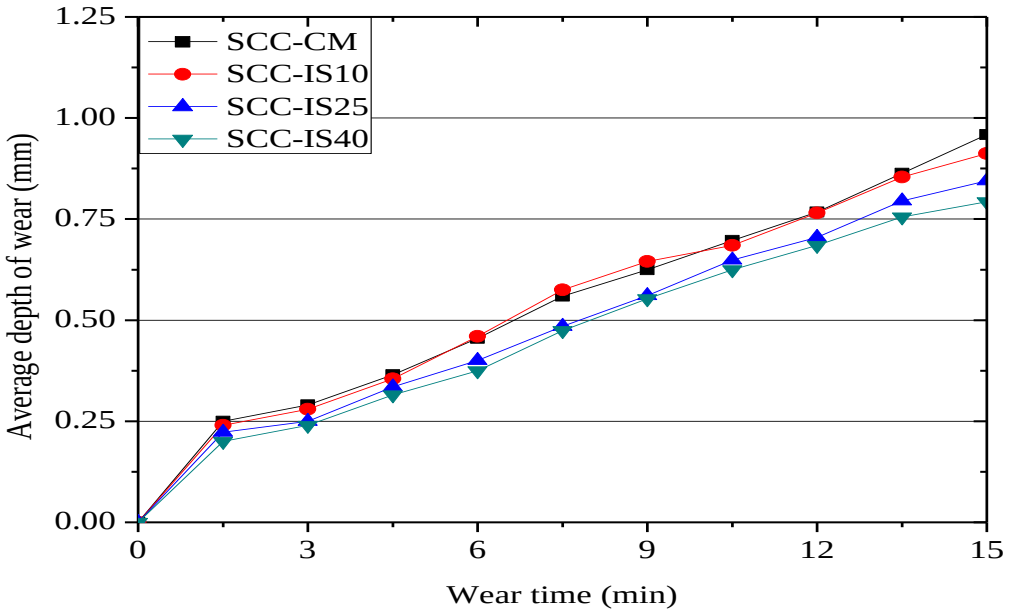

Fig 4.32: Variation in depth of wear with iron slag content in SCC at 28 days of curing age

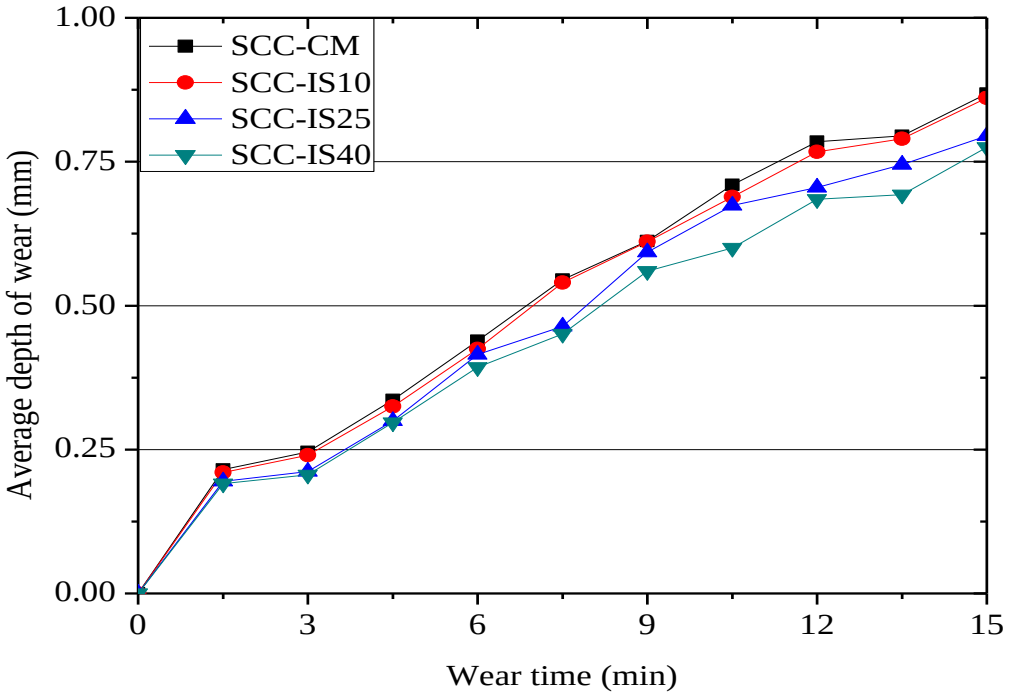

Fig 4.33: Variation in depth of wear with iron slag content in SCC at 91 days of curing age

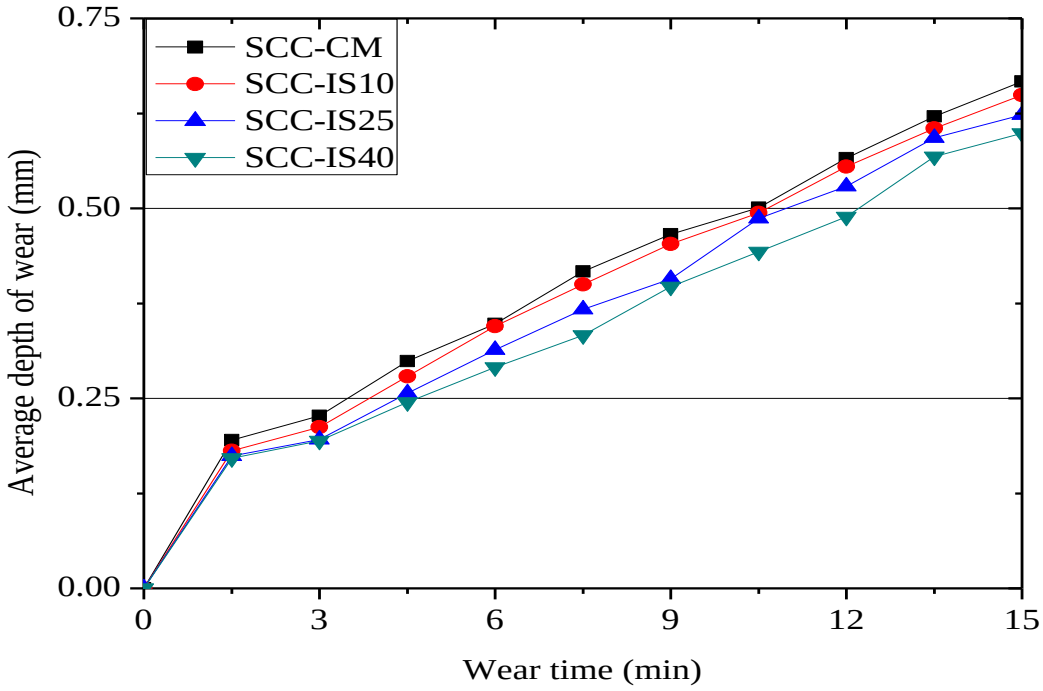

Fig 4.34: Variation in depth of wear with iron slag content in SCC at 365 days of curing age

At all ages, SCC mixes with iron slag content were shows lower depth of wear rate than control SCC. Results are displayed in Figs 4.35 to 4.38. Control SCC (SCC-CM), at 7 days, average depth of wear value was 0.647 mm and at 28, 91 and 365 days, depth of wear decreased about 18.18, 22.11 and 39.56% respectively. With 10% replacement (SCC-IS10), at 7 days age, the observed average value of depth was 0.626 mm. Further, at 28, 91 and 365 days the results value decreased about 16.20, 20.75 and 39.40%, respectively. When the iron slag content increased from 10 to 25% in SCC (SCC-IS25), it can be observed from the results, 7 days, average depth test result value was 0.598. Further, at 28, 91 and 365 days, the results value decreased about 20.50, 32.51 and 52.08%, respectively. With the further increase in iron slag content from 25 to 40% in SCC (SCC-IS40), decrease in average value of depth was about 11.50, 29.75 and 46.14% at 28, 91 and 365 days abrasion respectively as compared to 7 days average depth value of 0.481 mm.

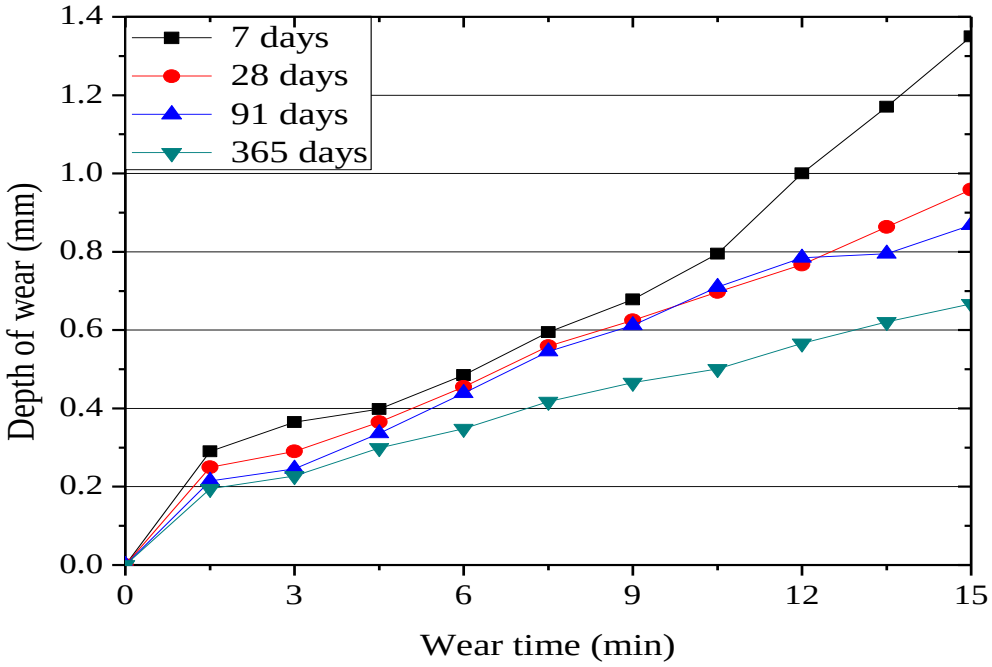

Fig 4.35: Variation in depth of wear with 0% iron slag content in SCC at various curing ages

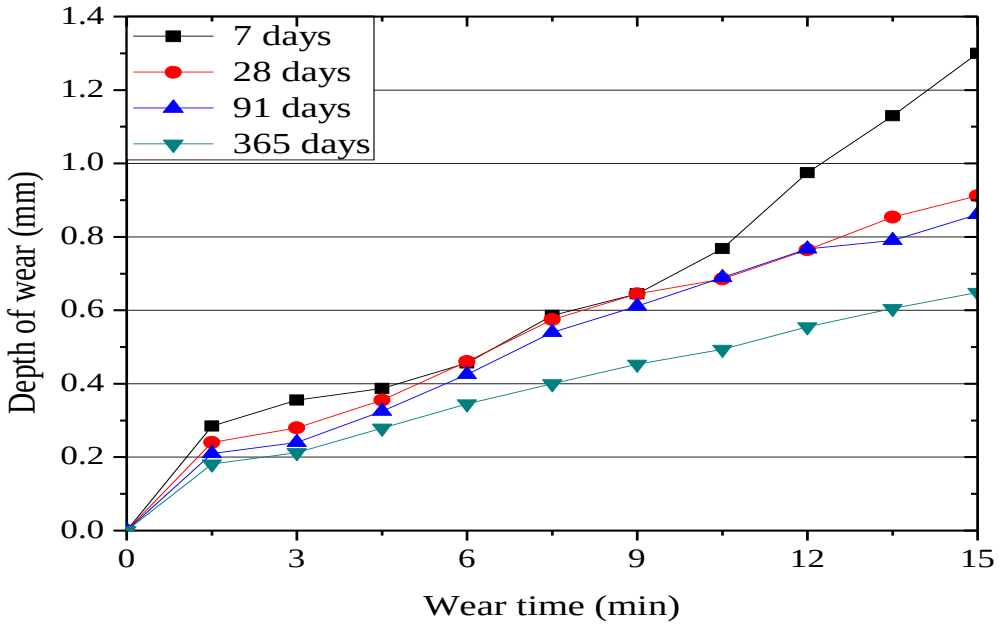

Fig 4.36: Variation in depth of wear with 10% iron slag content in SCC at various curing ages

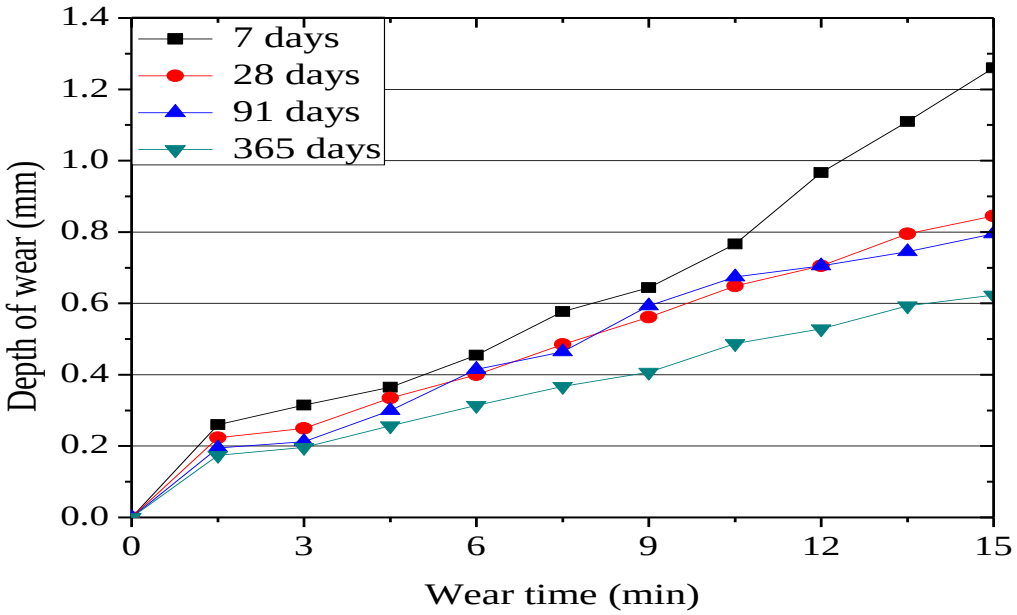

Fig 4.37: Variation in depth of wear with 25% iron slag content in SCC at various curing ages

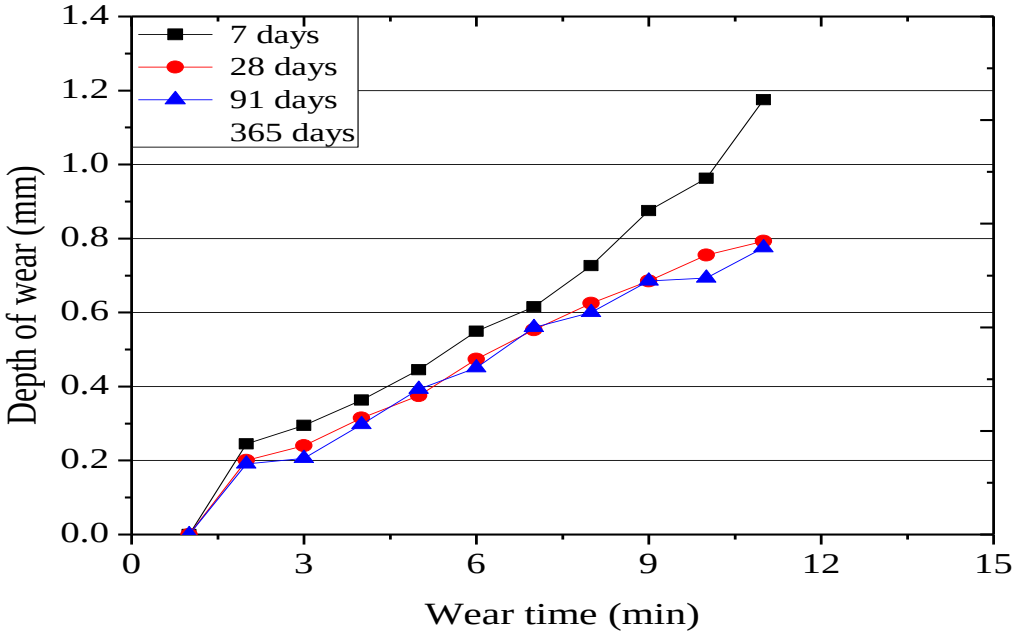

Fig 4.38: Variation in depth of wear with 40% iron slag content in SCC at various curing ages

4.4. NON DESTRUCTIVE TESTING

4.4.1. Ultra Sonic Pulse Velocity (UPV)

The pulse velocity results of SCC with iron slag and SCC control mixes are given in Table 4.9 and displayed in Figs 4.39 and 4.40. The pulse velocity results of SCC mixes with iron slag and control SCC mix were measured at 7, 28, 91 and 365 days. SCC incorporating iron slag exhibited similar trend of UPV results as in case of compressive strength. The pulse velocity result shows that as the percentage iron slag increased, ultra sonic pulse velocity also increases. All the result values of UPV were greater than 4000 m/s which depicts the 'excellent concrete quality' of SCC mixes. In control SCC, at 7 days, lower value of pulse velocity was found to be 4031 and higher value of pulse velocity was observed with 40% replacement at 365 days i.e 4720 m/s and between the values of UPV increased gradually.

The reason for increase in durability properties (rapid chloride permeability, abrasion resistance and ultra sonic pulse velocity) is silica in iron slag that reacts with calcium hydroxide and forms calcium silicates and aluminates hydrate which fills the voids, and improves the micro-structure of SCC, thereby enhancing its durability properties.

Table 4.9: Ultra-sonic pulse velocities through SCC specimens

SCC Mix	Pulse velocity (m/s) at curing period (days)			
	7	28	91	365
SCC-CM	4031	4150	4270	4370
SCC-IS10	4126	4190	4370	4560
SCC-IS25	4137	4220	4400	4600
SCC-IS40	4200	4260	4450	4720

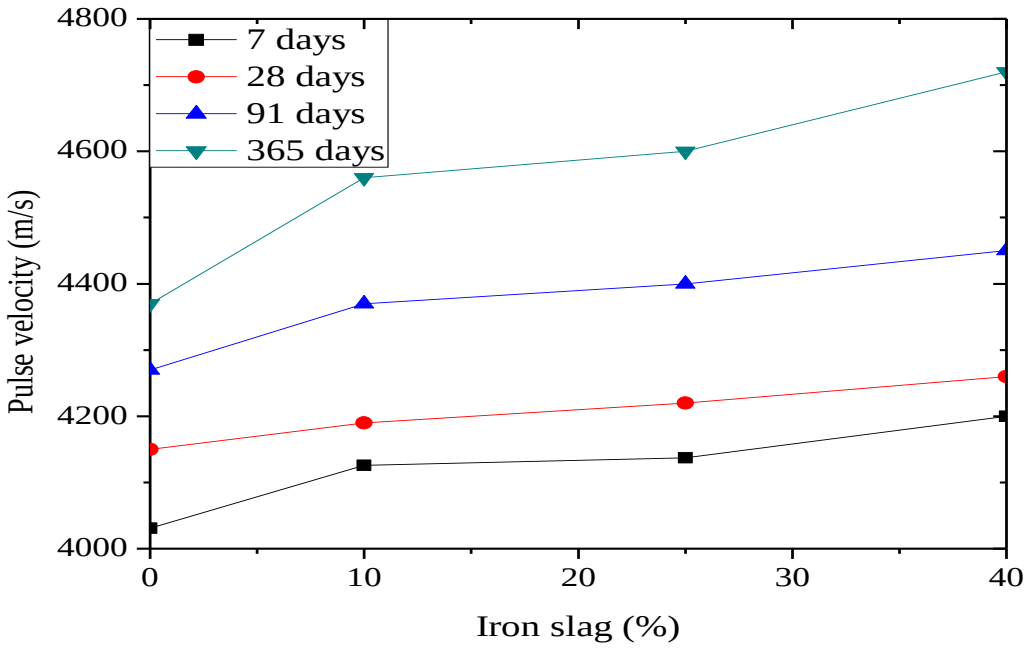

Fig 4.39: Effect of iron slag on pulse velocity of SCC

In control SCC (SCC-CM), at 7 days, ultra sonic pulse velocity value was 4031 m/s. Further, at 28, 91 and 365 days, pulse velocity increased about 3, 6 and 8.4% respectively. With 10% iron slag in SCC mix (SCC-IS-10), at 7 days, pulse velocity value was 4126 m/s and at 28, 91 and 365 days, pulse velocity increased about 1.6, 5.93 and 10.51 % respectively. When the iron slag content increased from 10 to 25% in SCC (SCC-IS25), pulse velocity value at 7-day was 4137 m/s and at 28, 91 and 365 days value increased about 2, 6.35 and 11.20% respectively. With the further increase in iron slag content from 25 to 40% in SCC (SCC-IS40), pulse velocity value increases about 1.5, 6 and 12.4% at 28, 91 and 365 days respectively, as compared to SCC-IS40 at 7 days (4200 m/s). The increase in ultra-sonic pulse velocity result shows that there is improvement in gel/space ratio due to continued hydration with age. The phenomenon also proved by SEM results that pore structure improves with increase of iron slag content and age. Decrease in pore spaces in SCC with iron slag resulted in increase of pulse velocities. All the result value of pulse velocity with or without iron slag content graded as excellent quality. The test results of pulse velocity are good in agreement with previous work reported by Peng and Hwang, 2010, Wang and Lin, 2013 and Sheen et al., 2015.

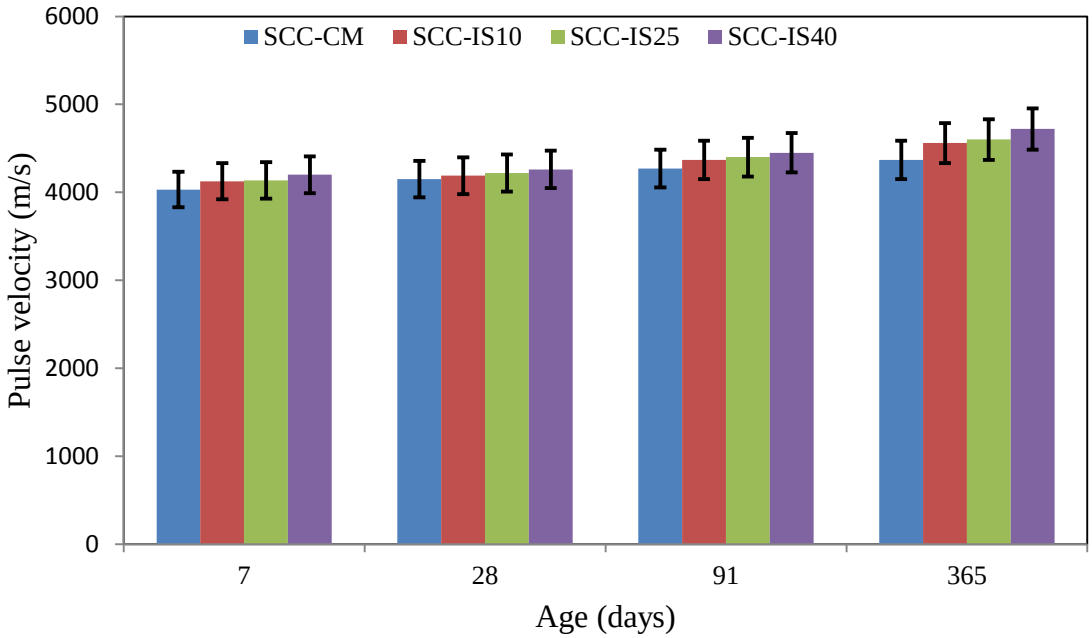

Fig 4.40: Ultra sonic pulse velocity of SCC verses age

4. 5. MICRO-STRUCTURAL PROPERTIES OF SCC

The mechanical parameters of concrete based on its intrinsic microstructure. The concrete structure mainly affected by the hydration period, w/c ratio, substitution of mineral admixture and cement type in the manufacturing of concrete. To assess the micro-structure of SCC, scanning electronic micrograph (SEM) technique was used in this study. SEM provides both topographic and compositional analysis of material. In this experimental study crushed pieces of SCC generated by crushing was mounted on the SEM stub and images was collected using SE image mode. SEM images of SCC-CM (0% iron slag), SCC-IS10 (10% iron slag), SCC-IS25,(25% iron slag) and SCC-IS40 (40% iron slag) are displayed in Figs 4.41-4.52 at age of 28, 91 and 365 days. These micrographs show that clear spread of CSH gel, voids and formation of ettringites in void spaces. Fig 4.41 shows in control SCC, at the age of 28 days. It was observed that micro voids and spread of CSH gel in some areas and formation of ettringites in void spaces. Fig 4.42 shows the similar mix proportion at the period of 91 days. Micro pores/voids, CSH gel and plates of calcium hydroxide were observed in the SE image. Fig 4.43 shows control SCC at 365 days, it was observed that spread of C-S-H gel, small voids and cracks. Fig 4.44 reveals that SCC mixes with 10% replacement of iron slag with fine

aggregates at the age of 28 days. Image being a more mature paste with limited space, reveals well crystal formation. Fig 4.45 depicts the same mix proportion at the age of 91 days. It was clearly observed that the formation of ettringites in void spaces and CSH gel is more widely spread. Fig 4.46 shows SCC mix with 10% iron slag. It was clearly observed that ettringites formation in void spaces and C-S-H gel in some areas. Fig 4.47 shows SCC mix with 25% iron slag replacement with fine aggregates at the age of 28 days. It was observed pore structure improved to greater extent and image shows the well crystal formation. Furthermore a similar mix proportion at the age of 91 days is illustrated in Fig 4.48. It was observed that dense CSH gel was fully spread over the micrograph leading to highly uniform and dense structure. The CSH formation serves as a thin pliable sheet of material. This would make concrete more resistant to aggressive environment. Fig 4.49 shows SCC mix with 25% iron slag replacement at 365 days, it was observed that CSH gel was fully spread on the micrograph leading to highly uniform and dense structure. The CSH formation serves as a thin pliable sheet of material Fig 4.50 shows SCC mix with 40% iron slag replacement at the age of 28 days. Image shows more mature paste with minimal void spaces and widely spread of CSH gel. Fig 4.51 reveals the same mix proportion at the age of 91 days.SCC mix, illustrates ettringites with its needle like habit calcium hydroxide crystals showing their characteristic cleavage. CSH gel identified its short needle like form and fine bundles and ettringite needles. Fig 4.52 shows the SCC mix with 40% replacement. Image shows more mature paste with minimal void spaces and widely spread of CSH gel. It was clearly observed from SEM images that internal structure of concrete gets denser after the inclusion of iron slag and no voids and ettringites formation was visible at 25 and 40% replacement and image area covered by thin layer of C-S-H gel. However, at 0% replacement level some voids are visible. It is concluded that, replacement of iron slag in SCC gives good effect to its strength and durability properties.

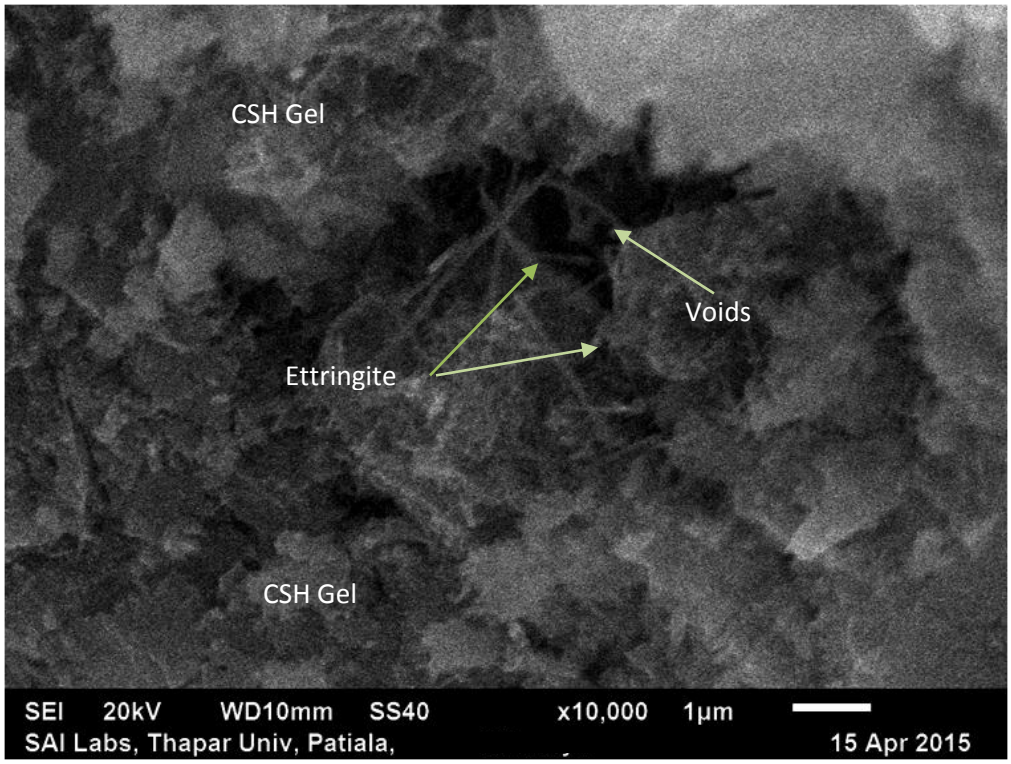

Fig. 4.41 SEM image of SCC (without iron slag) at 28 days

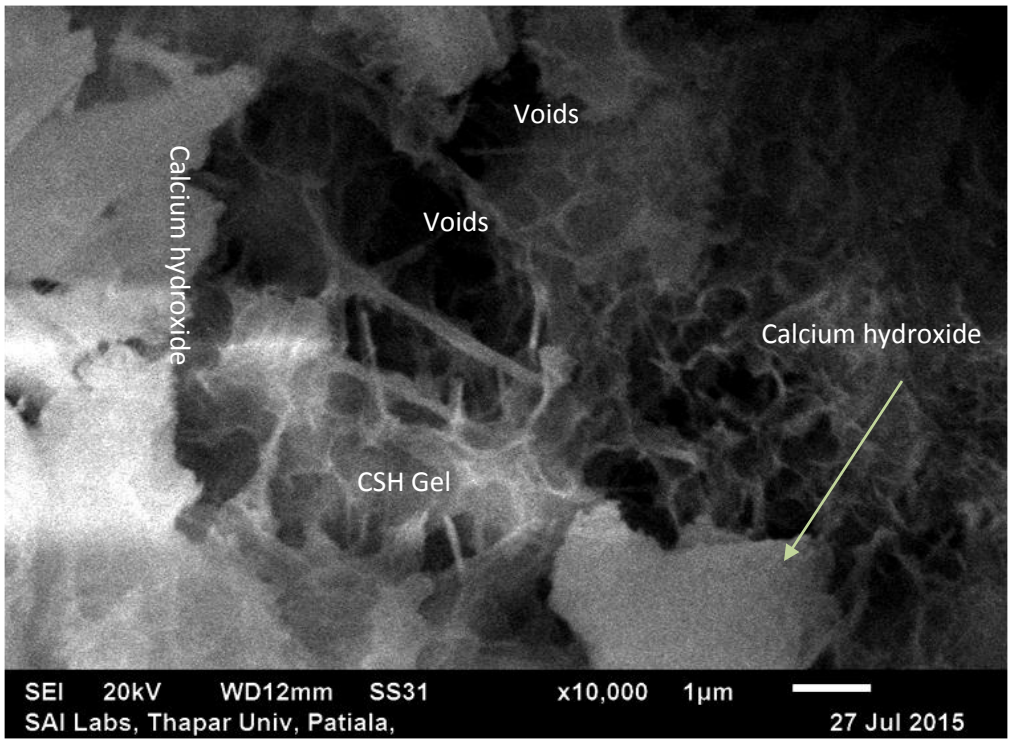

Fig 4.42: SEM image of SCC (without iron slag) at 91 days

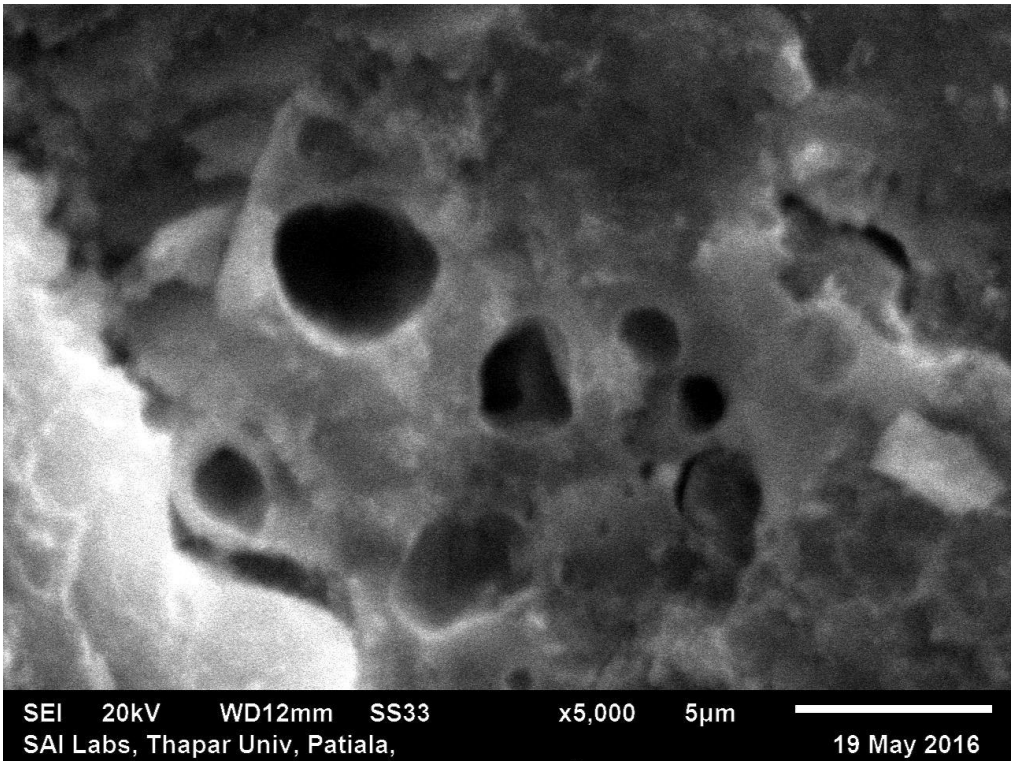

Fig 4.43: SEM image of SCC (without iron slag) at 365 days

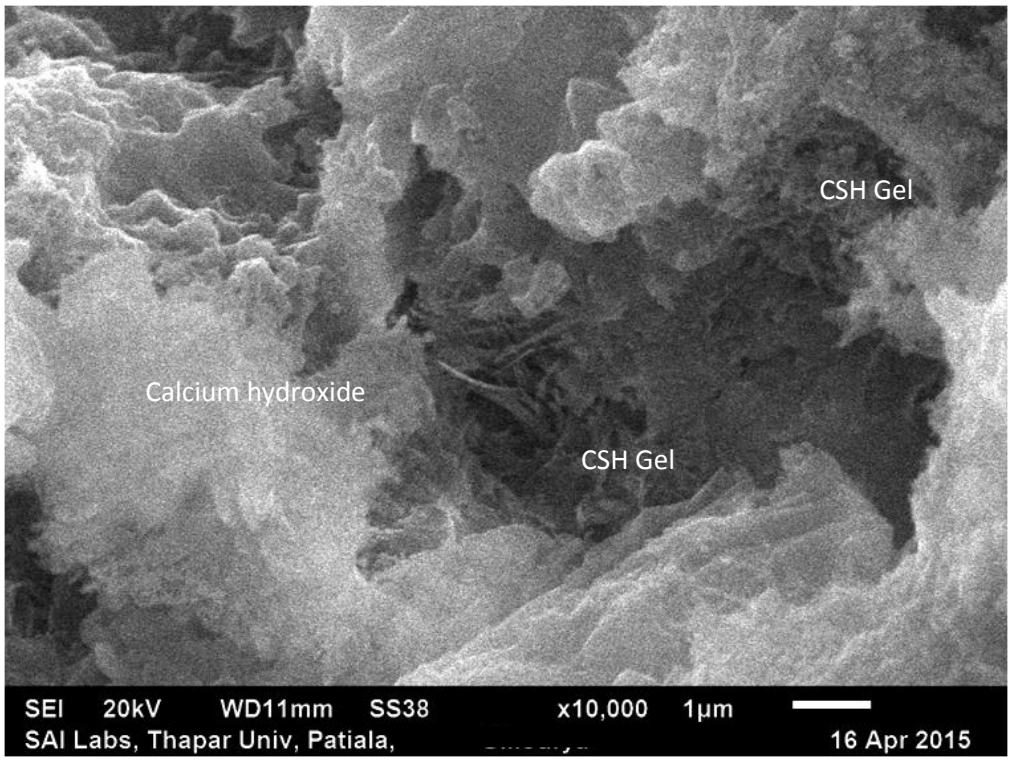

Fig 4.44: SEM image of SCC (with 10% of iron slag) at 28 days

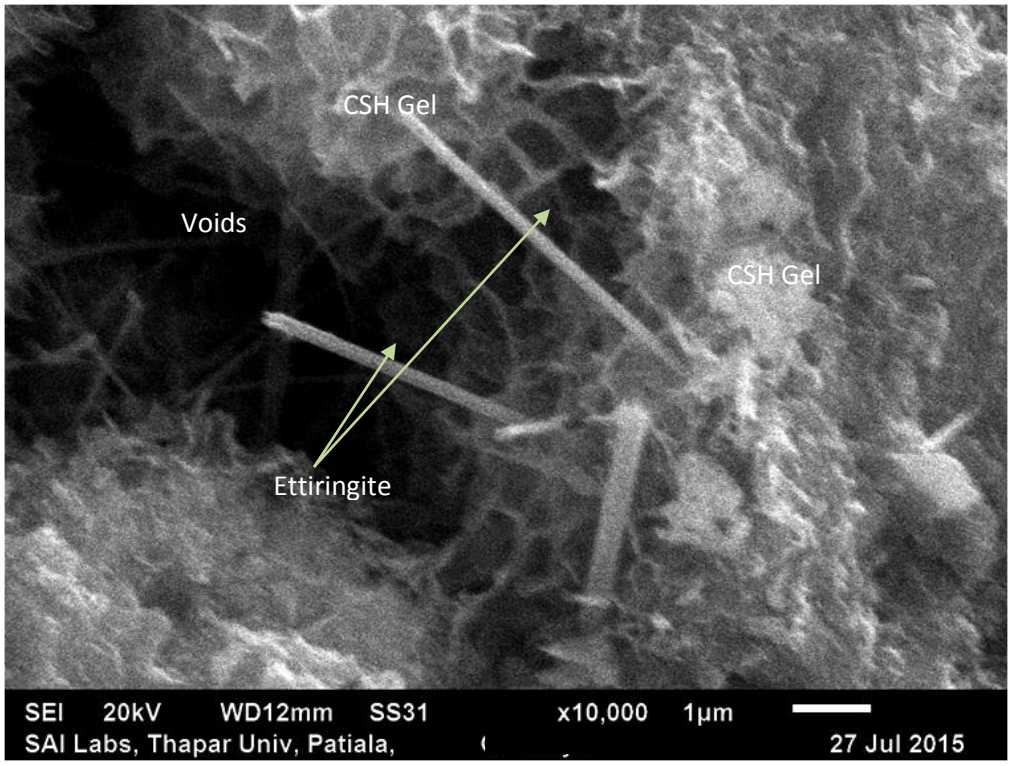

Fig 4.45: SEM image of SCC (with 10% of iron slag) at 91 days

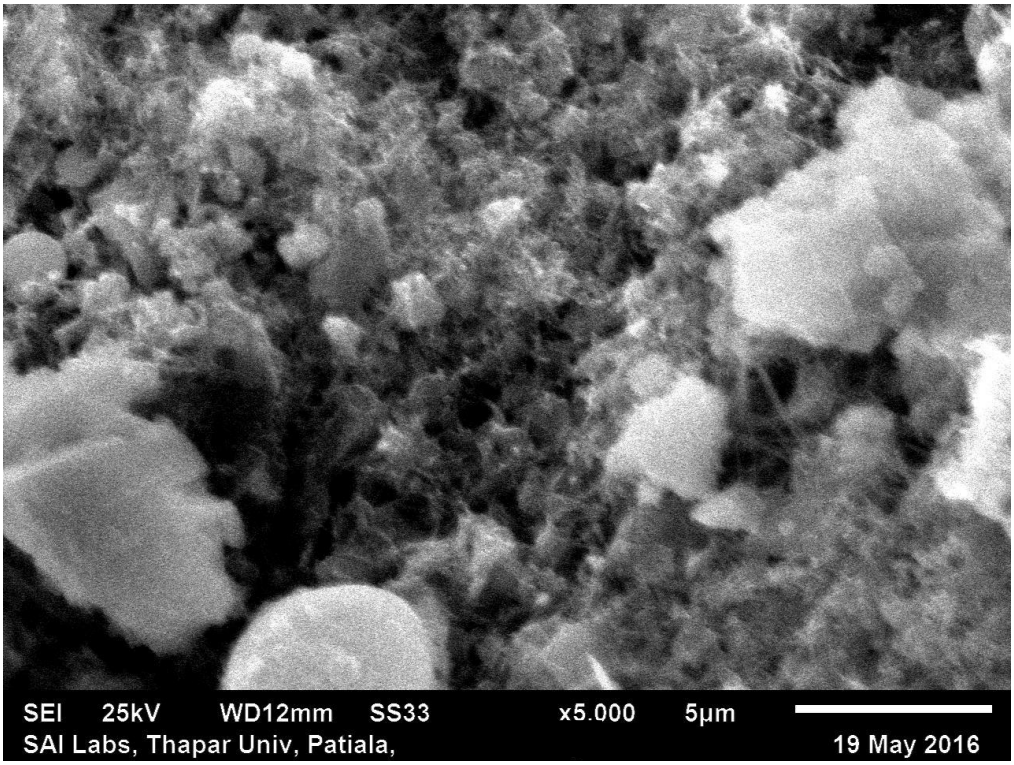

Fig 4.46: SEM image of SCC (with 10% iron slag) at 365 days

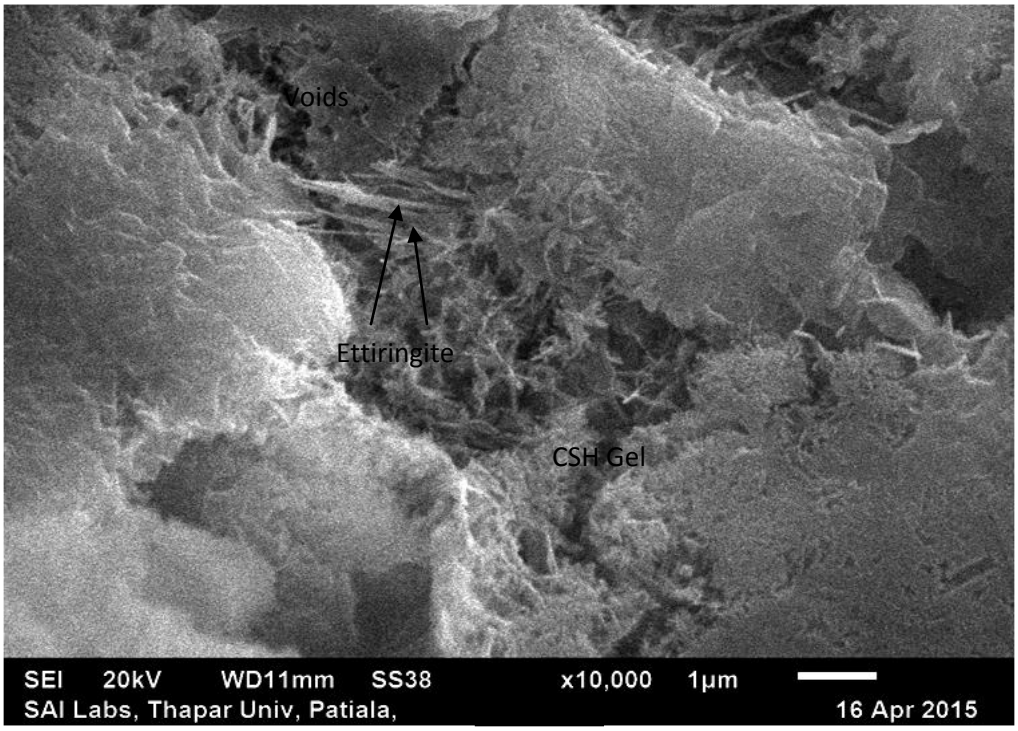

Fig 4.47: SEM image of SCC (with 25% of iron slag) at 28 days

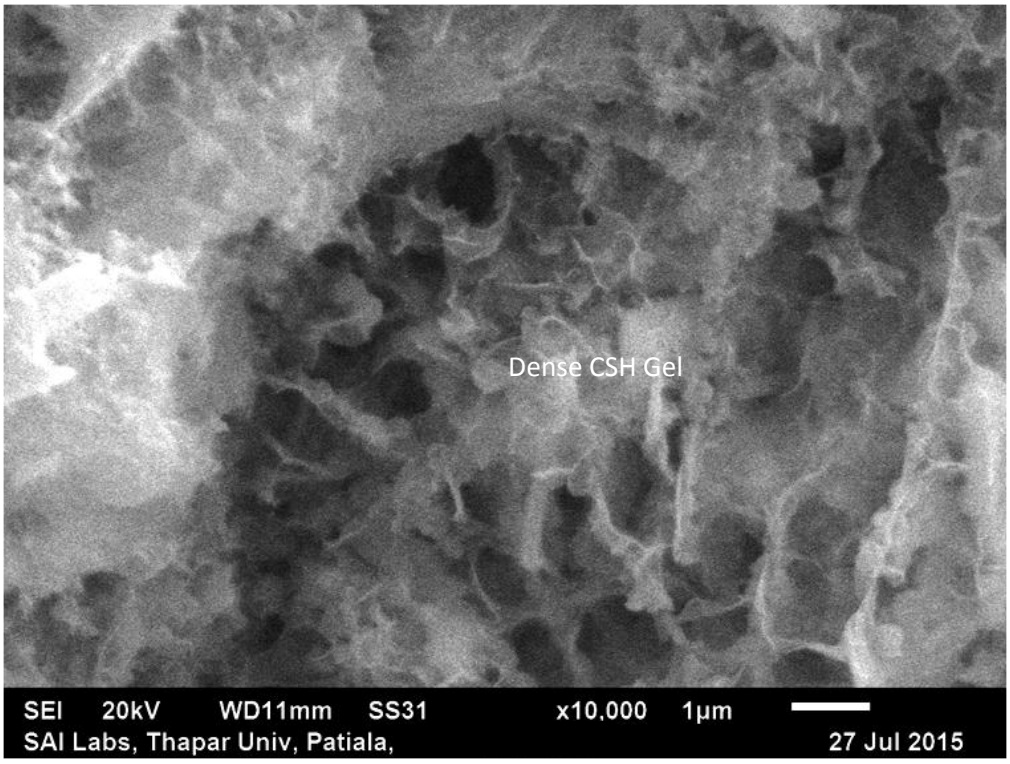

Fig 4.48: SEM image of SCC (with 25% of iron slag) at 91 days

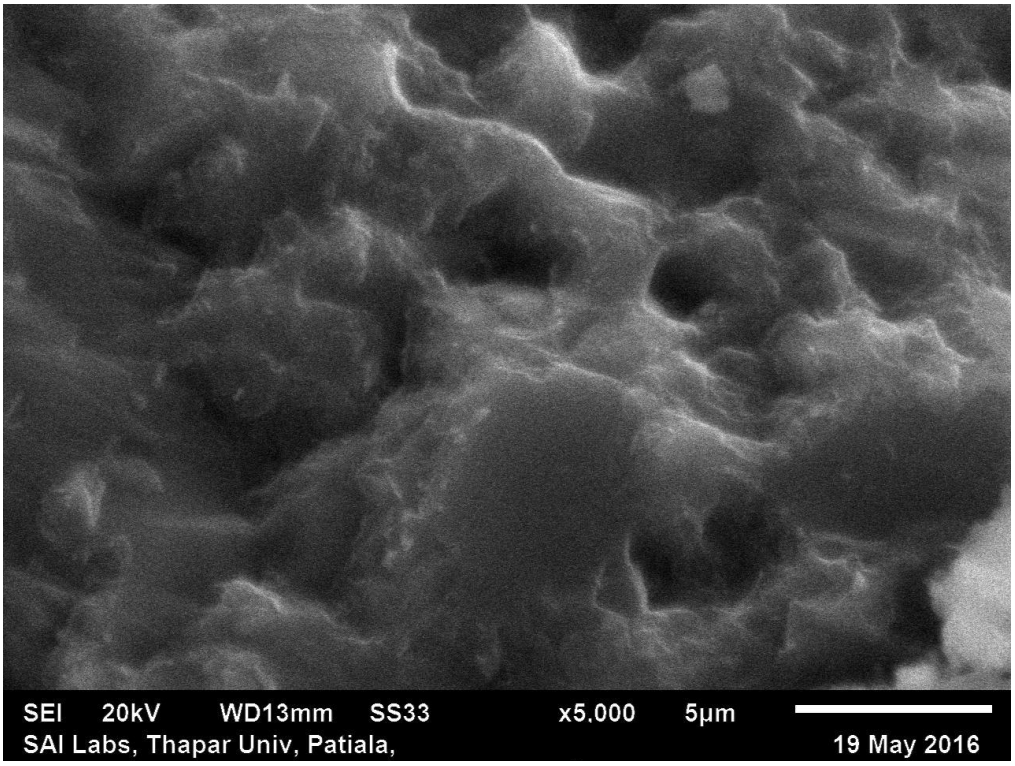

Fig 4.49: SEM image of SCC (with 25% iron slag) at 365 days

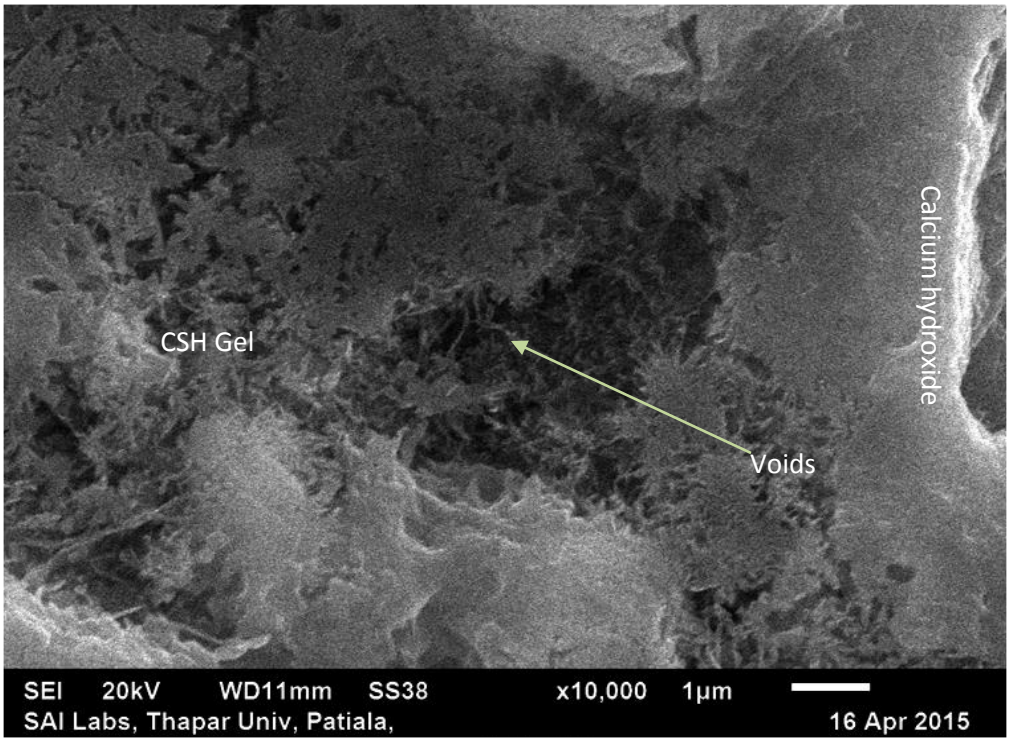

Fig 4.50: SEM image of SCC (with 40% of iron slag) at 28 days

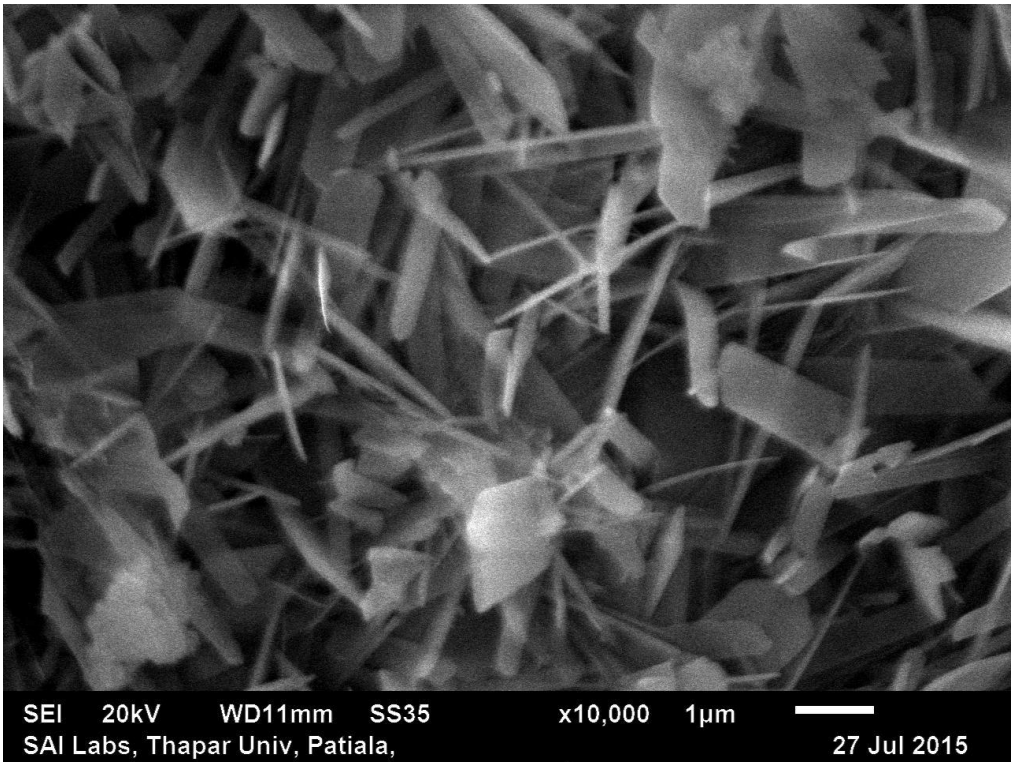

Fig 4.51: SEM image of SCC (with 40% of iron slag) at 91 days

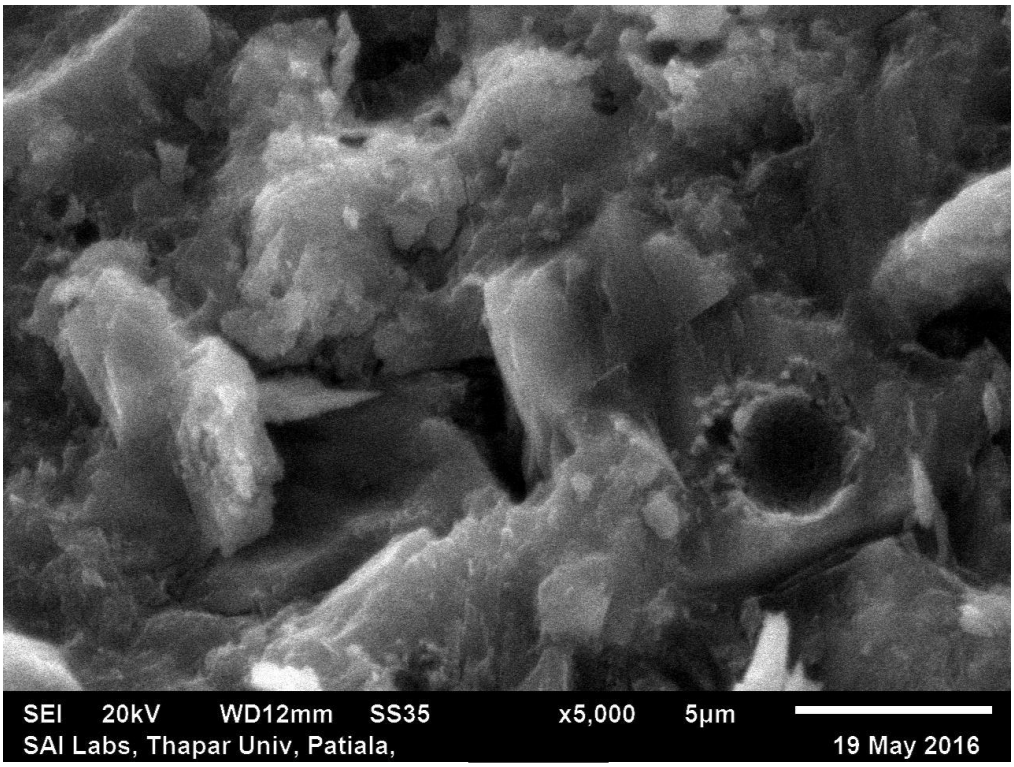

Fig 4.52: SEM image of SCC (with 40% iron slag) at 365 days

4.6. XRD PHASE ANALYSIS

X-ray spectrum of SCC mixes SCC-CM, SCC-IS10, SCC-IS25 and SCC-IS40 for 28, 91 and 365 days are presented in Figs 4.53-4.64. Cement paste sieved from 90µm sieve after separated from concrete samples. The XRD results were done for diffraction angle 2θ ranged between 10° to 70° and peaks were prepared. The XRD data for crushed samples were tested on Panalytical's X'Pert pro with Cu Kα radiation at SAI labs, Thapar University, Patiala. The X'Pert High Score Plus software was used to identify the phases.

The XRD shows the existence of hydrated phases such as quartz, calcium hydroxide, calcium silicate hydrates, calcium ion oxide, calcium silicates, calcite. One main problem occurred in the qualitative and quantitative analysis of SCC mixes was overlying of peaks. XRD analysis of all the mixes shows that there is no qualitative change in the phases present.

Weak peak and Broad base of CSH gel observed at 32°. Broad base peaks of CSH are at 29°, overlapping of calcite and calcium hydroxide at 47° and overlapping of quartz and CSH at 50°.

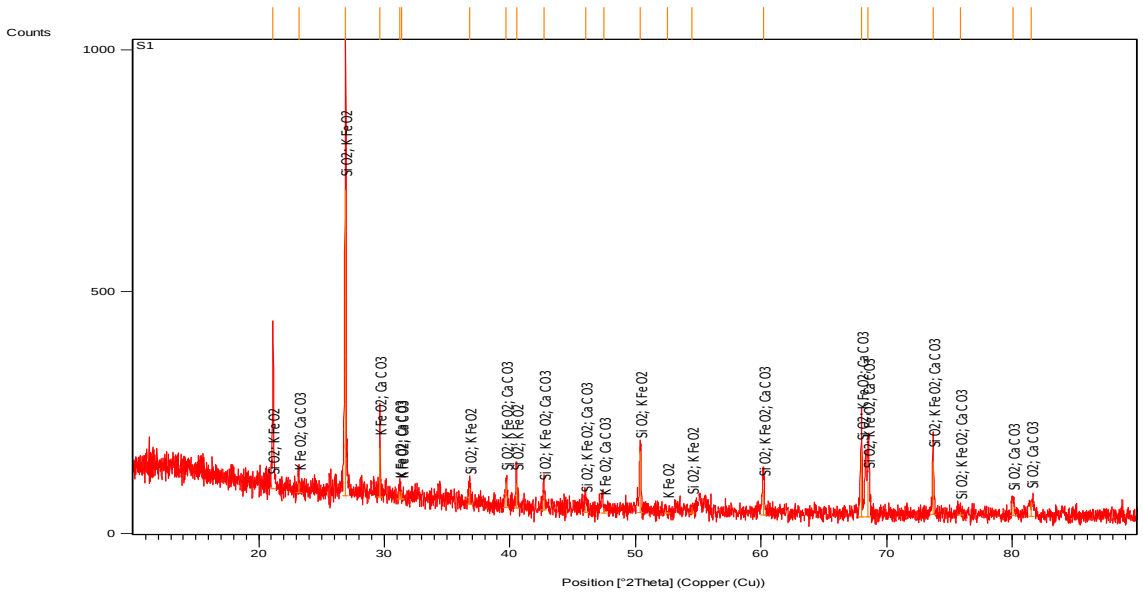

Fig 4.53: XRD spectra of SCC mix with 0 % iron slag at 28

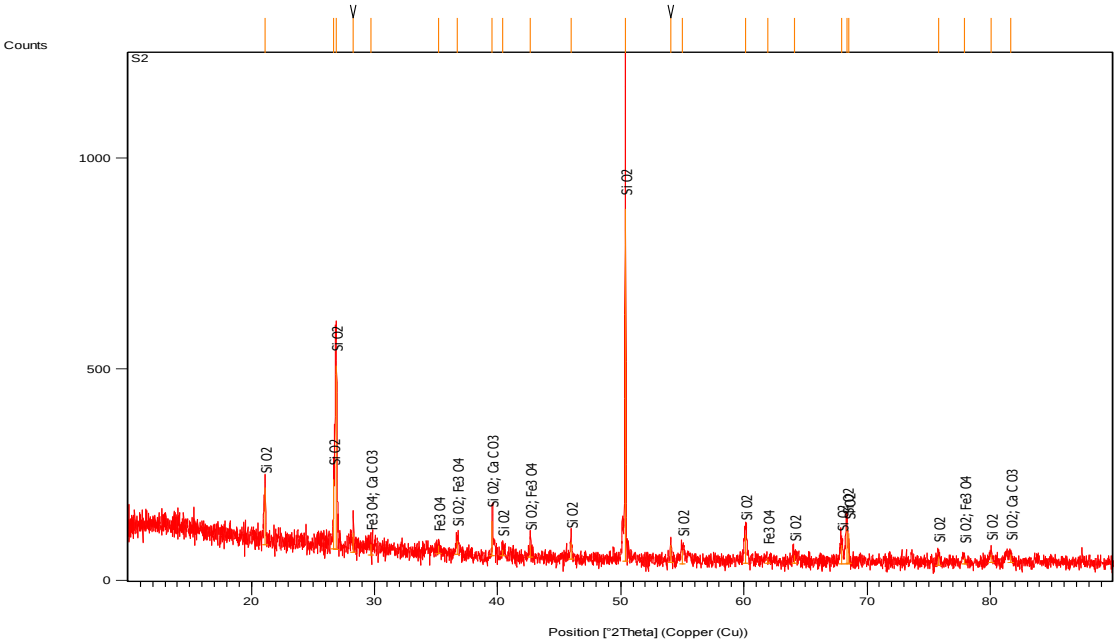

Fig 4.54: XRD spectra of SCC mix with 10 % iron slag at 28 days

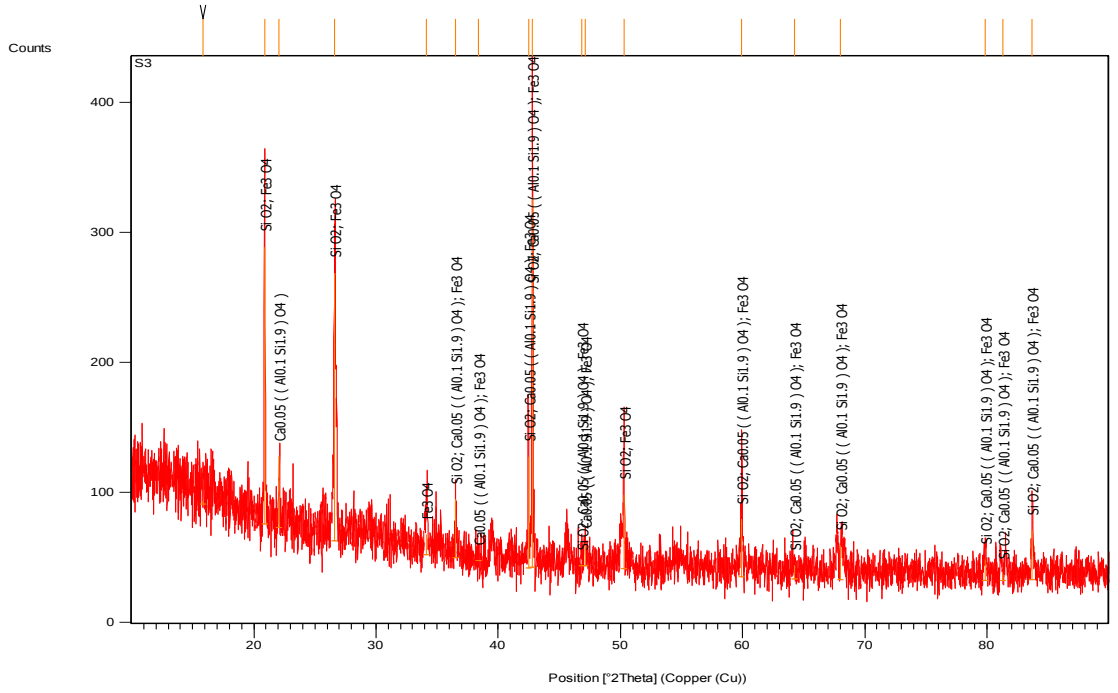

Fig 4.55: XRD spectra of SCC mix with 25% iron slag at 28 days

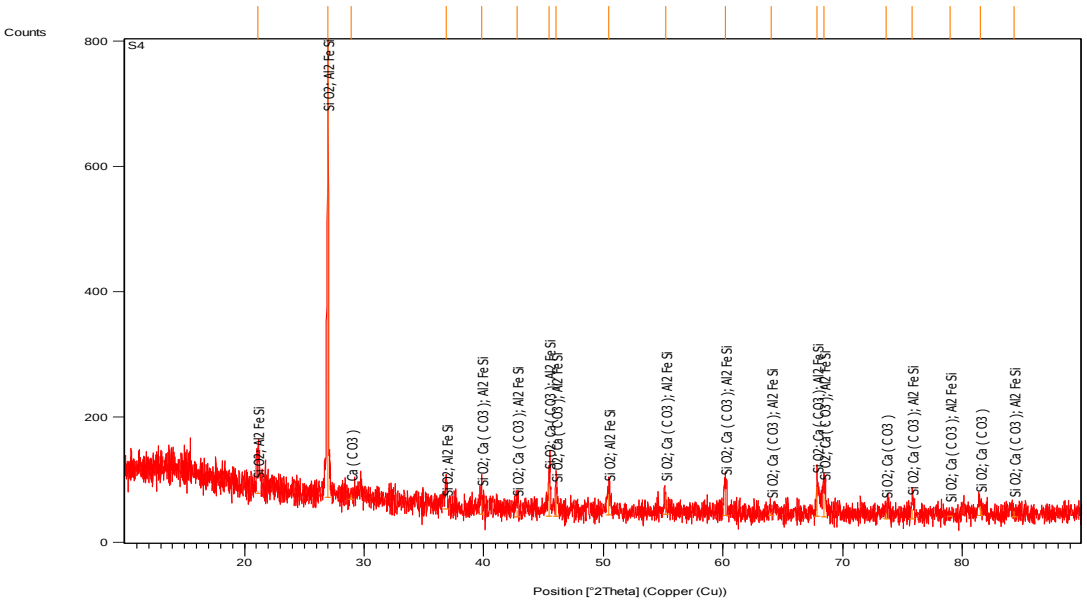

Fig 4.56: XRD spectra of SCC mix with 40% iron slag at 28 days

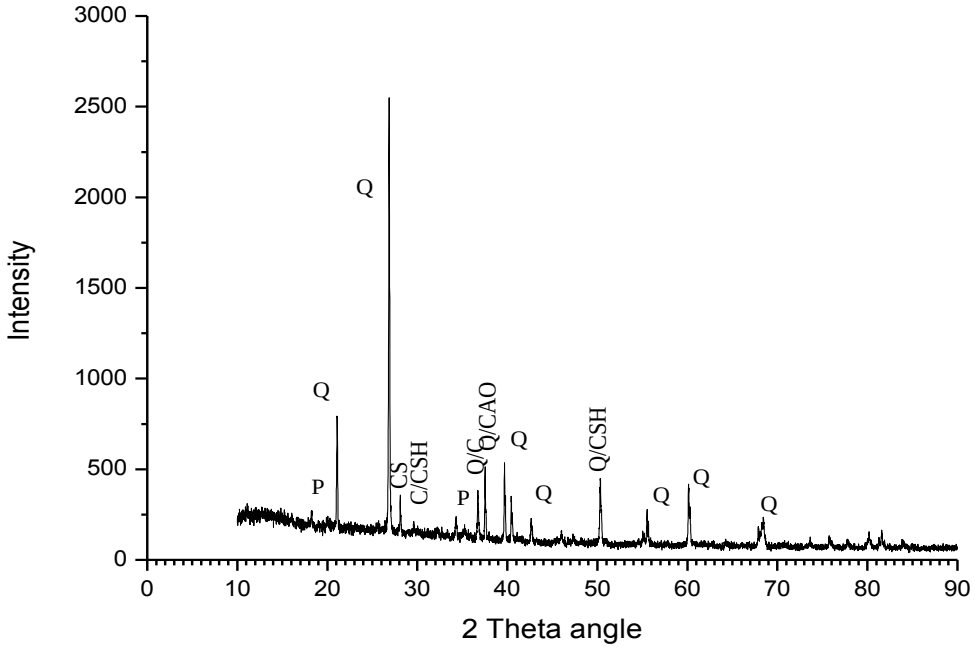

Fig 4.57: XRD spectra of SCC mix with 0% iron slag at 91 days ((CH- $Ca(OH)_2$), CSH-calcium silicate hydrates, Q- SiO_2, CS-calcium silicates, C-calcite)

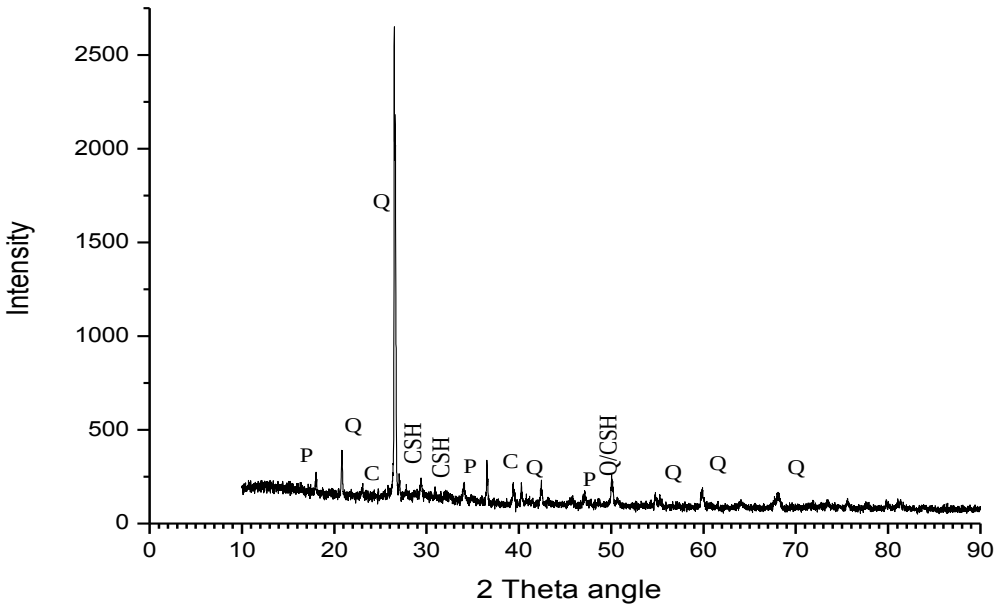

Fig 4.58: XRD spectra of SCC mix with 10% iron slag at 91 days ((CH- $Ca(OH)_2$), CSH-calcium silicate hydrates, Q- SiO_2, CS-calcium silicates, C-calcite)

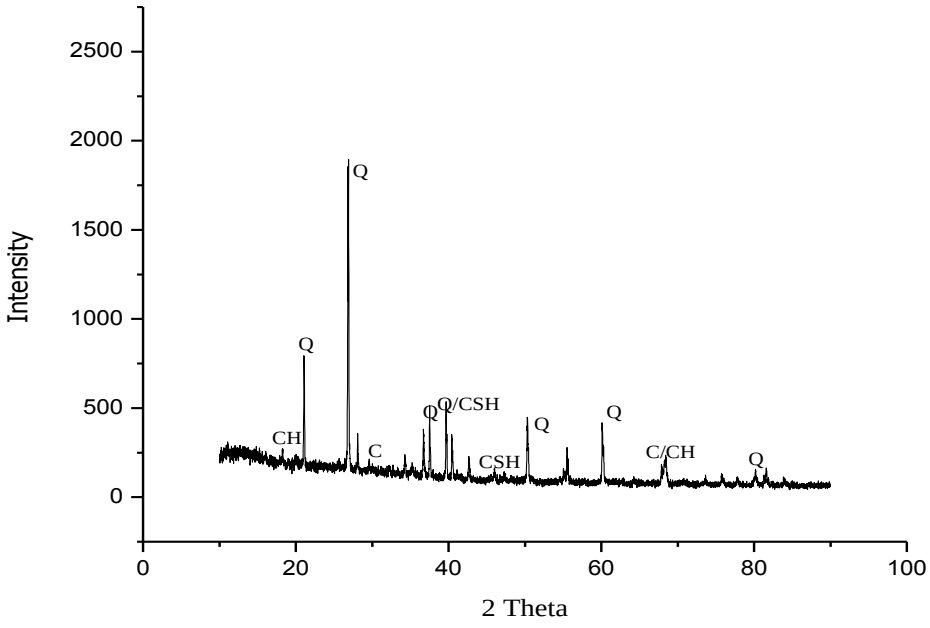

Fig 4.59: XRD spectra of SCC mix with 25% iron slag at 91 days ((CH- $Ca(OH)_2$), CSH-calcium silicate hydrates, Q- SiO_2, CS-calcium silicates, C-calcite)

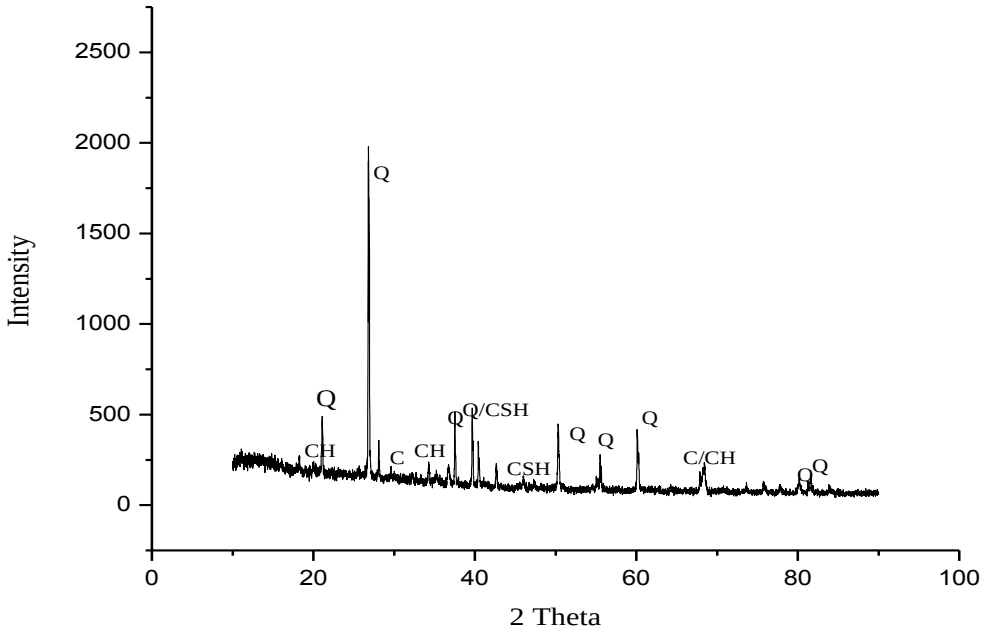

Fig 4.60: XRD spectra of SCC mix with 40% iron slag at 91 days ((CH- $Ca(OH)_2$), CSH-calcium silicate hydrates, Q- SiO_2, CS-calcium silicates, C-calcite)

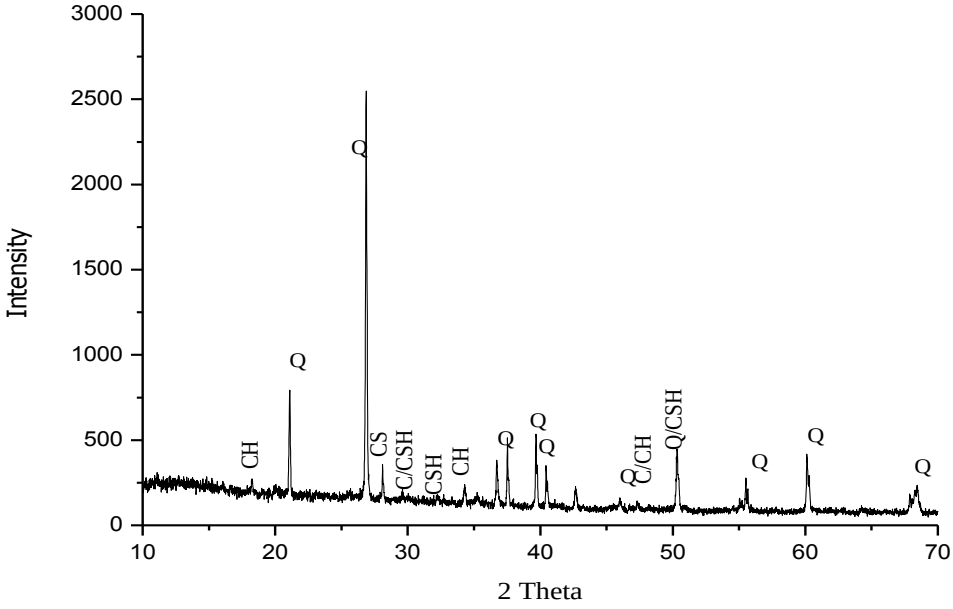

Fig 4.61: XRD spectra of SCC mix with 0% iron slag at 365 days ((CH- $Ca(OH)_2$), CSH-calcium silicate hydrates, Q- SiO_2, CS-calcium silicates, C-calcite)

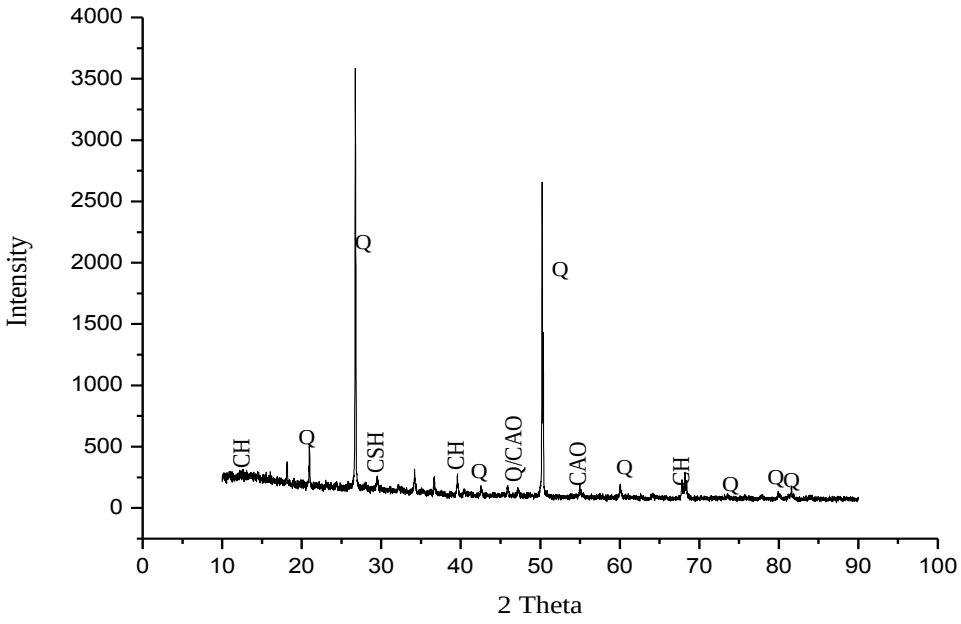

Fig 4.62: XRD spectra of SCC mix with 10 % iron slag at 365 days (CH-(CH-$Ca(OH)_2$), CSH-calcium silicate hydrates, Q- SiO_2 , CS-calcium silicates, C-calcite, CAO- calcium ion oxide)

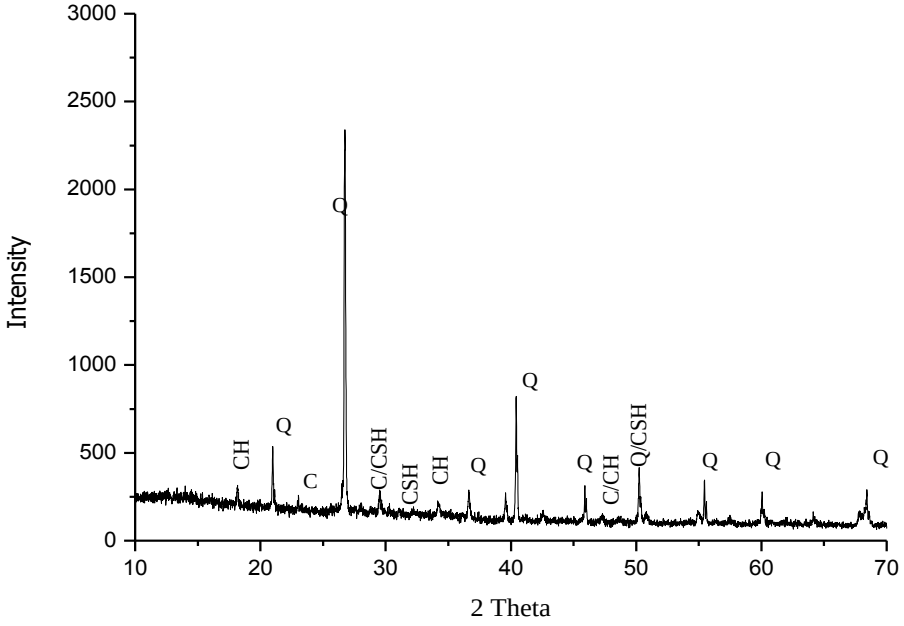

Fig 4.63: XRD spectra of SCC mix with 25% iron slag at 365 days (CH- $Ca(OH)_2$, CSH-calcium silicate hydrates, Q- SiO_2, CS-calcium silicates, C-calcite)

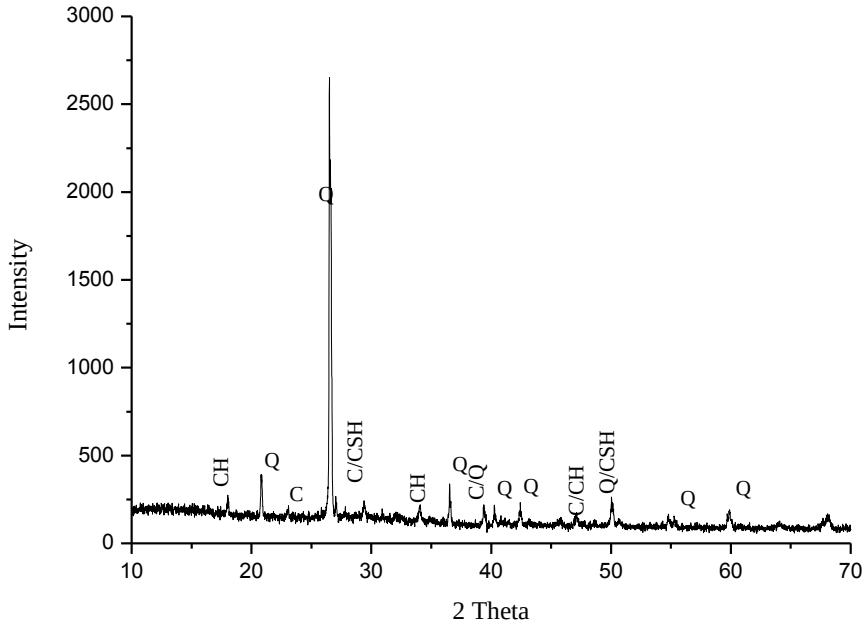

Fig 4.64: XRD spectra of SCC mix with 40% iron slag at 365 days (CH- $Ca(OH)_2$, CSH-calcium silicate hydrates, Q- SiO_2, CS-calcium silicates, C-calcite)

4.7. STATICAL ANALYSIS OF RESULTS

4.7.1. Comparative Study Of Strength And Durability Properties For The SCC Mixes by't – test'

Comparative study of strength and durability properties for the SCC mixes was done by't-test'. Mean score of SCC-IS10, SCC-IS25 and SCC-IS40 was higher than SCC-CM at all strength and durability properties and it was found to be statistically significant. ($p < 0.05$).

Table 4.10: Comparison of strength and durability properties of SCC mixes

	Mean±SD	**MD±SE**	**'t'- test**
Compressive strength			
SCC-CM	36.64±9.16	1.69±0.38	t=4.42,df=3
SCC-IS 10	38.33±9.90		p=.02*
SCC-CM	36.64±9.16	5.31±1.20	t=4.42,df=3
SCC-IS 25	41.95±11.56		p=.02*
SCC-CM	36.64±9.16	9.28±1.67	t=4.40,df=3
SCC-IS 40	45.92±12.45		p=.02*

Splitting Tensile Strength			
SCC-CM	2.70±0.95	0.20±0.06	t=3.37,df=3
SCC-IS 10	2.90±0.91		p=.04*
SCC-CM	2.70±0.95	0.52±.09	t=5.39,df=3
SCC-IS 25	3.22±0.89		p=.01*
SCC-CM	2.70±0.95	0.74±.05	t=13.8,df=3
SCC-IS 40	3.45±0.94		p=.01*
Flexural Strength			
SCC-CM	3.43±0.79	0.15±0.08	t=1.75,df=3
SCC-IS 10	3.58±0.94		$p=.17^{NS}$
SCC-CM	3.43±0.79	0.41±0.12	t=3.46,df=3
SCC-IS 25	3.85±0.74		p=.04*
SCC-CM	3.43±0.79	0.66±0.05	t=12.27,df=3
SCC-IS 40	4.10±0.82		p=.001*
Modulus of Elasticity			
SCC-CM	27.80±1.69	0.40±0.12	t=3.26,df=3
SCC-IS 10	28.20±1.92		p=.04*
SCC-CM	27.80±1.69	0.81±0.30	t=5.30,df=3
SCC-IS 25	28.61±1.80		p=.01*
SCC-CM	27.80±1.69	1.09±0.19	t=3.26,df=3
SCC-IS 40	28.89±1.97		p=.04*
Rapid Chloride Permeability			
SCC-CM	1192.75±265.99	247.73±207.29	t=1.19,df=3
SCC-IS 10	945.02±635.85		$p=.31^{NS}$
SCC-CM	1192.75±265.99	77±11.14	t=6.90,df=3
SCC-IS 25	1115.75±260.68		$p=.00^{*}$
SCC-CM	1192.75±265.99	123.50±27.77	t=4.43,df=3
SCC-IS 40	1069.50±229.67		$p=.02^{*}$
Sulphate Resistance			
SCC-CM	7.60±6.59	0.07±0.39	t=0.19,df=3
SCC-IS 10	7.67±6.31		$p=.86^{NS}$
SCC-CM	7.60±6.59	0.01±0.41	t=0.03,df=3
SCC-IS 25	7.58±6.45		$p=.97^{NS}$
SCC-CM	7.60±6.59	0.76±0.51	t=1.49,df=3
SCC-IS 40	8.36±7.54		$p=.23^{NS}$
	Mean±SD	**MD±SE**	**'t'- test**
Water Absorption			
SCC-CM	4.35±0.68	0.08±0.38	t=2.28,df=3
SCC-IS 10	4.27±0.74		$p=.10^{NS}$
SCC-CM	4.35±0.68	0.30±0.11	t=2.61,df=3
SCC-IS 25	4.05±0.74		$p=.08^{NS}$
SCC-CM	4.35±0.68	0.60±0.09	t=6.34,df=3
SCC-IS 40	3.75±0.52		$p=.00^{*}$
Ultra-sonic Pulse Velocity			
SCC-CM	4205.25±146.91	±1111.39	t=0.92,df=3

SCC-IS 10	3172.28±2115.30		p=.42^{NS}
SCC-CM	4205.25±146.91	1.24±25.21	t=4.91,df=3
SCC-IS 25	4329.25±188.98		p=.01*
SCC-CM	4205.25±146.91	1.72±24.63	t=6.99,df=3
SCC-IS 40	4377.50±182.64		p=.00*

df – degree of freedom, SD – Standard deviation, MD- mean difference
SE – standard error, * -Significant, NS- non significant

Table 4.10 describes comparison study of strength and durability properties for the SCC mixes. It depicts in compressive strength, mean value of SCC- CM was 36.64, mean value of SCC-IS10, SCC-IS25, and SCC-IS40 was 38.33, 41.95 and 45.92, respectively, which was higher than mean value of SCC-CM. It was found to be statiscally significant (p<.05) as calculated with t-test. In Splitting tensile strength mean value of SCC- CM was 2.70, mean value of SCC-IS10, SCC-IS25, and SCC-IS40 was 2.90, 3.22 and 3.45, respectively, which was higher than mean value of SCC-CM. It was found to be statiscally significant (p<.05) as calculated with t-test. As per flexural strength, mean value of SCC- CM was 3.43 and mean value of SCC-IS10 was 3.58, which was higher than SCC-CM but it was statiscally non significant (p>.05). Mean value of SCC-IS25 and SCC-IS40 was 3.85 and 4.10 which was higher than mean value of SCC-CM and was found to be statiscally significant (p<.05) as calculated with t-test. Regarding modulus of elasticity, mean value of SCC- CM was 27.80 mean value of SCC-IS10, SCC-IS25 and SCC-IS40 was28.20, 28.61 and 28.89, respectively, which was higher than mean value of SCC-CM. It was found to be statiscally significant (p<.05) as calculated with t-test. Mean value of SCC-CM in rapid chloride permeability was 1192.75 and mean value of SCC-IS10 was 945.02, which was lower than SCC-CM and it was statiscally non significant (p>.05). Mean value of SCC-IS25,SCC-IS40 was 1115.75 and 1069.50 which was lower than mean value of SCC-CM and was found to be statiscally significant (p<.05) as calculated with t-test. In sulphate resistance mean value of SCC- CM was 7.60, mean value of SCC-IS10, SCC-IS25 and SCC-IS40 was 7.67, 7.58 and 8.36, respectively, which was higher than mean value of SCC-CM and results was found to be statiscally Non significant (p<.05) as calculated with t-test. In water absorption mean value of SCC-CM was 4.35 which is higher than mean value of SCC-IS10, SCC-IS25 and SCC-IS40 (4.27,4.05 and 3.75) respectively. The results was found to be statistically significant with SCC-CM and SCC-IS40(p<.05). As per Ultra sonic Pulse velocity, mean value of

SCC- CM was4205.25 and mean value of SCC-IS10 was 3172.28, which was lower than SCC-CM and it was statiscally Non significant (p>.05).Mean value of SCC-IS25, SCC-IS40 was 4329.25 and 4377.50 which was higher than mean value of SCC-CM and was found to be statiscally significant (p<.05) as calculated with t-test.

4.7.2. Correlation Analysis of SCC properties

4.7.2.1. Relationship between Compressive Strength and Splitting Tensile Strength

Fig 4.65 shows the relation between splitting tensile strength and compressive strength of SCC. The relationships between compressive strength and splitting tensile strength together with the coefficient of determination R^2 obtained from test values of the present research work is mentioned below. The values of regression curve and data points indicate that good relationship between both the properties.

$F_t = 0.028 (F_c)^{1.263}$ $R^2 = 0.972$

Where

F_t = Splitting tensile strength of concrete in MPa

F_c = Compressive strength on concrete in MPa

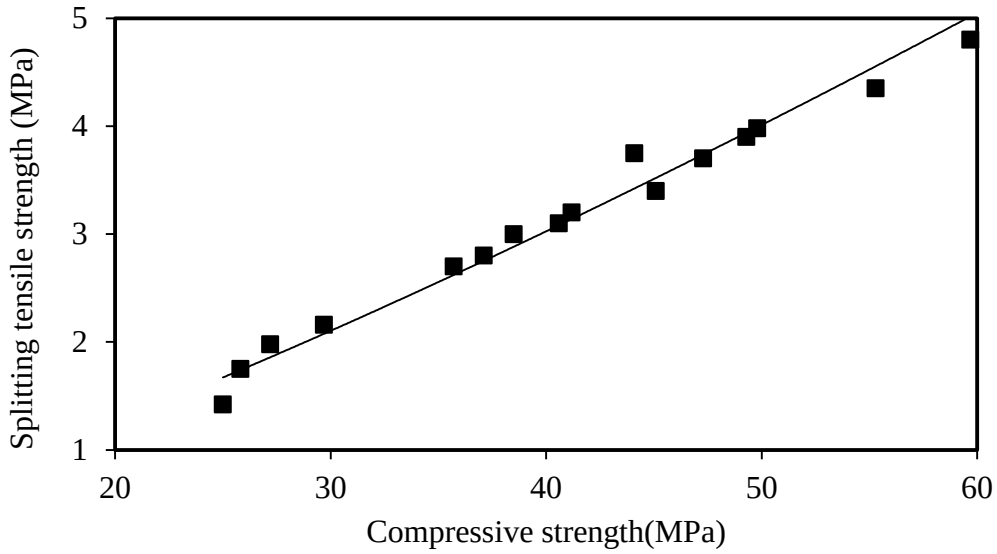

Fig. 4.65: Relation between compressive strength and splitting tensile strength of SCC

Table 4.11: Comparison of relation given in CEB-FIP, ACI318-99 and derived from present study

Compressive Strength of SCC mixes (MPa)	Splitting tensile strength (MPa) as per			Actual splitting tensile strength (MPa)
	$f_t=0.3(f_{cyl})^{2/3}$	$f_t= 0.56(f_c)^{1/2}$	$F_t = 0.028 (F_c)^{1.263}$	
35.7	3.25	3.34	2.55	2.7
37.1	3.30	3.41	2.68	2.8
41.2	3.58	3.59	3.095	3.2
45.1	3.80	3.76	3.43	3.4

4.7.2.2. Relationship between Compressive Strength and Flexural Strength

Fig 4.66 shows the relationship between compressive strength and flexural strength of SCC up to 365 days of curing period. The equation obtained from the properties is mentioned below. Coefficient of determination R^2 indicates good relevance between data points and regression curve.

$F_r = 0.145F_c^{0.889}$ $R^2 = 0.969$

Where,

F_r = Flexural strength of SCC in MPa

F_c = Compressive strength of SCC in MPa

Table 4.12: Comparison of relation given in IS: 456-2000, ACI, NZS-3101, EC-02 and derived from present study

Compressive Strength of SCC mixes (MPa)	Flexural strength (MPa) as per					Actual flexural strength (MPa)
	$0.7 f_c^{0.5}$	$0.62 f_c^{0.5}$	$0.6 f_c^{0.5}$	$0.6 f_c^{0.5}$	$0.145 F_c^{.889}$	
35.7	4.17	3.70	3.58	3.58	3.48	3.46
37.1	4.26	3.77	3.65	3.65	3.60	3.53
41.2	4.49	3.98	3.85	3.85	3.95	4.07
45.1	4.71	4.172	4.03	4.03	4.28	4.22

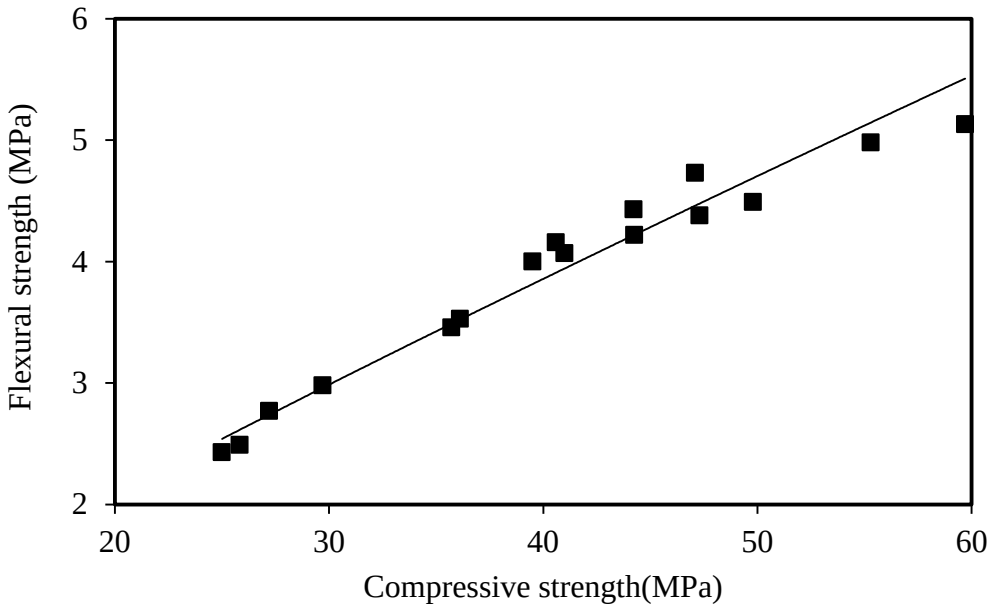

Fig. 4.66: Relation between compressive strength and flexural strength of SCC

4.7.2.3. Relationship between Compressive Strength and Modulus of Elasticity

Fig 4.67 shows the relationship between compressive strength and modulus of elasticity of SCC up to 365 days of curing period. The equation obtained from the properties mentioned below. Coefficient of determination R^2 indicates good relevance between data points and regression curve.

$E = 11.85 F_c^{0.237}$ $R^2 = 0.984$

Where,

E = Modulus of elasticity of SCC in GPa

F_c = Compressive strength of SCC in MPa

Table 4.13: Comparison of relation given in ACI, CEB-FIP and derived from present study

Compressive Strength of SCC mixes (MPa)	Modulus of elasticity (GPa) as per			Actual flexural strength (MPa)
	$63681\ f_c^{0.5}$	$22\ (f_c/10)^{1/3}$	$11.85\ F_c^{0.237}$	
35.7	38.01	33.66	27.61	27.9
37.1	38.78	34.32	27.85	28.19
41.2	40.80	35.20	28.56	28.71
45.1	42.85	36.30	29.27	28.87

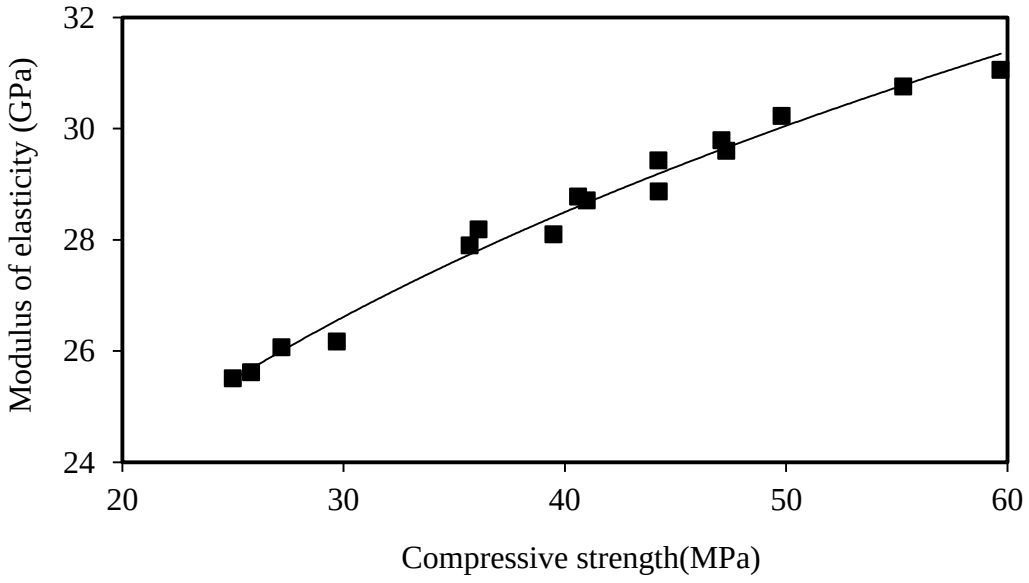

Fig. 4.67: Relation between compressive strength and modulus of elasticity of SCC

4.7.2.4. Relationship between Splitting Tensile Strength and Flexural Strength

Fig 4.68 shows the relationship between compressive strength and modulus of elasticity of SCC up to 365 days of curing period. The equation obtained from the properties mentioned below. Coefficient of determination R^2 indicates good relevance between data points and regression curve.

Fr = $0.842F_s + 1.13$ R^2 =0.964

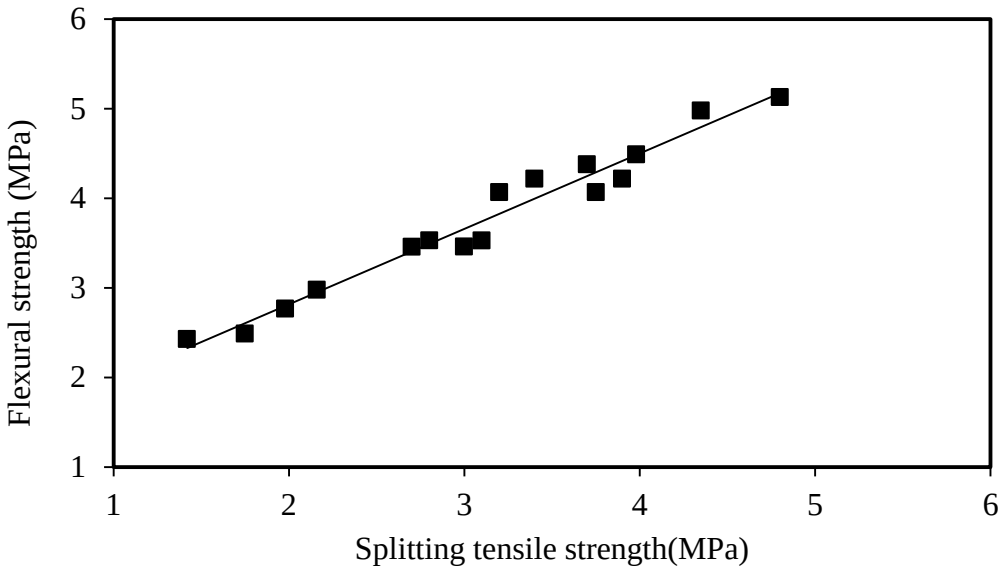

Fig. 4.68: Relation between splitting tensile strength and flexural strength of SCC

4.7.2.5. Relationship between Splitting Tensile Strength and Modulus of Elasticity

The regression equations and value of correlation coefficient R^2 between splitting tensile strength and modulus of elasticity are given in below mention equation and Fig 4.69. As evident from these results that value of correlation coefficient was 0.967. The high values of correlation coefficient indicate that there was strong relationship between the properties of SCC.

E = $23.27F_s^{0.181}$ R =0.967

E = Modulus of elasticity in GPa

F_s = Splitting tensile strength in MPa

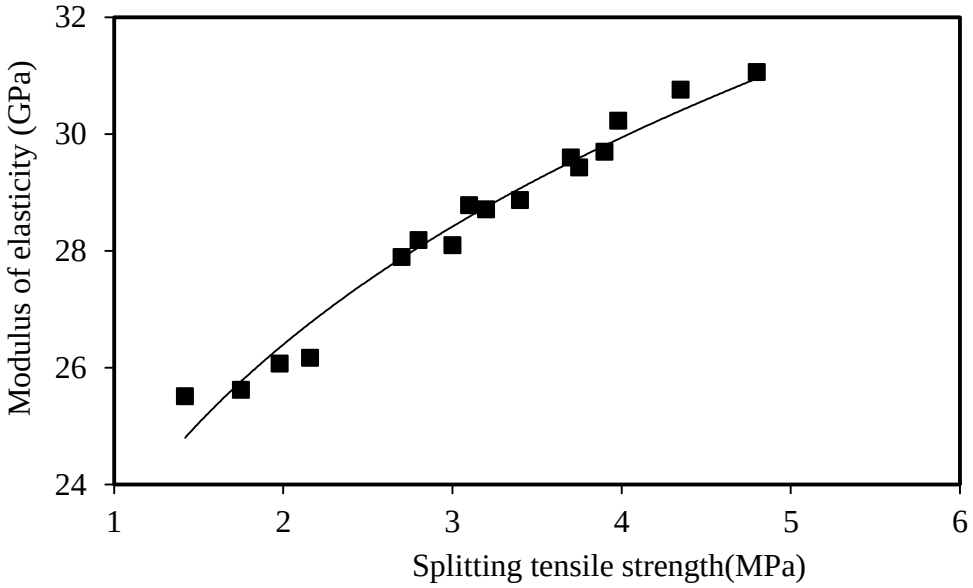

Fig 4.69: Relation between splitting tensile strength and modulus of elasticity of SCC

4.7.2.6. Relation between Compressive Strength and Chloride Permeability

Fig 4.70 displays that the relationship between compressive strength and cumulative charge passed of iron slag concrete mixes. Both properties related to its pore structure. The equation presenting the relationship between compressive strength σ and cumulative charge passed C, with the coefficient of R^2 given below.

$$\sigma = -20.15C + 1934 \quad R^2 = 0.854 \text{ (Present research)}$$

Where, σ = compressive strength in MPa, C= total charge passed (coulombs)
Coefficient value of R^2 shows good relation between data points and regression curve.

Singh and Siddique [31] reported the similar relationship of compressive strength and RCP.

$$\sigma = -0.0058Q + 53.627 \quad R^2 = 0.7665 \text{ (Singh and Siddique,(2014))}$$

σ= compressive strength in MPa, Q = total charge passed (coulombs)

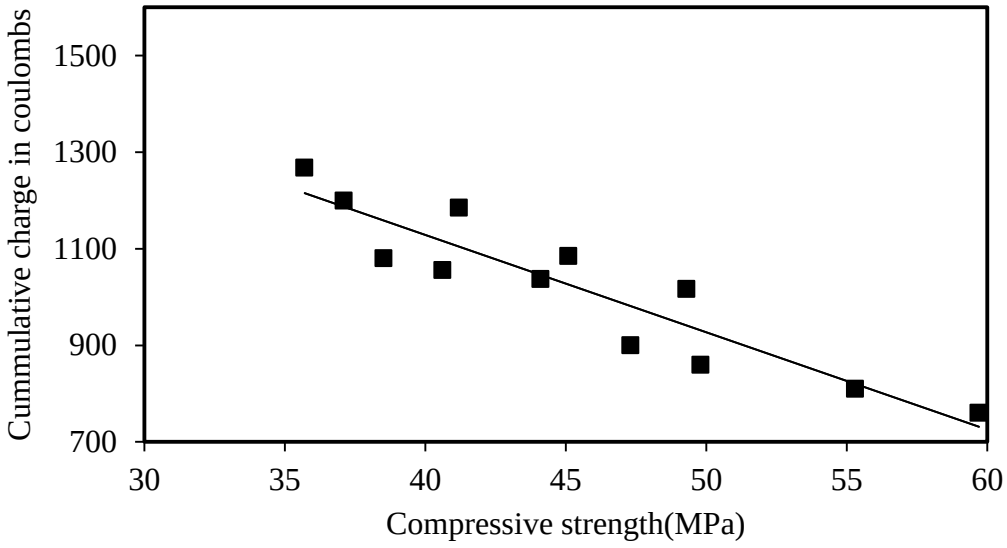

Fig. 4.70: Relation between compressive strength and Chloride permeability of SCC

4.7.2.7. Relation of Ultra-Sonic Pulse Velocity and Compressive Strength

Fig 4.71 demonstrates correlation of ultra-sonic pulse velocity and compressive strength for all collected results. Result report shows that the more the UPV value, the more the compressive strength was observed and relationship between them can be performed well with best-fit logarithmic formula as shown in equation and evidence by a good coefficient of determination (R^2=0.871)

F_c =220.1 ln(V)-1801 R^2 = 0.871

Where, F_c = compressive strength in MPa

V = Pulse velocity value in m/s

Sheen et al. presented a similar relationship between Ultra-sonic pulse velocity and compressive strength.

$$f'_c = 0.07 \times e^{0.0013 \times UPV} \quad (R^2 = 0.9677)$$

$$f_c = 0.0369 e^{0.0017 \times UPV} \quad (R^2 = 0.9462)$$

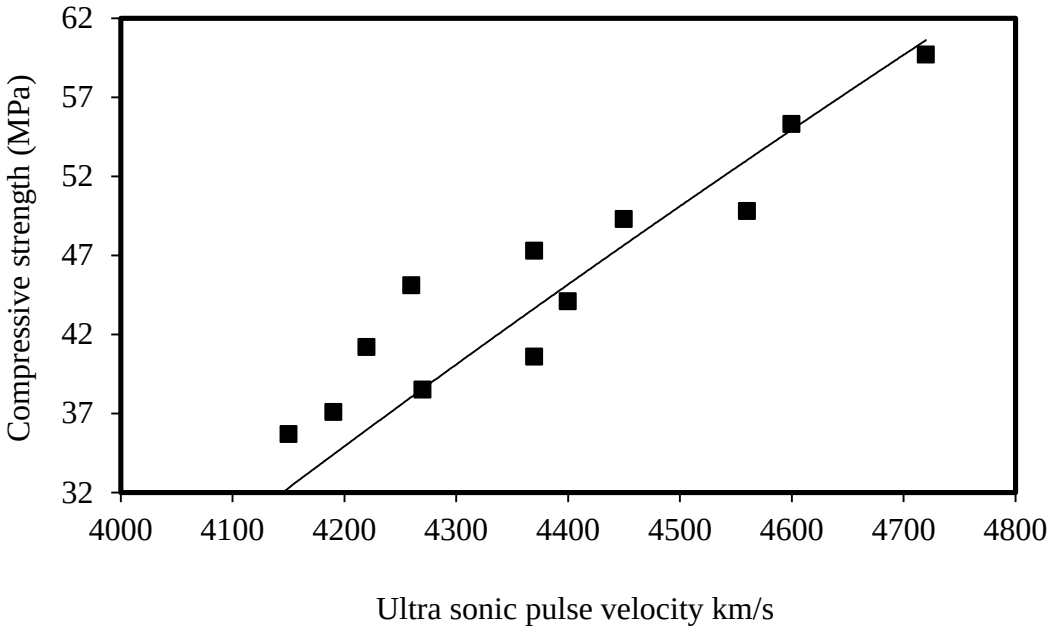

Fig. 4.71: Relation between compressive strength and ultra sonic pulse velocity of SCC

Table 4.14: Verification of relationship between pulse velocity and compressive strength

Pulse velocity (m/s)	Predicted compressive strength(Mpa)	Actual compressive strength (MPa)	Variation (%)
4270	38.89	38.5	+1.00
4370	43.99	40.6	+7.71
4400	45.49	44.1	+3.06
4450	47.98	49.3	-2.75

4.7.2.8. Relation of Compressive Strength and Abrasion Resistance

Fig 4.72 demonstrates correlation of abrasion resistance and compressive strength for all results up to 365 days. Result indicates that abrasion resistance of SCC increases with an increase of compressive strength and relationship between them can be performed well with best-fit logarithmic formula as shown in equation and evidence by a good coefficient of determination (R^2=0.897)

d = -0.401 Ln(F_t) +1.944, R^2 = 0.897 for 15 min abrasion (Present research)

d = -1.5992 Ln(x) + 7.728, R^2 = 0.9044 for 60 min abrasion (siddique, 2010)

d =-0.03951σ + 4.0444 R^2 = 0.6724 for 70 min abrasion (Naik et al., 1995)

The empirical parameters of the equation mentioned above obtained from the present research ate almost same as the reported by Siddique (2010) for fly ash concrete and reported by Nail et al (1995) for high strength concrete made with fly ash as replacement with cement.

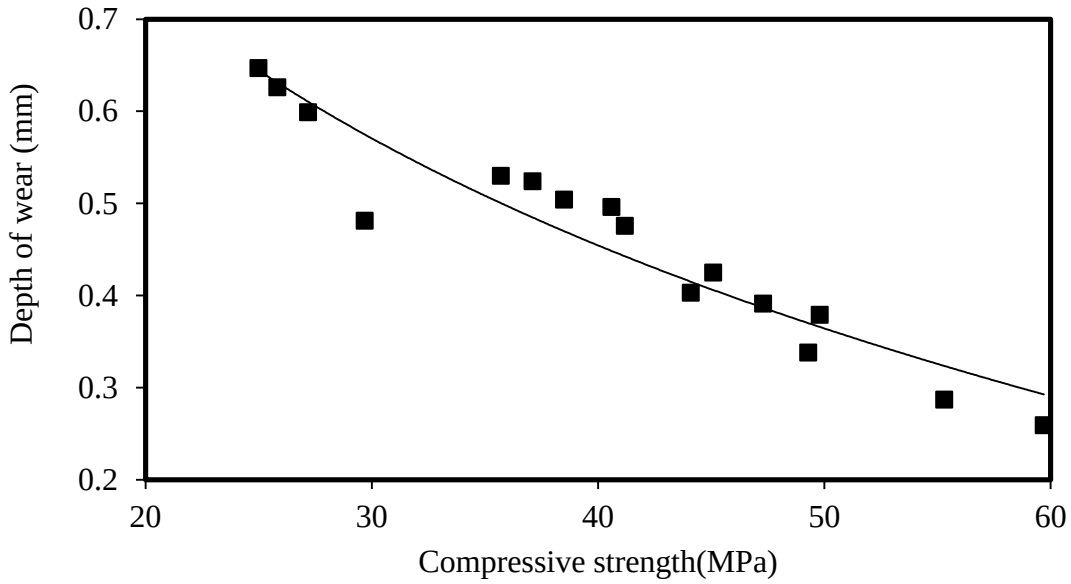

Fig 4.72: Relation between compressive strength and depth of wear of SCC

4.7.2.9. Relation between Chloride Permeability and Ultra-sonic Pulse Velocity

Fig 4.73 shows the relationship between ultra sonic pulse velocity and chloride permeability of SCC. Results shows the good relevance between regression curve and data points and coefficient of determination R^2 shows the strong relationship between them. Both the properties are related to pore structure if concrete matrix is dense, means

high pulse velocity and low chloride permeability. Equation mentioned below showing the relationship between chloride permeability (C) and pulse velocity (V) with coefficient of determination R.

$C = -1.152\ V + 6104 \qquad R^2 = 0.862$ (Author)

Where,

C = Charge passed through SCC in coulombs

V = Pulse velocity through SCC specimen in m/s

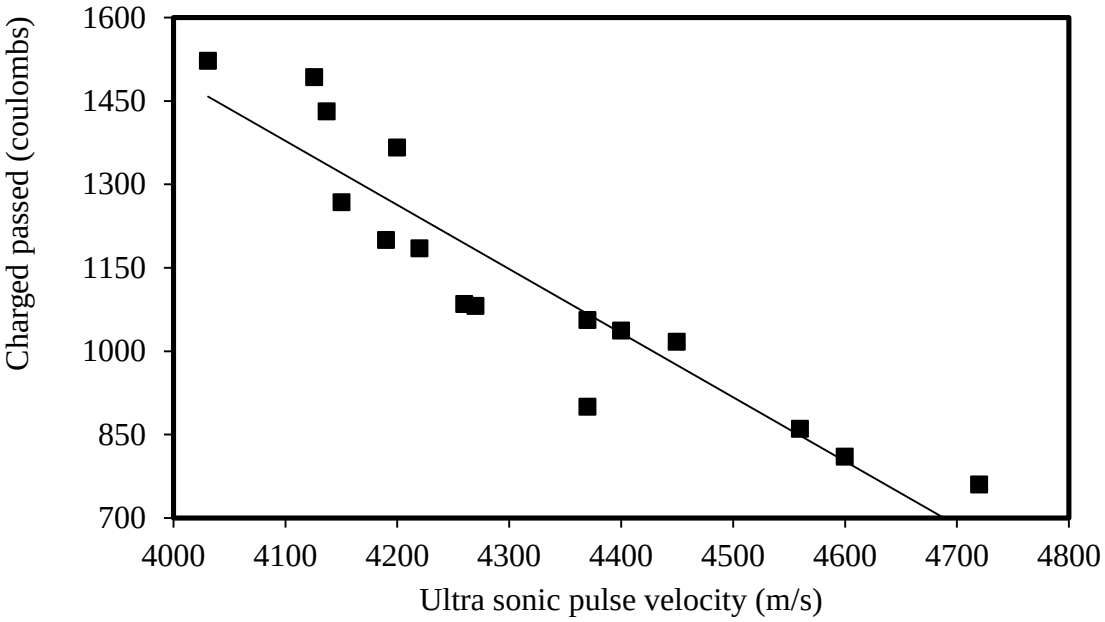

Fig. 4.73: Relation between chloride permeability and pulse velocity of SCC

CHAPTER-5

CONCLUSIONS

Test results indicate that iron slag can be used as suitable substitute for partial replacement of fine aggregates in the production of self-compacting concrete. Based on the investigation following conclusions are drawn.

5.1 FRESH SCC PROPERTIES

5.1.1. Slump Flow

Slump flow of SCC mixtures decreased on the addition of iron slag. At fixed water-powder ratio slump flow values of SCC mixtures decreased almost linearly with the increase in iron slag content.

Slump flow values of SCC mixtures were within the specified range (500-800mm) with and without replacement of iron slag with fine aggregates. But the inclusion of iron slag reduced the slump flow value as compared with the control SCC mixture. Higher the iron slag content in SCC mixtures lowers the slump flow. Slump value of iron slag SCC mixture decreased from 2.5 to 13% (790 to 690 mm) for 10 to 40% replacement of iron slag with fine aggregates in SCC.

5.1.2. L-Box

L-box ratios of SCC decreased with the increase in iron slag content. L-box ratios of SCC mixtures with or without inclusion of iron slag were within the specified range (0.8-1), but decreased with the increase in iron slag content. L-box ratio value decreases up to 8% with 40% replacement of iron slag with fine aggregates.

5.1.3. U-Box

U-box values of SCC mixture with or without iron slag were within the specified range(30- 35mm), but increased with the increase in iron slag content. U-box value increases 28mm to 31mm when 40% of iron slag replaced with fine aggregates.

5.1.4. V-funnel

Time of V-funnel test of SCC mixtures was within the limit (6-12 sec.) specified by EFNARC, 2005. Time span of V- funnel test values increased with the increase of iron slag content in SCC mixtures. Time span increase 10 to 12.5 seconds when 40% of iron slag replaced with fine aggregates in SCC mixtures.

Workability of SCC mixtures decreases due to increase of iron slag percentage cause may be multi-angle and rough in surface of iron slag aggregates. Increases friction between particles may responsible for the results.

5.2 STRENGTH PROPERTIES OF SCC

5.2.1. Compressive Strength

Compressive strength of SCC mixtures increased with the increase in iron slag percentage at all replacement levels. The reason for increase in strength was that silica in iron slag reacts with calcium hydroxide, forms calcium silicates and aluminates hydrates, which fill the voids and improve the micro-structure of SCC, thereby developing its strength.

Compressive strength of SCC mixtures at 28, 91 and 365 days with inclusion of iron slag (10, 25 and 40%) was 37.1 to 45.1 MPa, 40.6 to 49.3 MPa and 49.8 to 59.7MPa as against 35.7, 38.5 and 47.3MPa respectively, of control SCC mixture.

Higher replacement of iron slag with fine aggregates can be used to develop SCC with an adequate strength (45MPa). The compressive strength of SCC with 10, 25 and 40% iron slag dose at 28 days is marginally enough for the use in heavy reinforced concrete construction.

Compressive strength of SCC mixture with or without iron slag content was found to increase with increase in curing age.

5.2.2. Splitting Tensile Strength

Splitting tensile strength of SCC mixtures increased with the increase of iron slag and all SCC mixtures was found to increase with increase in curing age.

At 28, 91 and 365 days splitting tensile strength of SCC mixtures with iron slag (10, 25 and 40%) varied from 2.8 to 3.4MPa, 3.1 to 3.9MPa and 3.98 to 4.8MPa as compared to 2.7, 3.0 and 3.7MPa, respectively of control SCC mixture without iron slag.

Splitting tensile strength and compressive strength ratios of SCC mixture with iron slag content at 28, 91 and 365 days of curing age was 7.5 – 7.8, 7.9 – 8.5 and 7.9 – 8.0 as compared to 7.6, 7.8 and 7.8, respectively of SCC without iron slag content. With curing age, the effect of replacement of iron slag with fine aggregates in SCC on splitting tensile strength and compressive strength ratio was no so predominant.

5.2.3. Flexural Strength

Flexural strength of SCC mixture increases with the increase in iron slag and all SCC mixtures were found to increase with increase in curing age. At 28, 91 and 365 days, flexural strength of SCC mixtures with iron slag varied from 3.53 to 4.22MPa, 4.26 to 4.73MPa and 4.49 to 5.13MPa as against 3.46, 4.0 and 4.38MPa, respectively of SCC without iron slag content.

With age, the flexural strength of SCC mixtures improved at faster rate than iron slag content.

5.2.4. Modulus of Elasticity

Modulus of elasticity of SCC mixtures increased on inclusion of iron slag as replacement with fine aggregates. The modulus of elasticity value of SCC with iron slag content was 28.17 – 28.87GPa, 28.78 – 29.79GPa and 30.23 – 31.06GPa as compared to 27.90, 28.19 and 29.60GPa of control SCC at the age of 28, 91 and 365 days.

Modulus of elasticity of all SCC mixtures was found to increase with increase in age.

5.3 DURABILTY PROPERTIES OF SCC

5.3.1. Water Absorption

Water absorption in iron slag SCC mixtures decreased with the increase in iron slag content. With age, water absorption rate of SCC mixtures with iron slag reduced as compared to control SCC mixture.

At 28 days water absorption of control SCC mixture was 4.81%. After 40% replacement, of the absorption value was reduced to 4%.

5.3.2. Sorptivity

Sorptivity value decreased with the increase of iron slag content in SCC mixtures. The average cumulative absorption (I) in SCC mixtures with iron slag content was in range of 0.132 to 0.103 mm, 0.0987 to 0.0899 mm and 0.0801 to 0.0755 mm as against 0.145, 0.102 and 0.0830 mm of control SCC mixture at curing age of 28, 91 and 365 days.

Sorptivity value of all SCC mixtures was found to decrease with increase in age.

Sorptivity and water absorption generally related to the structural pores (inter-layer C-S-H) and porous paste, aggregate interface zone, especially more at initial stage, as concluded from SEM images matrix gets more denser after the inclusion of iron slag.

5.3.3 Sulphate Resistance

After the immersion in Mg_2So_4 solution, control SCC mixture was performed slightly better as compared to SCC mixtures with iron slag.

5.3.3.1. Loss in mass

Spalling and cracks were not found on any SCC specimens up to 365 days. No mass loss of all specimens was observed only white deposit were observed after 91 days of immersion period.

5.3.3.2. Loss in compressive strength

Compressive strength loss under sulphate attack was increased with the increase in iron slag content at replacement levels and at all ages. The percentage loss in compressive strength in SCC with iron slag content was 3.1 to 3.23%, 13.05 to 13.59% and 16.27 to 16.31% as compared with 2.8, 11.17 and 15.01% respectively, of SCC without iron slag content at 28, 91 and 365 days of curing.

5.3.4. Rapid Chloride Permeability

With age and iron slag content, resistance to chloride ion penetration of SCC mixtures increased as compared with control SCC mixture. The chloride permeability all of all SCC mixtures were graded as "low chloride ion penetration" up to the curing age of 91 days, after 91 days of curing period all SCC mixtures graded as "very low chloride ion penetration".

Chloride permeability value of SCC mixtures with iron slag at 28, 91 and 365 days of curing was in range of 1200 -1085 coulombs, 1056 – 1017 coulombs and 860 – 760 coulombs as against 1268, 1081 and 900 coulombs of control SCC respectively.

The addition of iron slag as fine aggregates in SCC has not much significant effect on resistance to chloride ion penetration. With age, iron slag SCC mixtures shows better resistance to chloride ion penetration.

5.3.5. Abrasion Resistance

SCC mixtures with iron slag demonstrated higher abrasion resistance than control SCC mixture. Average wear depth of all SCC mixtures was much below than 2mm for 7.5 minutes of wear time specified in BIS: 1237-2012 for heavy duty tiles.

At 28, 91 and 375 days curing age, for 15 minutes wear time, average wear depth of SCC with iron slag content was in the range of 0.524 to 0.425 mm, 0.496 to 0.338 and 0.379 to 0.259 mm as against 0.53, 0.504 and 0.391 mm respectively, of control SCC.

5.4 NON-DESTRUCTIVE TESTING

5.4.1. Ultra-sonic Pulse Velocity (UPV)

Pulse velocity of SCC mixtures with iron slag content was higher as compared to control SCC mixture.

All the test result values of UPV of SCC were in the range of 4150 to 4720 m/s at all replacement levels and at all ages. It shows the excellent concrete quality. Lower value of velocity in SCC was 4150 with 0% replacement on curing age of 28 days and higher value of velocity in SCC was 4720 with 40% replacement of iron slag with fine aggregates at the curing age of 365 days in between the values of UPV increased gradually.

5.5 MICROSTRUCTURE

Replacement of iron slag with fine aggregates in SCC gives good effect to its strength properties due to the quality of concrete in term of its density and porosity. SEM images indicate that internal structure of SCC gets denser after the inclusion of iron slag and the spread of CSH gel slightly less monolithic as compared with the images of SCC with iron slag content.

With age, internal structure of SCC improves due to filling the void spaces by the formation of ettringites in void spaces.

5.6 X-RAY DIFFRACTION PHASE ANALYSIS

XRD analysis showed the peaks of calcium silicate hydrates (CSH), portlandite (CH) quartz (Q), calcium silicates (CS), calcite (C). Phase composition of SCC paste did not change qualitatively, however phase proportions was observed on the inclusion of iron slag content in SCC.

REFERENCES

Afifudin, H., Nadzarah, W., Hamidah, M. S. and Noor, H. Microbial participation in the formation of calcium silicate hydrated (CSH) from bacillus subtilis. Procedia Engineering, 2011; 20: 159-165.

Afshoon, M and Sharifi, Y. Ground copper slag as a supplementary cementing material and its influence on fresh properties of self-consolidating concrete. The IES Journal Part A: Civil and Structure Engineering, 2014; 7(4): 229-242.

Aggarwal, P and Aggarwal, Y. Prediction of compressive strength of self-compacting concrete with fuzzy logic. World Academy of Science, Engineering and Technology, 2008; 847-854.

Aggarwal, P and, Aggarwal, Y., and Gupta, S.M. Modeling properties of self-compacting concrete: support vector machine approach. Computers and Concrete, 2008; 5(5): 1-12.

Ahamer, C.M., Fuchs-Eschlbock, S., Kolmhofer P.J., Rossler R., Huber, N and Pedarining J.D. Laser induced breakdown spectroscopy of major and minor oxides in steel slag: influence of detection geometry and signal normalization. Spectrochimica Acta Part: Atomic Spectroscopy, 2016; 122: 157-164.

Aliabdo, A.A and Suda, E.M. Re-use of waste marble dust in the production of cement and concrete. Construction and Building Materials, 2013; 50: 28-41.

ASTM C 1012-10. Standard test methods for length change of hydraulic-cement mortars exposed to sulphate solution. West Conshohocken, USA: ASTM International.

ASTM C 1202-10. Standard test methods for electrical indications of concrete's ability to resist chloride ion penetration. West Conshohocken, USA: ASTM International.

ASTM C 597-02. Standard test methods for pulse velocity through concrete. Conshohocken, USA: ASTM International.

ASTM C 642-06. Standard test methods for density, absorption and voids in hardened concrete. West Conshohocken, USA: ASTM International.

Awasthi, P.U and Mathews, M.P., Behavior of self-compacting concrete by partial replacement of fine aggregates with coal bottom ash. International Journal of Innovative Research in Advanced Engineering, 2015; 02(10): 45-52.

Baite, E., Messan, A., Hannawi, K., Tsobnang, F and Prince, W. Physical and transfer properties of mortar containing coal bottom ash aggregates from Tefereyre (Niger), Construction and Building Materials, 2016: 125; 919-926.

Balamuruga, G and Perumal, P. Use of Quarry Dust to Replace Sand in Concrete – An Experimental Study. International Journal of Scientific and Research Publications, 2013; 3(12): 1-4.

Bentz, D. P., Ehlen, M. A., Ferraris, C. F and Garboczi, E. J. Sorptivity-based service life predictions for concrete pavements. 7th International Conference on Concrete Pavements–Orlando, Florida, USA, Sept, 2001; 9-13.

Bernabeu, O. Rational production and improved working environment through using SCC: Final report of task 8.6 productivity and economy. Brite EuRam; 2000.

BIS: 1237-1980, Method for testing abrasion resistance of concrete, New Delhi, India: Bureau of Indian standards; 1980.

BIS: 3812-2003. Specifications for Pulverized fuel ash. Bureau of Indian Standards, New Delhi, India; 2003

BIS: 383-1970, Indian standard specifications for coarse and fine aggregates from natural sources for concrete New Delhi, India: Bureau of Indian standards; 1970.

BIS: 516-1959, Indian standard method of test for strength of concrete, New Delhi, India: Bureau of Indian standards; 1959.

BIS: 5816-1999, splitting tensile strength of concrete method of test, New Delhi, India: Bureau of Indian standards; 1999.

BIS: 8112-1989, Indian standard 43 grade OPC specifications, New Delhi, India: Bureau of Indian standards; 1989.

Brindh, D., Baskaran, T and Nagan, S. Assessment of corrosion and durability characteristics of copper slag admixed concrete. International Journal of Civil and Structural Engineering, 2010; 1(2): 192- 211.

British Standard Institute. Concrete, specifications, performance, production and conformity, 2000, London,(BS EN 206-9).

Brouwers, H.J.H and Eijk Van, R.J. Chemical reaction of fly ash, 11th International Conference on the Chemistry of Cement (ICCC). The Cement's Contribution to the Development in the 21th Century, 2003.

Cachim, P., Velosa, A.L and Ferraz, E. Substitute materials for sustainable concrete production in Portugal. KSCE Journal of Civil Engineering, 2014; 18(1): 60-66.

Comité Euro-International du Béton. High-Performance Concrete, Recommended Extensions to the Model Code 90—Research Needs, CEB Bulletin d'Information, 1995; 228: 46.

Corinaldesi, M and Moriconi, G. The role of industrial by-products in self-compacting concrete. Construction and Building Materials, 2011; 25(8): 3181-3186.

Damtoft, J.S., Lukasik, J., Hertfort, D., Sorrentino, D and Gartner, E.M., Sustainable development and climate change initiatives, Cement and Concrete Research, 2008; 38(2): 115-127.

Domone, P.L. A review of the hardened mechanical properties of self-compacting concrete. Cement and Concrete Composites, 2007; 29(1): 1-12.

Domone, P.L. Self-compacting concrete: an analysis of 11 years of case studies. Cement and Concrete Composites, 2006; 28(2): 197-208.

EFNARC, European guidelines for self-compacting concrete: specification, production and use. Self-compacting concrete European project group; 2005.

Etxeberria, M., Pacheco, C., Meneses, J. M and Beerridi, I. Properties of concrete using metallurgical industrial by-product as aggregate. Construction and Building Materials, 2010; 24: 1594-1600.

Eurocode, EN 206-9 Concrete -Part 9: Aditional rules for Self compacting concrete, 2010.

Fadaee, M., Mirhosseini, R., Tabatabaei, R and Fadaee, M.J. Investigation on using copper slag as part of cementitious material in SCC, Asian Journal of Civil Engineering (BHRC), 2015; 16 (13): 368-381.

Gayarre, F.L., Boadella, I.L., Perez, C.L.C., Lopez, M.S and Cabo, A.D. Influence of the ceramic recycled aggregates in the masonry mortars properties. Construction and Building Materials, 2017; 132: 457-461.

Goodier, C.I. Development of self-compacting concrete, Proceedings of the Institution of Civil Engineers, Structures and Buildings, 2003; 156(4): 405-414.

Gunny, Y., Sari, Y. D., Yalcin, M., Tuncan, A and Donmez, S. Re-usage of waste foundry sand in high strength concrete. Waste Management 2010; 30: 1705-1713.

Hall, C. Water sorptivity of mortars and concretes. Magazine of Concrete Research, 1989; 41: 51-61.

Hameed, M.S and Sekar, S.S. Properties of green concrete containing quarry rock dust and marble sludge powder as fine aggregate, ARPN Journal of Engineering and Applied Sciences, 2009; 4(4): 83-89.

Hendrik, G and Oss, V.U.S. Iron and steel slag, Geological Survey, Mineral Commodity Summaries,2015.

Hiltunen, A. Waste management as a business in integrated steel making. Proc. Gorham/Intertech's 13th International Iron & Steel Development Forum – Managing

Steel Mill Wastes & By-Products: Crisis and Opportunity, Antwerp, Belgium, 1998; 11-14.

Holton, I. Update on research and development taking place in self-compacting concrete. Department of Trade and Industry and BRE, 2004 UK.

Human, T and Siddique, R. Properties of mortar incorporating iron slag. Leonardo journal of science. 2013; 23: 53-60.

Ilangovana, I., Mahendrana, N and Nagamanib, K. Strength and durability properties of concrete containing quarry rock dust as fine aggregate. ARPN Journal of Engineering and Applied Sciences, 2008; 3(5): 20-26.

Indian Minerals Yearbook (Part-II) 51th edition slag-iron and steel, government of India, ministry of mines, Indian bureau of mines, indira bhavan, civil lines, Nagpur-440001.

IS: 383-1970, Indian standard specifications for coarse and fine aggregates from natural sources for concrete New Delhi, India: Bureau of Indian standards; 1970.

Ismail, N.K., Hussin, K and Idris, M.S. Physical, chemical and mineralogical properties of fly ash. Journal of Nuclear and Related Technology, 2007; 4: 47-51.

Ismail, Z.Z and AL-Hashmi, E.A. Reuse of waste iron as a partial replacement of sand in concrete. Waste Management.2008; 28:2048-2053.

Joulazadeeh, M.M and Joulazadeh, F. Slag value added steel industry by product. Archives of Metallurgy and Materials, 2010; 55(4).

Kalyoncu, R.S. U.S geological survey mineral year book, Slag-Iron and Steel 2000.

Khatib, J.M. Effect of initial curing on absorption and pore size distribution of paste and concrete containing slag. KSCE Journal of Engineering, 2014; 18(1): 264-272.

Khatib, J.M. Performance of self-compacting concrete containing fly ash, Construction and Building Materials, 2007; 2(1): 1-12.

Khatib, J.M and Ellis, D.J. Mechanical properties of concrete containing foundry sand. ACI Special Publication, SP- 200, 2001: 733-748.

Kim, B., Prezzi, M and Salgado, M. Geotechnical Properties of Fly and Bottom Ash Mixtures for Use in Highway Embankments, Journal of Geotechnical Engineering. 2005; 131(7): 914-924.

Kitamura, H., Nishizaki, T., Ito, H., Chikamatsu, R., Kamada, F., and Okudate, M. Construction of prestressed concrete outer tank for LNG storage using high strength self-compacting concrete. Proceedings of the International Workshop on Self-Compacting Concrete,1999: 262-291.

Kothei, L and Malathy, R. Mechanical properties of self-compacting concrete with partial replacement of natural sand by steel slag. International journal of earth sciences and engineering 2012; 05(01): 635-639.

Kou, S.C and Poon, C.S. Properties of Self-Compacting Concrete Prepared with Recycled Glass Aggregate, Cement and Concrete Composites, 2008; 31(2): 107-113.

Law, D.W., Adam, A.A., Molyneaux, T.K and Patnaikuni, I. Durability assessment of alkali activated slag (AAS) concrete. Mineral and Structures, 2012; 45: 1425-1437.

Ling, T.C., Poon, C.S and Kou, S.C. Influence of recycled glass content and curing conditions on the properties of self-compacting concrete after exposure to elevated temperatures. Cement & Concrete Composites, 2012; 34: (265–272).

Liu, M. Incorporating ground glass in self-compacting concrete, Construction and Building Materials. 2010; 25: 919–925.

Madheswaran, C.K., Ambily, P.S., Dattatreya, J.K and Rajamane, N.P. Studies on use of copper slag as replacement material for river sand in building constructions. Journal of Institution of Engineering(India): Series A, 2014; 95(3): 169-177.

Malathy, R and Govindasamy, T. Development of mix design chart for various grades of self-compacting concrete. ICI Journal, 2006; 7(3): 19-28.

Maslehuddin, M., Alfarabi, M., Shammem, M., Ibrahim, M and Barry, M. Comparison of properties of steel slag and crushed lime stone aggregate concrete. Construction and building material, 2003; 17: 105-112.

Mehta, P.K and Monteito, P. Concrete micro-structure properties and materials. 3rd ed. New York Mc-Graw hill Professionals; 2006.

Milicevic, I., Stirmer, N and Pecur, I.B. Residual mechanical properties of concrete made with crushed clay bricks and roof tiles aggregate after exposure to high temperatures. Journal of Materials, 2016; 9(4): 295.

Mishra, S., Yamamoto, A., Tsutsumi, T and Motohashi, K. Application of rapid chloride permeability test quality control of concrete. Special Publication ACI, 1994; 145:487-502.

Monshi, A and Asgarani, M.K. Producing Portland cement from iron and steel slags and limestone. Cement and Concrete Research, 1999; 29: 1373-1377.

Naik, T. R., Singh, S.S and Hossain, M. M. Abrasion resistance of high strength concrete made with class C fly ash. ACI Material Journal, 1995; 92(6): 649-59.

Naik, T. R., Singh, S.S and Ramme, B.W. Performance and leaching assessment of flow able slurry. Journal of Environmental Engineering, 2001:359-368.

Netinger, I., Rukavina, M. J., Serdar, M and Bjegovic, D. Steel slag as valuable material for concrete production. Technical Gazette, 2014; 21: 1081-1088.

Netinger, I., Rukavina, M.J and Mladenovic, A. Improvement of post-fire properties of concrete with steel slag aggregate. The 9th Asia- Oceania on Fire Science and Technology, Procedia Engineering, 2013; 62: 745-753

Nevile, A.M. Properties of concrete. 3rd edition, ELBS and Longman, Singapore 1989.

Niewiadomski, P., Cwirzen, A and Hola, J. The influence of an additive in the form of selected nanaparticles on the physical and mechanical characteristics of self-compacting concrete. Procedia Engineering, 2015; 111: 601-606.

Okamura, H and Ouchi, M. Self-compacting Concrete, development, present use and future. Proc. First International RILEM Symposium on self-compacting concrete (Stockholm, Sweden), Skarendhal, A. and Petersson, O. Eds. RILEM Publications S.A.R.L 1999; 3-14.

Omar, M.O., Abd Elhameed, G.D., Sherif, M.A and Mohamadien, H.A. Influence of limestone waste as partial replacement material for sand and marble powder in concrete properties. HBRC Journal, 2012; 8(3): 193-203.

Omran, A. F., Morinn, E.D., Harbec, D and Hamou, A.T. Long-term performance of glass-powder concrete in large-scale field applications**.** Construction and Building Material, 2017; 135: 43-58.

Ouda, S. A and Gawwad, H.A.A. The effect of replacing sand by iron slag on physical, mechanical and rheological properties of cement mortar. HBRC journal, 2015.

Ozawa, K., Maekawa, K and Okamura, H. Development of high performance concrete. Faculty of engineering journal. University of Tokoyo; 1992.

Pai, B.H.V., Nandy, M., Krishnamoorthy, A., Sarkar, P.K and Ganapathy, C.P. Experimental study on Self-compacting concrete containing industrial by-product. European scientific journal 2014; 10(12).

Parrott, L. Water absorption in cover concrete. Materials and Structures; 1992; 25: 284-292.

Patel, A., Bhuva, P., George, E and Bhatt, D. Compressive strength and modulus of elasticity of self compacting concrete. National conference on recent trends in engineering and technology 2011.

Pellegrino, C and Gaddo, V. Mechanical and durability characteristics of concrete containing EAF slag as aggregates. Cement and Concrete Composite, 2008; 31: 663-671.

Peng, Y.C and Hwang, C.L. Carbon steel slag as cementitious material for self-consolidating concrete. J Zhejiang Univ-Sci A (Appl phy & eng) 2010; 11(7): 488-494.

Peter, J.A., Lakshmanan, N and Manoharan, P.D. SCC for under-reamed piles. Indian Concrete Journal, 2009; 83(6): 20-28.

Raharjo, D., Subakti, A and Tavio, A. Mixed concrete optimization using fly ash, silica fume and iron slag on the SCC's compressive strength. The 2nd International Conference on Rehabilitation and Maintaince in Civil Engineering, Procedia Engineering, 2013; 54: 827-839.

Rai, B., Kumar, S and Satish, K. Effect of fly ash on mortar mixes with quarry dust as fine aggregate. Advances in Materials Science and Engineering, 2014: 1-7.

Rakshvir, M and Barai, S.V. Studies of recycled aggregate based concrete. Waste Management Research, 2006; 24(3): 225-234.

Regev, L., Ronald, L.M and Alalon, O. Economics feasibility of waste separation source: Case study of neighborhoods in Haifa, Israel. Presentation at the Proceeding of the Twenty-Ninth International Conference on Solid Waste Technology and Management. Philadelphia, PA, March 30-April 2, 2014.

Sabapathy, Y.K., Balasubramaniam, V.B., Shankari, N.S., Kumar, Y and Ravichandra, D. Experimental investigation of surface modified EOF steel slag as coarse aggregate in concrete,. Journal of King Saud University-Engineering Sciences, 2016 *(Article in press).*

Sahmaran, M., Lachemi, M., Erdem, T.K and Yucel, H.E. Use of spent foundry sand and fly ash for the development of green self-consolidating concrete. Material and structures, 2011; 44(7): 1193-1204.

Sahu, A.K., Kumar, S and Sachan, A.K. Crushed stone waste as fine aggregates for concrete. The Indian Concrete Journal, 2003; 1: 845-848.

Santamaria, A., Gozalez, J.J., Losanez, M.M., Vegas, I., Arribas, I and Roji, E. Selff-compacting concrete containing EAF slag as aggregates. The 8th Euroslag Conference, Euroslag 2015.

Schutter, G. D., Bartos, P., Domone, P and Gibbs, J. Self-Compacting Concrete. Dunbeeath, Scotland: Whittles Publishing, 2008.

Sengupta, A and Santhanam, M. Influence of aggregate characteristics on uniformity of SCC. Indian Concrete Journal, 2009; 83(6): 50-60.

Serina, N., Jelle, B.P., Sandberg, L.I.C., Gao, T and Wallevik, OH. Experimental investigations of aerogel-incorporated ultra-high performance concrete. Construction and Building Material, 2015; 77: 307,316.

Shakhmenko, G., Korjakins, A and Bumanis, G. Concrete with microfiller obtained from recycled lamp glass, Modern building materials, structures and techniques. The 10th International Conference. Vilnius, Lithuania (2010).

Shalabi, F.I., Asi, I.M and Qasrauri, H.Y. Effect of by-product steel slag on engineering properties of clay soil. Journal of King Saud University-Engineering Sciences, 2016 *(Article in Press)*

Sharifi, Y., Houshiar, M and Aghebati, B. Recycled glass replacement as fine aggregates in self-compacting concrete, Frontier of structure and civil engineering 2013; 7(4): 419-428.

Sheen, Y.N., Le, D.H and Sun, T.H. Greener self-compacting concrete using stainless steel reducing slag, Construction and Building Material, 2015; 82:341-350.

Sheen, Y.N., Huang, C.J., Sun, T.H and Le, D.H. Engineering properties of self compacting concrete containing stainless steel slags, Procedia Engineering, 2016; 142: 79-86.

Sheen, Y-N., Le, D-H and Sun, T-H. Innovative usages of stainless steel slag in developing self compacting concrete, Construction and Building Material 2015; 101: 268-276.

Siddique, R and Bennacer, R. Use of iron and steel industry by-product (GGBS) in cement paste and mortar. Resources, Conservation and Recycling, 2012; 69: 29-34.

Siddique, R and Kadri, E.H. Effect of metakaolin and foundry sand on the near surface characteristics of concrete. Construction and Building Materials, 2011; 25(8): 3257-3266.

Siddique, R. Wear resistance of high volume fly ash concrete. Leonardo Journal of Science, 2010; 17: 21-36.

Siddique, R and Kunal. Design and development of self-compacting concrete made with coal bottom ash. Journal of Sustainable Cement-Based Materials.2015; 4(3-4): 225-237.

Sideris, K.K., Tassos, C and Chalzopoulos, A. Production of durable self-compacting concrete using ladle furnace slag (LFS) as filler material. 7th Scientific-Technical Conference Material Problem in Civil Engineering (MATBUD'2015), 2015; 108: 592-597.

Singh, M and Siddique, R. Strength properties and micro-structural properties of concrete containing coal bottom ash as partial replacement of fine aggregate**,** Construction and Building Material, 2014; 50: 246-256.

Singh, M and Siddique R. Compressive strength, drying shrinkage and chemical resistance of concrete incorporating coal bottom ash partial or total replacement of sand. Construction and Building Material, 2014; 68: 39-48.

Singh, S.P., Goel, S and Singh, P. Fatigue analysis of plain and fiber reinforced self-consolidating concrete. ACI Material Journal, 2012; 109 (5): 573-582.

Sivarama, B., Manohar, S and Selvam, S. Nobel method of placing SCC by bottom up pumping, ICI Journal, 2006; 7(1): 33-40.

Smarzewski, P and Hunek, D.B. Mechanical and durability related properties of high performance concrete made with coal cinder and waste foundry sand. Construction and Building Materials, 2016; 121: 9-17.

Soya, M., Sugits, S., Tsukinaga, Y., Aba, M and Tokuhasi, K. Properties of self compacting concrete with slag as fine aggregates. Exploiting waste in concrete, Proceeding Of International Seminar: held at the University of Dundee, Scotland, UK 1999:121-130.

Srinivas, C.H and Muranal, S.M. Study of the properties of concrete containing copper slag as a fine aggregates, International Journal of Engineering Research and Technology, 2015; 4(2).

Tanikella. P and Olek, J. Incorporating physical and chemical characteristics of fly ash in statical modeling of binder properties. Purdue University, 2010.

Tersawy, S.H and Ali, E.E. Recycled glass as a partial replacement for fine aggregate in self compacting concrete. Construction and Building Materials, 2012; 35: 785–791.

The Concrete Society, BRE, Technical report No.62 self-compacting concrete: a review. Day RTU, Holton IX, editors, Camberley, UK, Concrete society, Surrey 2005; GU17 9AB, UK.

Tittarelli, F and Moriconi, G. Use of GRP industrial by-products in cement based composites, Cement and Concrete Composite, 2010: 32(3); 219-225.

Tomasiello, S and Felitti, M. EAF slag in self compacting concrete. Facta universitatis series: architecture and civil engineering, 2010; 8: 13-20.

Torgal, F.P. 1 – Introduction to the environmental impact of construction and building materials, Eco-efficient Construction and Building Materials, 2014: 1-10.

Valcuende, M., Benito, F., Parra, C and Minano, I. Shrinkage of self-compacting concrete made with blast furnace slag as fine aggregates. Construction and Building Material, 2015; 76: 1-9.

Vanjare, M.B and Mahure, S.H. Experimental Investigation on Self Compacting Concrete Using Glass Powder. International Journal of Engineering Research and Applications (IJERA), 2012; 2(3): 1488-1492.

Viacava, R.I., Aguado, D.C.A and Sensale, R.D.G. Self-compacting concrete of medium characteristic strength. Construction and Building Materials, 2012; 30: 776-782.

Wang, H.Y and Huang, W.L. A study on the properties of fresh self-consolidating glass concrete (SCGC), Construction and Building Materials, 2010; 24: 619–624.

Wang, H.Y and Lin, C.C. A study of fresh and engineering properties of self compacting high slag concrete (SCHSC). Construction and building material, 2013; 42: 132-136.

www.fhwa.dot.gov/publications/research/infrastructure/structures/97148/ssa1.cfm

Yoo, J.H., Choi, J.J and Choi, D.S. Self compacting concrete incorporating atomized steel slag aggregates. First International Symposium on Design and Use of Self-Consolidating Concrete (SCC) in China; 2005: 253-260.

Yuksel, I and Genc, A. Properties of concrete containing Non-ground ash and slag as fine aggregates. ACI Material Journal, 2007; 103(3): 203-208.